Società Chimica Italiana
Divisione di Spettrometria di Massa

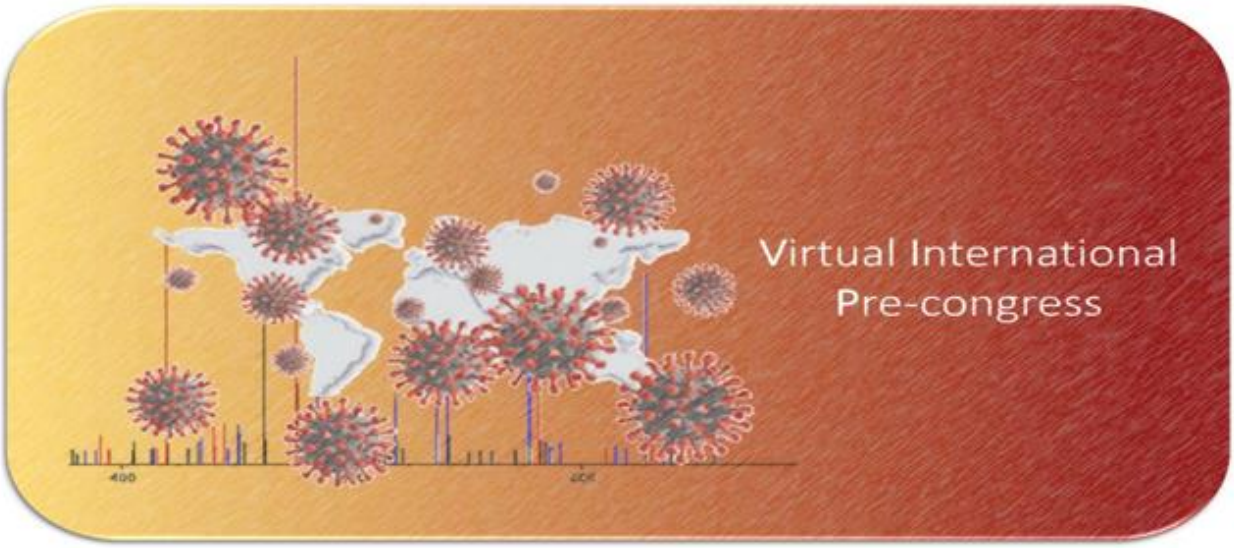

1st online edition

MASSA 2020 VIP

Book of Abstracts

ISBN 9788894952025

Committees

Scientific & Organizing Committee

Gianluca Bartolucci	Università di Firenze
Cecilia Bergamini	ARPAE, Bologna
Giuliana Bianco	Università della Basilicata, Potenza
Donatella Caruso	Università di Milano
Riccardo Flamini	CREA-VE, Conegliano (TV)
Roberta Galarini	Ist. Zooprofil. Sper. Umbria, Marche, Perugia
Gianluca Giorgi	Università di Siena
Emanuela Gregori	Istituto Superiore di Sanità, Roma
Valentina Lazazzara	Fondaz. E. Mach, S. Michele all'Adige (TN)
Fulvio Magni	Università di Milano Bicocca
Giorgio Mellerio	Università di Pavia
Paola Montoro	Università di Salerno
Sabino Napoletano	Min. Interno, Roma
Luciano Navarini	illycaffè, Trieste
Valeria Filippi	Arpa Toscana, Livorno
Michele Mazzetti	Arpa Toscana, Livorno
Daniela Cecconi	Università di Verona

MASSA 2020 –VIP- Virtual International Pre-Congress is kindly supported and sponsored by:

Scientific Program

Summary

ORAL PRESENTATIONS

Omics

An integrated MS approach reveals the conformational dynamics of lipopolysaccharide outer membrane insertase LptDE

***F. Fiorentino*[1], *J. B. Sauer*[1,2], *X. Y. Qiu*[1], *P. J. Stansfeld*[2,3], *S. Mehmood*[1,4], *J. R. Bolla*[1] *and C. V. Robinson*[1]**

[1]Department of Chemistry, University of Oxford, South Parks Road, Oxford OX1 3QZ, UK, [2]Department of Biochemistry, University of Oxford, South Parks Road, Oxford OX1 3QU, UK, [3]School of Life Sciences and Department of Chemistry, University of Warwick, Gibbet Hill Campus, Coventry, CV4 7AL, UK, [4]Current address: The Francis Crick Institute, 1 Midland Road, London NW1 1ST, UK

Keywords: *HDX – MS, native mass spectrometry, membrane proteins*

Introduction

Lipopolysaccharide (LPS) is a glycolipid present in the outer membrane (OM) of Gram-negative bacteria essential for cellular structural stability and protection from xenobiotics. Newly-formed LPS molecules are inserted in the outer leaflet of the OM through the heterodimer formed by the OM protein LptD (presenting a β-barrel transmembrane domain and a periplasmic β-jellyroll) and the lipoprotein LptE [1]. Given its key role in LPS transportation, LptDE has been described as an ideal target for antimicrobial drugs [2]. Although the crystal structure of this complex has been solved [1,3], details about the conformational changes following LPS binding to LptDE remain elusive. Here we integrate native mass spectrometry (nMS) and hydrogen-deuterium exchange mass spectrometry (HDX-MS) to investigate the influence of substrate and inhibitor binding on the conformational dynamics of LptDE.

Materials and Methods

LptDE was purified according to standard chromatographic methods and incubated with LPS, the inhibitor thanatin or both ligands. The HDX reaction was initiated by a 12× dilution into deuterated buffer (0.03% DDM, 20 mM Tris, 200 mM NaCl adjusted to pH 8 using DCl at 20 °C) for a time course of 10s, 60s, 1000s, 5000s and 7hrs. The labelling reaction was quenched with ice cold buffer brought to pH 2.0 with HCl and containing 15 mM TCEP. Following on-line digestion using pepsin immobilized column and separation on a nano-Acquity UPLC column, peptides were analysed using a hybrid ESI-Q-TOF mass spectrometer (Synapt G2-Si, Waters). Data was processed using DynamX (Waters), Deuteros, HX-Express 2.0 software packages and an in-house Python script. Native mass spectrometry was performed using Thermo Q-Exactive UHMR platforms modified for the transmission of high molecular weight membrane protein assemblies [4]. Before NMS analysis, purified protein complexes were buffer exchanged into ammonium acetate buffer containing detergents at twice the critical micelle concentration. Data were processed using Thermo Scientific Xcalibur and UniDec (University of Oxford) software.

Results

We performed nMS experiments with Re-LPS, an LPS substructure consisting of the lipid A moiety and two ketodeoxyoctonic acids (Kdo) residues belonging to the core oligosaccharide. This LPS analogue has been found to have the same endotoxin activity as LPS and has thus been used to investigate the functionality of the Lpt system in previous studies [5]. Mass spectra recorded using optimised conditions exhibited concentration-dependent binding of Re-LPS (Fig. 1a, left). Next, we performed nMS competition experiments in the presence of the antimicrobial peptide thanatin (1 μM) with increasing concentrations Re-LPS from 0 to 20 μM. Interestingly, additional adduct peaks observed in the mass spectra showed the simultaneous binding of Re-LPS and thanatin to LptDE (Fig. 1a, right), thus suggesting non-competitive binding of the peptide inhibitor towards the substrate. To dissect the conformational dynamics of LptDE, we performed HDX-MS experiments. The peptide coverage of the whole complex (70.5% sequence coverage for LptD and 87.4% for LptE) allowed a thorough investigation of the conformational dynamics of the protein in

both apo and ligand-bound states. The analysis of deuterium uptake of apo-LptDE indicated that the majority of the peptides belonging to LptD β-jellyroll undergo exchange dynamics according to the EX1 or EXX (mixed EX1- EX2) regimes [6]. Indeed, these peptides present the characteristic bimodal isotopic distribution upon deuterium uptake. Incubation with LPS induced a significant increase of deuterium uptake in the β- jellyroll region of LptD and led to an increased rate of the correlated exchange rate of the segments characterised by EX1/EXX kinetics. These results suggest that the enhanced dynamics of the protein in the presence of the substrate is related to conformational opening of the β-jellyroll. LPS incubation also showed decreased deuterium uptake (following EX2 kinetics) on peptides corresponding to strands β1-β2 of LptD β-barrel (Fig. 2). Remarkably, these segments are involved in the process of LPS extrusion from the β-barrel and are adjacent to the putative exit gate, located at the β1-β26 edge. HDX-MS analysis of LptDE bound to thanatin, a peptidomimetic LPS transportation inhibitor, indicated a slower rate of correlated exchange in the β-jellyroll compared to the apo protein, suggesting reduced conformational opening. Moreover, we uncovered additional peptides belonging to the N-terminal region of the β-jellyroll with reduced deuterium uptake. We integrated HDX-MS analysis with complementary techniques (native MS, structure alignment, and MD simulations) and concluded that this region may represent the binding site for thanatin. Furthermore, LptD β-jellyroll remains in the closed conformation in the presence of both LPS and thanatin, indicating that the disruption of LPS transport played by thanatin relies on a ligand-induced conformational change rather than competition for the same binding site. In conclusion, we demonstrated that the substrate induces opening of the complex and elucidated the influence of antibiotic peptide binding to the protein.

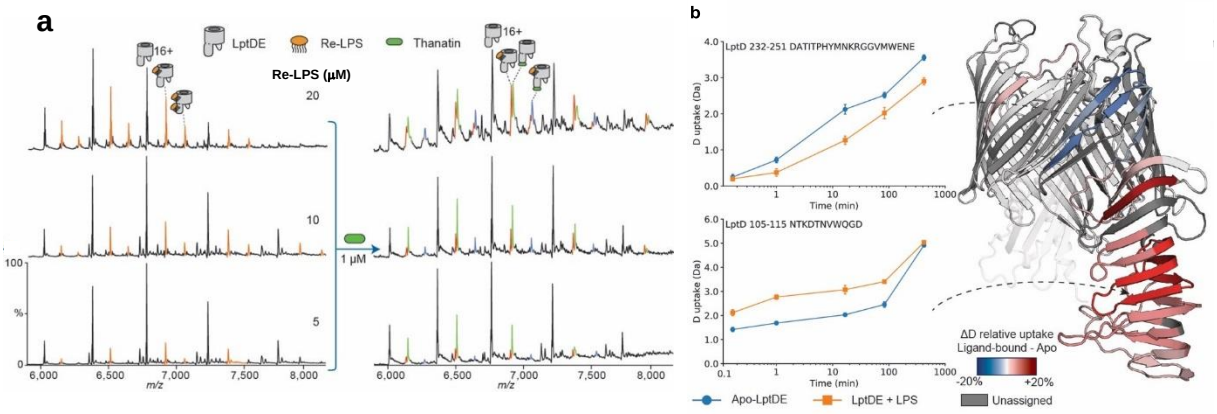

Fig.1 (a) nMS analysis of LptDE ligand binding properties. LptDE in 0.5% C8E4 was incubated with increasing concentrations of Re-LPS (left, orange peaks). Then, Re-LPS-bound LptDE was supplemented with 1 μM thanatin (right). New charge state series corresponding to LptDE bound to thanatin (green) and both Re-LPS and thanatin (purple) are observed. Each data point and standard deviation are calculated from the average of five observed charge states in three independent experiments. Error bars represent standard deviations (n = 3).
(b) Conformational dynamics of LPS-bound LptDE. Left: the deuterium uptake of representative peptides (105- 115, β-taco and 232-247, β-barrel) plotted as a function of labelling time (0.167-420 min) for apo-LptDE (blue) and LPS-bound LptDE (orange). Error bars indicate standard deviations (n= 4). Right: difference in relative deuterium uptake (scaled for the number of residues of each peptide) at the 16.67 min labelling time mapped on the crystal structure of LptD. Only peptides showing significant difference are colored. Red and blue indicate increased and decreased deuterium uptake, respectively.

References

1. H. Dong, et al.; *Nature* 511, (2014) pp 52-56.
2. G. Andolina, et al.; *ACS Chem. Biol*. 13, (2018) pp 666-675.
3. I. Botos, et al.; *Structure* 24, (2016) pp 965-976. 4.
4. J. Gault, et al.; *Nat. Meth.* 13, (2106) pp 333-336
5. R. Xie, R. J. Taylor, & D. Kahne; *J. Am. Chem. Soc.* 140, (2018) pp 12691-12694.
6. D. D. Weis, et al.; *J. Am. Soc. Mass Spectrom.* 17, (2006) pp 1498-1509

The metabolic plasticity of malignant primary cholangiocytes: a multiplatform mass spectrometry strategy

L. Brunelli [1,2], ***G. Sestito*** [1], ***M.A. Polidoro*** [3], ***C. Soldani*** [3], ***B. Franceschini*** [3], ***G. Torzilli*** [4], ***M. Donadon*** [4], ***A. Lleo*** [3,5] ***and R. Pastorelli*** [1,2]

[1]Protein and Metabolite Biomarkers Unit, Mass Spectrometry Laboratory, Istituto di Ricerche Farmacologiche Mario Negri IRCCS, Milano, [2]Italian Metabolomics Network (metabonet.it), [3]Hepatobiliary Immunopathology Laboratory, Humanitas Clinical and Research Center – IRCCS, Humanitas University - Rozzano (Italy), [4]Department of Surgery - Division of Hepatobiliary & General Surgery, Humanitas Clinical and Research Center – IRCCS, Humanitas University - Rozzano (Italy), 5Division of Internal Medicine and Hepatology, Department of Internal Medicine, Humanitas Clinical and Research Center, Humanitas University - Rozzano (Italy)

Keywords: *intrahepatic cholangiocarcinoma, conditioned medium, metabolomics*

Introduction

Intrahepatic cholangiocarcinoma (iCCA) is a malignancy that arise from biliary epithelial cells (BECs) that lining biliary tree. It is the second most common primary liver tumor and surgical resection is the only curative approach because pharmacological therapies are generally unsuccessful [1,2]. Due to the complexity of the in vivo cellular interactions, the mechanisms and metabolic activation pathways are largely unknown. There is a need for better understanding tumor characteristics and pathogenesis and for tailoring effective therapies. In this perspective, it is vital to dissect the involved biochemical pathways and key players in iCCA development and progression.

Materials and Methods

We have isolated and in-vitro cultured tumoral iCCA and their normal biliary cell counterparts from 15 patients, which underwent liver surgery at the Humanitas Clinical Institute. With the aim to decipher the metabolic asset and the influence of extracellular metabolic composition of the metabolic capability of malignant primary cells, we profiled the cell exo-metabolome by high-resolution mass- spectrometry. Specifically, we used multiplatform metabolomics strategies including untargeted FIA, central cellular metabolites targeted profiling and target Biocrates p180kit to profile the conditioned medium derived from iCCA primary cells cultured in different media metabolic composition. We also evaluate the effect of different metabolic dependencies by proliferation tests.

Results

Multiplatform metabolomics approaches of metabolites uptake and release in the conditioned culture media of iCCA cells showed that iCCA cells modify medium composition by altering metabolites belonging to biochemical pathways linked to central cellular metabolism compared to normal primary biliary cells (Fig.1A). Further, we highlighted the capability of tumour cells to reprogram nutrient uptake and utilization in presence of different metabolic medium composition (RPMI-1640, Ready- To-use) to accommodate and sustain mitochondrial functionality. Specifically, we imputed in pyruvate the main metabolic actor able to foster mitochondrial machinery revealed by the augmented metabolites extrusion, in Ready-to-use medium, of metabolic intermediates (e.g. aspartate, citrate, lactate) associated with their lowering in the intracellular space. This was indicative of an augmented cellular metabolism exerted by the Ready-To-use medium in iCCA cells. The presence of environmental pyruvate is able not only to foster the cell metabolic machinery but also to specifically sustain iCCA in-vitro cancer cell proliferation. Indeed, we cultured over-time primary iCCA cells in four different formulation of RPMI-1640 medium covering different nutrient combinations (without pyruvate and glutamine, with only pyruvate, with only glutamine, with both pyruvate and glutamine) and observed the capability of pyruvate to trigger cancer cell proliferation.

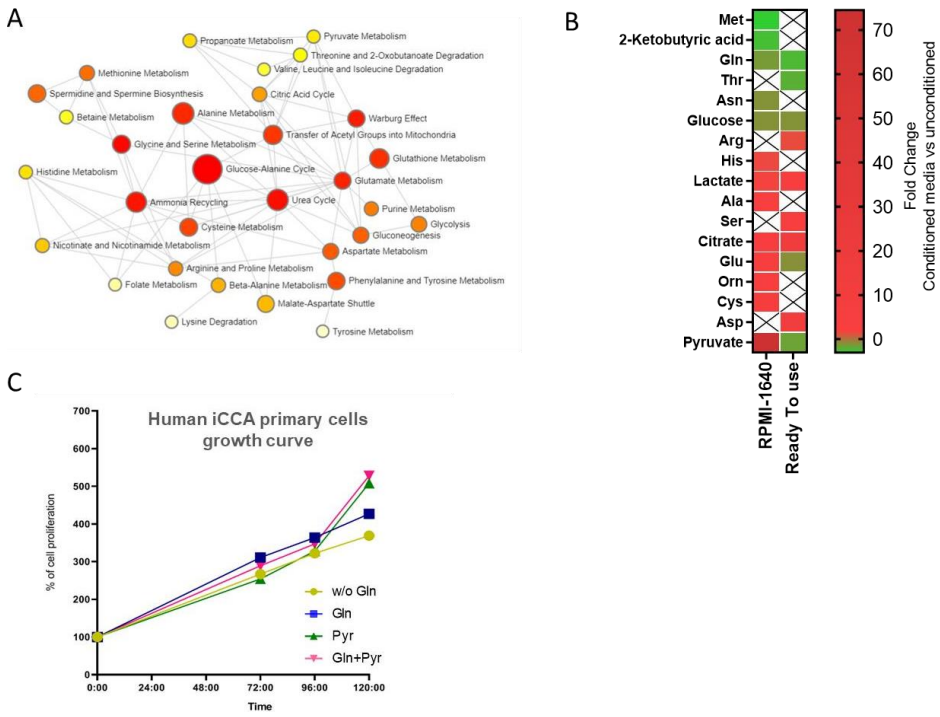

Fig. 1. ***A.*** *Metabolic network representative of the significant enriched pathways (MetaboAnalyst, p <0.05, FDR <0.05) using the significant altered metabolites (p<0.05, Mann–Whitney–Wilcoxon test) between iCCA conditioned medium and RPMI-1640. The red circles indicate significant enriched pathways in iCCA primary cells conditioned medium (p <0.05, FDR <0.05). Metabolomics data from central cellular target, untargeted-FIA, Biocrates p180 kit integrated approaches (n=15iCCA, n=5 primary biliary cells).* ***B.*** *Heat map representative to the significantly altered (p<0.05, Mann–Whitney–Wilcoxon test) metabolite uptake and release (fold change of metabolites abundance in conditioned media vs unconditioned) between iCCA cultured in ready to used (n=8) and in RPMI-1640 (n=15).* ***C.*** *iCCA cells proliferation curve performed with WST-1 assay. iCCA cells were seeded in a 96-well plates at 1 X 103 cells/well and grown in four different media composition (w/o pyruvate and glutamine, only pyruvate, only glutamine, and with pyruvate and glutamine). Cell proliferation were monitored over time (T0-T120 hours)*

Discussion/Conclusions

The use of multiplatform metabolomics approaches, increasing the metabolite coverage, converged to define the activation of glutaminolytic pathway that fuels iCCA primary cells anabolic processes as already observed for sever other cancers such as NSCLC, pancreatic cancer [3,4,5]. Interestingly, we highlighted the capability of iCCA cancer cells to modulate their metabolic machinery to adapt plastically at different extracellular metabolic composition. Such ability together with the capability of pyruvate to augment cancer cell proliferation raises the concern that interfering only with the glutaminolityc pathway may not be sufficient for altering the mitochondrial machinery in this cell context. To avoid possible metabolic escaping of iCCA to metabolic targeting, there is the strong need to take into consideration physiological context that better mimics the metabolic composition of the in-vivo tumor environment.

References

1. J.M. Banales, V. Cardinale, G. Carpino, et al. *Nat Rev Gastroenterol,* 13 (2016), pp 261-80.
2. S. Buettner, J. Van Vugt, J. N. IJzermans, et al. *Onco Targets Ther*. 10 (2017), pp 1131–42.
3. E.Caiola, F. Falcetta, S. Giordano, et al, *J Exp Clin Cancer Res.* 37 (2018) pp 302.
4. E. M Kerr, C. P Martins, *FEBS J*, 285 (2018), pp 28-41.
5. J.Bott1, J. Shen, C. Tonelli, et al. *Cell reports*. 29 (2019), pp 1287-1298.

ESI-MS highlights the selective interaction of small molecules with G-quadruplex nucleic acids

***G. Ribaudo*[1], *A. Ongaro*[1], *M. Memo*[1] *and A. Gianoncelli*[1]**

[1]Department of Molecular and Translational Medicine, University of Brescia, Viale Europa 11, 25123 Brescia, Italy

Keywords: *G-quadruplex, nucleic acids, drug discovery, CID*

Introduction

In the context of drug discovery, G-quadruplex nucleic acids represent attractive targets for developing small molecules that trigger biological effects. These arrangements, constituted by stacked guanine nucleobases, can be formed by guanine-rich sequences, such as those that are present in telomeres, promoter genes and viral genomes. Compounds with peculiar structural features can interact with G-quadrupexes, improving or affecting their stability. In particular, this strategy is pursued in medicinal chemistry for selectively interfering with gene expression, uncontrolled cell proliferation and viral replication. Acridines, naphthalene diimides, anthracenes and anthraquinones are among the synthetic small molecules studied as non-covalent G-quadruplex binders, along with some natural compounds such as flavonoids. G-quadruplex ligands generally bear a planar scaffold and flexible side chains to efficiently interact with the nucleic acid [1].
In this contribution, we will present the practical application of an experimental approach, consisting in a cell free, mass spectrometry-based test for screening small molecules interacting with biologically relevant G-quadruplex structures and for the evaluation of their sequence selectivity.

Materials and Methods

Commercially available chemicals and oligonucleotides were obtained from Sigma-Aldrich. Nucleic acid samples were heat-denatured and folded in 150 mM ammonium acetate before incubation with ligands, selected from a library of natural and synthetic compounds. Ligand stock solutions were prepared in methanol. The final concentration of the oligonucleotide was 5 μM in 150 mM ammonium acetate, with a 10:1 ligand/oligo ratio. Samples were acquired after an equilibration time of 30 minutes by direct infusion electrospray (ESI) on a Thermo Scientific LCQ Fleet ion trap mass spectrometer. The instrument was set in negative ionization mode with a 3.4 kV capillary voltage, 120 °C capillary temperature and a flow rate of 5 μL/min. Collision-induced dissociation (CID) experiments were performed on the DNA/ligand complexes by isolating the precursor ion in the trap and increasing the "normalized collision energy" parameter. Additional and confirmative high resolution analyses were carried out on Waters Xevo G2 and Thermo Scientific LTQ Orbitrap spectrometers in negative ionization mode.
Exact mass for the G-quadruplex sequence (5'-AGGGTTAGGGTTAGGGTTAGGGT-3'): 7270.774 Da. Exact mass for double stranded DNA (dsDNA) sequence (5'-ACTATTTACGTATAATGA-3', 5'-TCATTATACGTAAATAGT-3',): 10987.922 Da. Binding affinity was calculated according to the formula: $BA= (\Sigma I_{bound\ DNA}/(\Sigma I_{free\ DNA} + \Sigma_{bound\ DNA}))$ x 100. In CID studies, relative intensity (%) of the DNA/ligand signal was plotted against the applied energy expressed in eV (logarithmic scale). Relative I (%) = $(I_{complex}/(I_{complex} + I_{dissociation\ products}))$ x 100 [2-4].

Results

G-quadruplex DNA stabilization mediated by small molecules is an attractive approach to modulate the transcription of guanine-rich sequences and contrast unregulated cell proliferation. On the other hand, interference with viral nucleic acid is a promising, emerging strategy for the development of innovative antivirals. In this communication, the potential of ESI-MS in probing the interaction of small molecules with different DNA structures is exemplified. A pool of natural, semi-synthetic and synthetic compounds bearing a planar scaffold, such as anthracenes, anthraquinones and flavonoids were tested against a G-quadruplex-forming sequence containing the human telomeric TTAGGG repeat. A dsDNA oligonucleotide was used as control and G-quadruplex/duplex selectivity ratio was estimated on the basis of BA values. CID experiments were used to investigate the relative gas-phase kinetic stability of the complexes. MS fragmentation pattern, combined with molecular docking, provide insights on the interaction motif of the compounds with G-

quadruplex (Figure 1) [5]. Moreover, the ligand-DNA complex formation in solution was further confirmed by fluorescence titrations for most promising compounds.

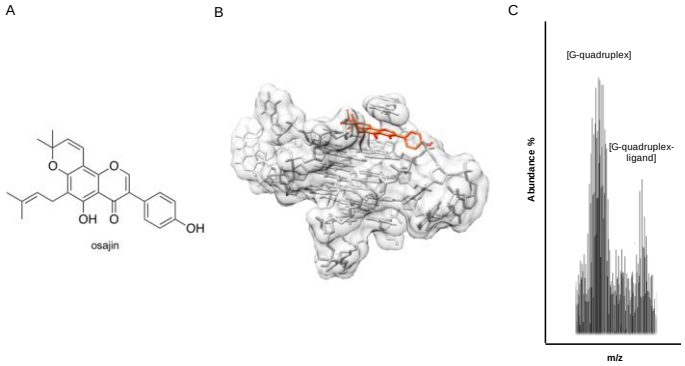

Fig. 1. Chemical structure of osajin, a natural isoflavone (A), and its predicted interaction pattern with G-quadruplex DNA (PDB ID: 3CE5; B). A representative interaction spectrum is also reported (C).

Discussion/Conclusions

Natural and synthetic small molecules targeting G-quadruplex were screened using ESI-MS against G-quadruplex and dsDNA sequences. This screening highlighted a small set of compounds capable of selectively targeting and efficiently stabilizing G-quadruplex. The preliminary results encourage further studies for elucidating the potential application of such compounds as antiproliferative and antiviral agents selectively interacting with G-quadruplex structures, presumably showing limited cross-reactivity with off-target sequences.

References

1. R. Rigo, M. Palumbo, C. Sissi; *Biochim. Biophys. Acta - Gen. Subj.*, 1861 (2017), pp 1399-1413.
2. R. Ferreira, A. Marchand, V. Gabelica; *Methods* 57 (2012), pp 56-63.
3. F. Rosu; *Nucleic Acids Res*. 30 (2002), pp 82e–82.
4. A. Tjernberg, S. Carnö, F. Oliv, K. Benkestock, P.O. Edlund, W.J. Griffiths, D. Hallén; *Anal. Chem.* 76 (2004), pp 4325-4331.
5. G. Ribaudo, A. Ongaro, G. Zagotto, M. Memo, A. Gianoncelli; *Nat. Prod. Res*. (in press, DOI: 10.1080/14786419.2019.1680670).

Analysis of Oxysterols profile in Zebrafish Embryos by HPLC-MS/MS

F. Fanti[1], C. Merola[1], A. Vremere[1], E. Oliva[1], M. Perugini[1], M. Amorena[1], D. Compagnone[1], and M. Sergi[1]

[1]University of Teramo, Faculty of Bioscience and Technology for Food, Agriculture and Environment, 64100 TE, Italy

Keywords: *Oxysterols, Zebrafish embryos, LC-MS/MS*

Introduction

Zebrafish. is an in vivo model used in toxicology to estimate the effects of xenobiotics in particular during embryos growth and their teratogenic consequences. [1] The knowledge of the profile of the oxysterols in zebrafish, during the early embryonic stages, provides important information on the role and biological function of these molecules [2]. This work reports the development and validation of a LC-MS/MS method for the determination of 7 different oxysterols in zebrafish embryos; sample was treated with a combination of liquid/liquid extraction (LLE) followed by micro solid phase extraction (μSPE) clean-up in order to remove matrix interference and obtain a suitable enrichment factor of the analytes.

Materials and Methods

Embryos at 3/4hpf and at 24hpf were counted and dispersed in 5 mL of water were sonicated in ice and then vortexed, then 300 μL of $CHCl_3$ and 300 μL of MeOH were added to 300 μL of sample; they were shaken by orbital shaker for 30 min at 300 rpm. Then, another portion of 300 μL of CHCl3 was added and samples were shaken again for 30 min at 300 rpm. Finally, 300 μL of H2O were then added and the resulting mixture was shaken for 30 min at 300 rpm, for a total extraction time of 1.5 h. The resulting mixture was centrifuged at 4°C for 5 min at 9600 g. The extracted $CHCl_3$ portion was taken from each sample and dried with N_2 stream. Samples were resuspended in 112 μL of a precipitant solution 1900 g. The supernatant was taken, added with 88 μL of H2O, vortexed and processed by μSPE for clean-up. Samples were analysed with a Nexera LC20AD chromatographic system (Shimadzu, Kyoto, Japan) coupled with a Qtrap 4500 mass spectrometer (Sciex, Toronto, ON, Canada). The chromatographic run was performed using a Kinetex C18 XB 100x2.1mm packed with 2.6 μm particles, with column oven maintained at 40°C. Flow rate was set at 0.6 mL min-1; phase A was H2O and phase B ACN/MeOH both acidified with formic acid (25 mM).

Results

Validation was performed on embryos at 2 different stage of development (3 and 24 hpf). LODs and LOQs values were evaluated in according with EMA Guideline on bioanalytical method validation. To test the proposed analytical method, different zebrafish embryos samples were analysed. Different oxysterols were detected as preliminary data. In particular, the 25OH and 27OH were detected both in embryos at 3-4 hpf and 24 hpf.

Discussion/Conclusions

In conclusion, a robust and reliable analytical method for the analysis of oxysterols in zebrafish embryos was developed and validated. In particular the determination of oxysterols profiles induced both enzymatically and nonenzymatically, in zebrafish embryos will be useful to understand the correlation between oxysterols profile and developmental abnormalities induced by xenobiotics exposure.

References

1. A. Zampelas, E. Magriplis, *Nutrients*. 11 (2019).
2. Y.C.M. Staal, J. Meijer, et al., *Arch. Toxicol*. 92 (2018) pp 3549–3564

MALDI mass spectrometry imaging of the mouse ovarian folliculogenesis

G. Fiorentino[1,2], A. Smith[3], F. Orellana[1], F. Magni[3], S. Garagna[1,2] and M. Zuccotti[1,2]

[1] Department of Biology and Biotechnology "Lazzaro Spallanzani", University of Pavia, Italy, [2] Center for Health Technologies, University of Pavia, Italy, [3] Department of Medicine and Surgery, University of Milano-Bicocca, Italy

Keywords: *MALDI-MSI, LC-ESI-MS/MS, ovary*

Introduction

The mammalian ovary is a highly dynamic organ that cyclically undergoes morpho-functional changes. From puberty, at each ovarian cycle, a pool of primordial follicles (type 1, T1) is recruited, grows through to the secondary (T4) to pre-ovulatory (T8) stage, until ovulation of a mature oocyte. The correct follicle growth and acquisition of oocyte developmental competence are strictly related to a continuous, but still poorly understood, remodelling of the ovary and crosstalk between follicle cells and oocytes. The objective of this study was the *in-situ* identification of the peptide signature of each growing follicle type, from T4 to the fully-grown T8, combining MALDI mass spectrometry imaging (MALDI-MSI) with Liquid Chromatography Electrospray Ionization Tandem Mass Spectrometry (LC-ESI-MS/MS).

Materials and Methods

A 25-day-old mouse ovary was fixed in 10% Formalin, dehydrated, embedded in Paraffin wax, and a total of 130 6-µm serial sections were placed onto four ITO glass slides.

Following proteins digestion with 20 ng/µL trypsin o/n at 40°C, sections were coated with a matrix of α-cyano-4-hydroxycinnamic acid (10 mg/mL in 50:50 acetonitrile:water w/0.4% trifluoroacetic acid) for peptides extraction and *in-situ* crystallization. Mass spectra were acquired by using the ultrafleXtreme MALDI–TOF mass spectrometer (Bruker Daltonik GmbH) in a reflectron-positive ionisation mode, within the mass range of m/z 750 to 3,500. The matrix was irradiated by a Smartbeam 3D laser with a pixel width of 20 µm, allowing peptides ionisation [1]. Then, mass spectra were imported into the SCiLS Lab MVS 2019c Pro software (http://scils.de/; Bremen, Germany) to perform intensity normalization and remove background noise.

After MALDI-MSI, the matrix was used for further LC-ESI-MS/MS analysis with the Dionex UltiMate 3000 rapid separation (RS) LC nano system coupled with an Impact HD™ UHR-QqToF (Bruker Daltonik, Germany). Peptides obtained were identified using the Mascot software (version 2.4.0), in Swissprot proteins database, with a peptide tolerance of 20 ppm, a fragment mass tolerance of 0.05 Da, and trypsin as digestive enzyme.

Using SCiLS Lab MVS 2019c Pro software, Principal Component Analysis (PCA) and Receiver operating characteristic (ROC) analysis were performed on MALDI-MSI mass spectra.

Results

A total of 382 mouse proteins were identified with LC-ESI-MS/MS, 75 of which resulted involved in key ovarian functions: follicle growth (21), oocyte maturation (9), ovulation (5), oocyte developmental competence (26), fertilisation (3), luteolysis (1), angiogenesis (1) and ovary pathologies (9).

Figure 1 shows the eight main follicle types [2], their size in diameter and the number of follicles analysed with MALDI-MSI. At least 1,674 for T4 and up to 6,184 for T8 mass spectra were analysed.

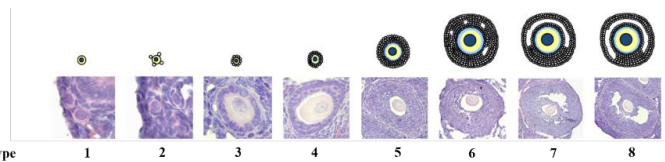

Follicle type	1	2	3	4	5	6	7	8
Diameter (µm)	15	20	30	60	100	150	300	400
Number of follicles	59	95	63	17	15	14	8	5

Fig. 1

PCA, first performed comparing the mass spectra of each follicle type (red dots) to the whole folliculogenesis (grey dots), showed a clusterisation of data in a specific region of the 3D representation, and suggested a shift in the spectra localisation from T5 to T8 (Figure 2).

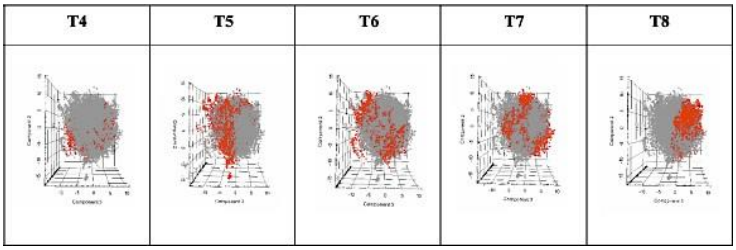

Fig. 2

When performed to compare the mass spectra of each individual follicle to those of its follicle class, PCA data clusterisation was well represented with the five T8 fully-grown follicles. Figure 3 shows the mass spectra of the whole T8 group (separated into large and small clouds of blue dots), and the single T8.1, T8.2 or T8.3 follicles (red dots) localised in the large blue cloud, T8.4 across the large and small clouds, whereas T8.5 was exclusively part of the small cloud.

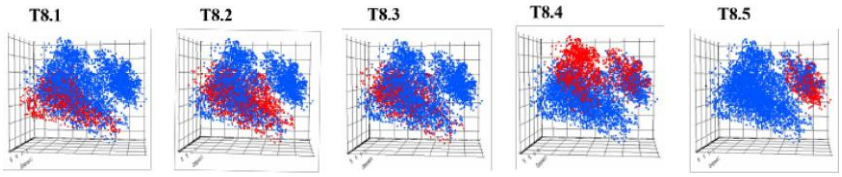

Fig. 3

ROC analysis of T8.1 (smallest in size) *vs* T8.5 (biggest in size) mass spectra, localised at the two most distant poles, highlighted the presence of 45 proteins differentially expressed ($p < 0.05$), 43 of which were up-regulated and 2 down-regulated. Of these, 10 are well known to be involved in key ovarian functions, including ALDOA, SMC1A, HYOU1 (follicle growth), LAMA2, NUCL (oocyte maturation), CSPG2 (ovulation), 1433T, DNMT1, FILIA and MATER (oocyte developmental competence).

Discussion/Conclusions

This study is the first to use MALDI-MSI on the mammalian ovary and represents proof-of-concept of the possibility to draw a map of the peptide content of each follicle type growing inside the gonad. The organ was entirely serially sectioned to allow the acquisition of information on the whole follicles throughout folliculogenesis, thus acquiring thousands mass spectra for each follicle type. Although PCA analysis summarised in Figure 2 suggests a changing profile of the peptide content during follicle growth from T5 to T8, this did not result significative with the ROC analysis applied, perhaps due to the intrinsic biological variability existing within and between growing follicle classes. Folliculogenesis, as most of differentiation processes, displays a continuum of molecular and physiological changes that, likely, the cytological classification used here [2] only partially takes into consideration. Instead, a strong significative difference was highlighted between T8 follicles, with 45 proteins clearly differentially expressed. This difference may be explained with the presence within the pre-ovulatory compartment of developmental competent or incompetent fully-grown follicles, which explains the up-/down- regulation of key maternal-effect proteins stored inside the oocyte and crucial for pre-implantation development.

References

1. A. Smith, et al.; *Journal of Proteomics*, 191 (2019), pp 114–123.
2. H. Peters; *Acta Endocrinologica*, 62 (1969), pp 98–116

Molecular portraits of diffuse large B-cell lymphoma: towards the discovery of novel phenotypes

A. Smith[1], A. Buzzi[1], G. Motta[2], F. Melle[2], V. Tabanelli[2], V. Denti[1], I. Piga[1], C. Chinello[1], D. Russo[3], S.A. Pileri[2] and F. Magni[1]

[1]University of Milano-Bicocca, Department of Medicine and Surgery, Clinical Proteomics and Metabolomics Unit, Vedano al Lambro, Italy, [2]Division of Diagnostic Haematopathology, European Institute of Oncology, IRCCS, Milan, Italy, [3]Department of Clinical and Experimental Sciences, University of Brescia, Brescia, Italy

Keywords: *MALDI-MSI; proteomics; lymphoma*

Introduction

Diffuse large B-cell lymphoma (DLBCL) is the most common lymphoid malignancy and can be considered a sort of "Pandora's box", with the disease encompassing a range of neoplasms which cannot be further classified using traditional histopathology. DLBCL are classified in two subgroups, activated B cells (ABC) and germinal centre B cells (GCB), depending on their cell of origin (COO) [1] and work is ongoing to discover further subgroups that can explain the heterogeneous outcomes in terms of patient outcome and sensitivity to targeted therapies [2].

Materials and Methods

MALDI mass spectrometry imaging was performed on FFPE tissue microarray cores from patients with ABC (n=16) and GCB (n=16) subtypes of DLBCLs. All mass spectra were acquired in reflectron positive mode, within the *m/z* 700 to 3000 range, using a rapifleX MALDI Tissuetyper™ (Bruker Daltonik GmbH, Bremen, Germany) MALDI-TOF/TOF MS equipped with a Smartbeam 3D laser operating at 2.5 kHz frequency. MALDI-MS images were acquired with a beam scan setting of 6 µm and a raster sampling of 10 µm in both x and y dimensions.
COO was determined by gene expression profiling using the NanoString nCounter Analysis System.

Results

Each core was histologically annotated in order to define the neoplastic cells and the tumour microenvironment (TME). When comparing the neoplastic cells of the ABC and GCB subtypes, 8 *m/z* signals were observed to have a differential intensity with an AUC $\geq$ 0.8 (2 ↑ in ABC; 6 up ↑ GCB). Considering the TME, a total of 43 *m/z* signals were observed to have a differential intensity (21 ↑ in ABC; 21 ↑ in GCB). Whilst those signals up-represented in ABC co-localised to both the stromal regions and neoplastic cells, those up-represented in GCB had a specific localisation within the TME and, in particular, in regions with an evident accumulation of extracellular matrix (ECM). This included proteins associated with ECM deposition such as fragments of collagen (CO1A2; *m/z* 852.41, CO1A1; *m/z* 1105.65) and fibrinogen (m/z 1117.63). Text 11 pts justified.

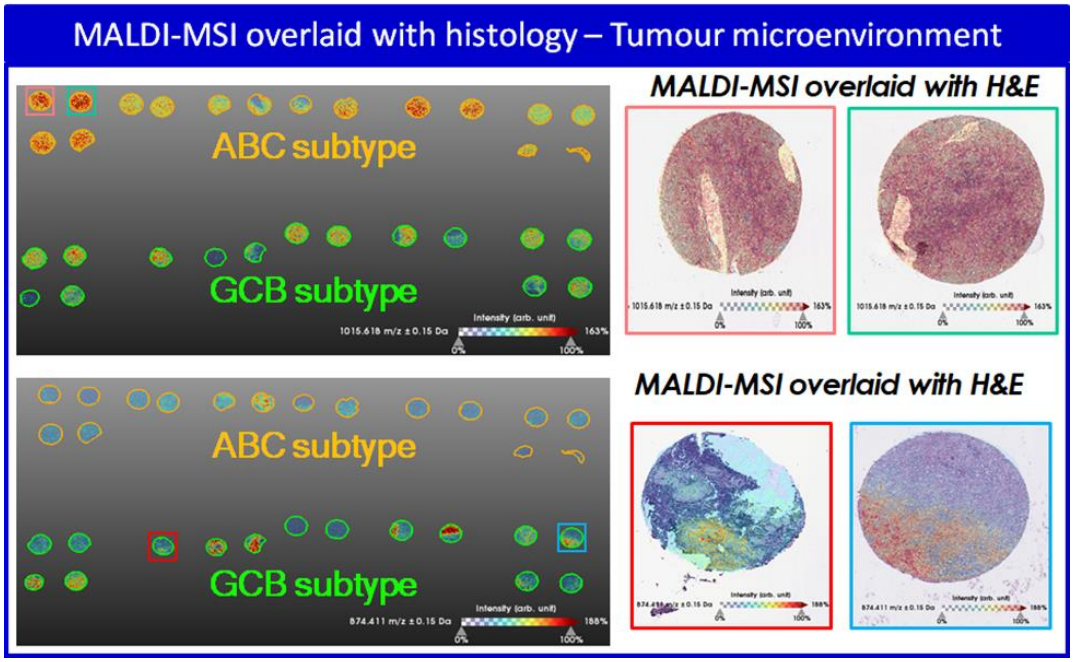

Fig. 2.. Exemplary MALDI-MS images overlaid with its hematoxylin and eosin stained counterpart. (Top, left)) the increased signal intensity of m/z 1015.62 (Alpha-1-antitrypsin) in ABC DLBCL and tissue distribution within both the stroma and tumour regions (right). (Bottom) the increased signal intensity of m/z 874.41 0 (Alpha-actinin 4) in GCB DLBCL and tissue distribution within TME regions represented by an accumulation of extracellular matrix or tissue scarring. Colour intensity scales are provided.

Discussion/Conclusions

This work highlights the utility of performing spatially resolved molecular imaging in the search for novel molecular subtypes of DLBCL and indicates specific protein signatures of the TME. Our final goal will be to integrate this proteomics data with that obtained using gene expression profiling to refine personalised medicine strategies in the treatment of DLBCL.

Funding

This work received funding from the 2019 Gilead Fellowship Program and Regione Lombardia POR FESR 2014-2020. Call HUB Ricerca ed Innovazione: ImmunHUB.

References

1. A. A. Alizadeh, M. B. Eisen, R. E. Davis et al. *Nature*. 2000; 403(6769): 503–11.
2. S. A. Pileri, M.C. Vegliante, S. Ciavarella *Oncotarget*. 2019; 18; 10(40): 3991–3993.

Molecular signatures of Hashimoto's thyroiditis liquid biopsies revealed by mass spectrometry imaging

***I. Piga*[1], G. Capitoli[2], F. Clerici[1], A. Mahajneh[1], V. Brambilla[3], S. Galimberti[2], F. Magni[1] and F. Pagni[3]**

[1]Proteomics and Metabolomics, School of Medicine and Surgery, University of Milano-Bicocca, Vedano al Lambro, Italy, [2]Bicocca Bioinformatics Biostatistics and Bioimaging B4 Center, School of Medicine and Surgery, University of Milano - Bicocca, Monza, Italy, [3]Department of Medicine and surgery, UNIMIB, Pathology, Monza, Italy

Keywords: *MALDI-MSI, Hashimoto's thyroiditis, proteomics*

Introduction

Hashimoto's thyroiditis (HT), also known as chronic autoimmune thyroid disorder, is the most common cause of hypothyroidism worldwide. It is caused by antibodies-mediated immune processes that attack and damage thyroid cells, with diffuse lymphoplasmacytic infiltration (B and T lymphocytes cells) and progressive fibrosis. HT diagnosis is often challenging and based on a combination of serological, ultrasound examinations and cytological tests. However, its etiology and pathogenesis remain so far unclear and its progression to hypothyroidism is often associated with papillary thyroid carcinoma, requiring further, even surgical, treatments.

Matrix-assisted laser desorption/ionisation mass spectrometry imaging (MALDI-MSI) is a powerful tool to detect the proteomic signature and to spatially localize proteins directly on cytological samples.

Hence, the first aim of this study was to characterize the MALDI-MSI proteomic signature of both lymphocytes and epithelial cells from fine needle aspiration (FNA) samples of Hashimoto's thyroiditis. Then we combined MALDI-MSI data with supervised and unsupervised statistical approaches in order to compare HT with hyperplastic (Hp) and papillary thyroid carcinoma (PTC) proteomic profiles.

Materials and Methods

Real thyroid FNAs were collected from patients (San Gerardo Hospital, Monza, Italy) and transferred into CytoLyt solution, centrifuged and re-suspended in PreservCyt solution [1]. Cytospin spots have been positioned onto conductive slides and MALDI-MSI proteomics analysis was performed within the mass range 3,000–20,000 *m/z*, using an ultrafleXtreme MALDI-TOF/TOF. Regions of interest (ROIs) containing pathological areas (thyrocytes clusters and lymphocytes regions) were comprehensively annotated by pathologist. A pixel-by-pixel based statistical approach was used and a cohort of 27 patients (9Hp, 9 PTC and 9 HT) was included in the training phase. Further 16 patients (3 Hp, 8 HT and 5 PTCs) were used for validation.

Results

MALDI-MSI underlines different proteomic profiles for lymphocytes and epithelial cells in HT samples, with one signal specifically localized in the inflammatory background and one localized in thyrocytes cells regions. Moreover specific proteomic signatures were obtained when comparing HT, Hp and PTC cytological samples. The unsupervised principal component analysis (PCA) highlights three clusters, with a clear separation between PTC and Hp, and a slight overlap between Hp and HT groups. This similarity does not surprise, in fact, thyrocytes cells in Hp and HT samples share common morphological characteristics, but differences are related with the abundant inflammatory background of HT samples. Finally a pixel-by-pixel based statistical approach built on the three classes HT, Hp and PTC confirmed that HT lesion belongs to the group of benign lesions but with peculiar signature characteristics of the lymphocytic background.

Discussion/Conclusions

The present study introduces an original methodological approach to build a proteomic diagnostic tool in thyroid cytopathology by taking advantage of MALDI-MSI technology and its capability to discriminate specific signatures of different cellular components, preserving both proteins spatial localization and the morphology of the cytological sample. The next step will be to further integrate these preliminary results,

with the identification of statistically-relevant HT signals in order to be potentially used in the future for diagnosis, follow-up, personalized treatments and for the management of Hashimoto's thyroiditis patients.

Acknowledgments

This work was funded thanks to AIRC (Associazione Italiana per la Ricerca sul Cancro) MFAG GRANT 2016 - Id. 18445 and from Regione Lombardia POR FESR 2014-2020. Call HUB Ricerca ed Innovazione: ImmunHUB.

References

1. I. Piga et al; *Proteomics Clinical Application*, 13 (2019), 1700170.

HILIC-ESI-MS with All Ion Fragmentation (AIF) Scans for a high throughput lipidomic strategy

***G. Ventura*[1], *M. Bianco*[1], *C. D. Calvano*[2,3], *I. Losito*[1,2] *and T. R. I. Cataldi*[1,2]**

[1]Department of Chemistry, University of Bari Aldo Moro, via Orabona 4, 70126 Bari, Italy; [2] SMART Inter-Departmental Research Center, 70126 Bari, Italy [3] Department of Pharmacy-Drug Sciences, University of Bari Aldo Moro, via Orabona 4, 70126 Bari, Italy

Keywords: *lipidomics, HILIC-ESI-MS, All Ion Fragmentation*

Introduction

Phospholipids (PL) play different but essential roles in biological systems [1, 2], so their description, in terms of intact molecules and class including linked fatty acids (FA) composition, is fundamental. The examination of fatty acyl chains is typically performed using a preliminary PL extraction [3] followed by derivatization and gas chromatography (GC) with mass spectrometry (MS) detection [4]. The conversion to volatile and thermally stable products is time-consuming since long reaction times are required, and sample loss is possible. Furthermore, at least two different strategies are required to obtain information on both intact phospholipids and fatty acid composition of each lipid class.

Materials and Methods

Having high sensitivity, high selectivity along with good mass accuracy, scan speed, and dynamic range, hybrid quadrupole-orbital trap mass spectrometers are an interesting choice in lipidomic studies; such instruments enable the so-called all ion fragmentation (AIF) acquisition, a data-independent analysis in which all ionized molecules are fragmented without prior isolation of a selected precursor ion, already employed in lipidomics [5].

Liquid chromatography in lipid analysis represents a great advantage for complex mixtures. PL separation can be achieved by hydrophilic interaction liquid chromatography (HILIC) in which single peaks/bands are obtained almost corresponding to each specific PL class, thus minimizing the suppression effect between classes [6].

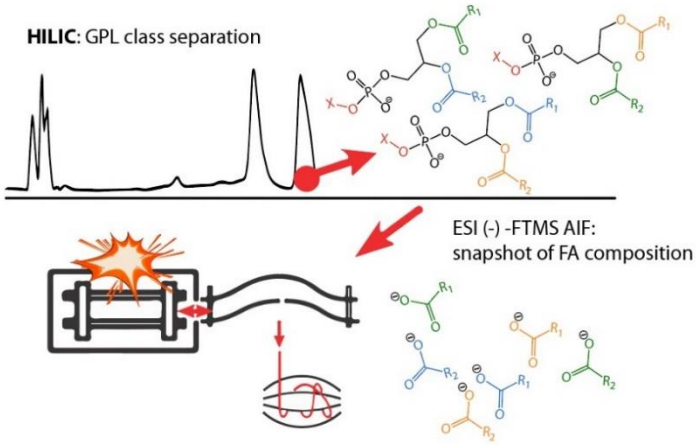

Fig. 3. HILIC-ESI-FTMS AIF scan acquisitions, in negative ion mode, allow to obtain information on linked fatty acyl chains of a specific lipid class.

Results

According to the adopted ESI polarity, HILIC-ESI MS using AIF analyses can be exploited to identify two important features of PL; while the polar head can be inferred in both polarities, the fatty acyl chain composition of each PL class can be attained in negative ion mode. Such an identification of carboxylate anions can be obtained without recurring to prior chemical derivatization of PL, e.g., generation of FAME followed by GC-MS analysis [7], so really speed up the whole lipidomic investigation.

Discussion/Conclusions

Firstly, the advantages of HILIC-ESI-FTMS by AIF scans were assessed on a mixture of class-specific phospholipid standards and then proved on different real samples, namely the lipid extracts of human peripheral blood mononuclear cells and dermal fibroblasts for biomarker discovery purposes, and human plasma and food samples through an effortless characterization of linked fatty acyl chains. These results confirmed that the combination of AIF scan and HILIC separation can be a reproducible and helpful tool in both targeted and untargeted lipidomics, thus improving the biological information gained in just one run.

References

1. J. Wang, C. Wang, X. Han; *Anal. Chim. Acta.* 1061 (2019), 28–41.
2. X. Han; *Nat. Rev. Endocrinol.* 12 (2016), 668–679.
3. B. Fuchs, R. Süß, K. Teuber, M. Eibisch, J. Schiller; *J. Chromatogr. A.* 1218 (2011), 2754–2774.
4. I. Brondz; *Anal. Chim. Acta.* 465 (2002), 1–37.
5. S. Eliuk, A. Makarov; *Annu. Rev. Anal. Chem.* 8 (2015), 61–80.
6. I. Losito, R. Patruno, E. Conte, T.R.I. Cataldi, F.M. Megli, F. Palmisano; *Anal. Chem*, 85 (2013), 6405–6413.
7. G. Ventura, M. Bianco, C.D. Calvano, I. Losito, T.R.I. Cataldi; *Molecules*, 25 (2020), pp 2310.

Capillary Flow LC-MS Using Micro Pillar Array Columns: Combining Nano Flow Sensitivity with Analytical Flow Robustness and Throughput for Bottom-Up Proteomics

***C. Mitterer*[1], *G. V. Raemdonck*[1], *J. Op De Beeck*[1], *P. Jacobs*[1] *and G. Desmet* [2]**

[1]PharmaFluidics, Ghent, Belgium, [2] Vrije Universiteit Brussel, Brussels, Belgium

Keywords: *capillary flow LC-MS, high-throughput proteomics, Micro Pillar Array Columns*

Introduction

Mass-spectrometry based proteomics has become an essential tool in biological, biomedical and biopharmaceutical research. Due to the increased sensitivity that can be achieved compared to analytical flow LC-MS, the majority of LC-MS based proteomics research is performed within the nanoflow LC regime, with flow rates typically below 1 µL/min and total run times exceeding 60 min. Compared to the LC-MS methods employed in other 'omics' fields, the need for separation power often prevails over sample throughput, making relatively long separations the gold standard in LC-MS based proteomics. However, capillary and microflow LC-MS solutions are recently gaining interest as the demand for large quantitative studies with increased throughput and robustness is growing and the sensitivity of MS instrumentation has increased significantly.

Materials and Methods

A micro pillar array column-based solution for capillary flow LC-MS is presented in this work. Compared to the nanoflow compatible pillar array formats, an increase in effective channel cross section close to 5-fold has been accomplished without affecting chromatographic separation performance. Chromatographic performance for alkylphenones and tryptic peptides was benchmarked against several state-of-the art packed bed alternatives (0.3 mm diameter, 150 mm length, 1.7/2/3 µm diameter C18 functionalized particles) using both data dependent and data independent ms acquisition methodologies. The performance was evaluated over the entire capillary flow range (1-10 µL/min) for solvent gradients ranging from 10 to 120 min in length.

Results/Conclusions

Using optimal LC methods for a variety of LC-MS based proteome analysis needs, the recently launched PharmaFluidics' µPAC™ capLC column provides versatile output in terms of separation performance and throughput. As a consequence of the low column back pressure, the column can be operated over a range of flow rates, enabling analytical scientists to tune LC methods according to the sample complexity or to the size of the sample set. Three common separation needs in LC-MS proteome research have been identified and tailored LC methods with optimal output in terms of data productivity and sensitivity have been developed. For large sample sets where maximum throughput is required, a high flow rate method with a sample turnover rate of 65 samples per day is advised. By operating the µPAC™ capLC column at a flow rate of 10 µL/min and running a 17.5 min solvent gradient, total overhead time (including sample pick up, column void time and column equilibration) can be reduced to 17% of the total analysis time, leaving 83% of the total time available for data generation. When looking for medium throughput but maximum data productivity, a routine LC program is advised that combines increased sensitivity with increased separation power. At a flow rate of 5 µL/min, column void time increases, but the relative contribution of overhead time can be reduced by applying longer solvent gradients (54 min), which yields a sample turnover rate of 24 samples per day with 89% of effective MS time use. By increasing the gradient duration even further, this could even approach 97%. However, the maximum outcome in terms of chromatographic performance and subsequent peptide/protein group identifications would not be achieved. When comprehensive analysis with no limit on time consumption per sample is at hand, lowering the flow rate even further to 2 µL/min will give the best results. Comprehensive proteome analysis using a 108 min solvent gradient at a sample turnover rate of 12 samples per day results in maximum peak capacity (335 measured at peak base) and the highest sensitivity (more efficient electrospray ionization at lower flow rates). In addition to the flexible operation benefits, the perfect order and unique control of stationary phase design result in excellent chromatography

at the highest level of LC reproducibility. With peptide retention time variation of respectively 0.75s (0.12%), 1.13 s (0.08%) and 1.81s (0.07%), a set of exceptionally reproducible, robust and versatile LC-MS based proteomics workflows is demonstrated.

SWATH-MS based label-free quantitative analysis to investigate the proteomic effects of lactic acid bacteria on keratinocytes

J. Brandi[1], S. Cheri[2], M. Manfredi[3], C. Di Carlo[1], F. Federici[4], E. Rizzi[4], L. Manna[4], U. Marini[4], M. T. Valenti[2], E. Marengo[5] and D. Cecconi[1]

[1]Department of Biotechnology, Proteomics and Mass Spectrometry Laboratory, University of Verona, 37134 Verona, Italy, [2]Department of Medicine, Section of Internal Medicine D, University of Verona, Verona 37134, Italy, [3]Department of Translational Medicine and Center for Translational Research on Autoimmune Diseases, University of Piemonte Orientale, Novara, Italy, [4]Sintal Dietetics s.r.l., Castelnuovo Vomano, Teramo, Italy, [5]Department of Sciences and Technological Innovation, University of Piemonte Orientale, Alessandria, Italy;

Keywords: *keratinocytes; lactic acid bacteria; proteomics*

Introduction

The human skin is the largest organ of the body, involved in a variety of functions which acts mainly as a protective barrier preventing the entry of potential pathogens. It is densely colonized with a complex microbial community also referred as "microbiota". In particular, skin homeostasis is regulated by microorganisms, which act on keratinocytes and on their cytokine release, make certain the good state of skin health [1]. The alteration of skin homeostasis is often the consequence of infections of wounds and of inflammatory diseases, such as dermatitis, acne, or psoriasis.

Different studies have demonstrated that the topical application of lactic acid bacteria (LAB) can improve skin health or combat skin diseases [2, 3]. Therefore, the present study was performed to investigate the proteomics effects on keratinocytes treated with LAB strains by using a label free strategy based on SWATH-MS. In particular, the human HaCaT keratinocytes treated with six different LAB including *Lactobacillus paracasei* SGL 04, *Lactobacillus plantarum* SGL 07, *Lactobacillus fermentum* SGL 10, *Lactobacillus brevis* SGL 12, *Lactobacillus casei* SGL 15 and *Lactobacillus salivarius* SGL 19, were analyzed by proteomics.

Materials and Methods

Before proteomics, in order to assess the effects of LAB on wound healing, scratch, migration, and proliferation assays were performed on HaCaT cells after exposure to LAB lysates. The LAB anti-inflammatory effect was also evaluated measuring secreted cytokines by multiplex technology. Then, in order to elucidate the molecular mechanisms underlying the effects of LAB induced on keratinocytes, a proteomic analysis was carried out using high resolution mass spectrometry (SWATH-MS). Moreover, to characterize the function of proteins identified by quantitative proteomics analysis, gene ontology (GO) annotation and pathway enrichment analyses were performed [4].

Results and Discussion

The results obtained demonstrated that the six selected LAB lysates increase the proliferation and migration of keratinocytes, and that certain LAB lysates, improve the closure of wounds, a property which can be connect to their induction effect on keratinocyte migration. In addition, all the LAB lysates significantly reduced the release of the pro-inflammatory cytokines and chemokines from keratinocytes. Then a label-free quantitative proteomics analysis was conducted for studying alterations in protein abundances and understanding the mechanisms responsible for the wound healing and the anti-inflammatory effects of LAB on keratinocytes. We identified a total of 1154 proteins, and among them 162, 229, 196, 291, 158, and 138 proteins were found differentially expressed in the six LAB treated keratinocytes compared to the control. Gene ontology annotation of deregulated proteins revealed that most of the deregulated proteins were either cytoplasmic or secreted proteins. In addition, by using Reactome database we found that the dysregulated proteins of HaCaT cells were highly associated with pathways that can be mainly related to the anti-inflammatory effect of LAB (i.e. neutrophil degranulation, immune system, infectious disease, interleukin-1 signalling, cytokine signalling in immune system).

Furthermore, the proteomics analysis indicated that the LAB lysates induced the keratinocyte expression of protein-arginine deiminase type-1, a fundamental protein for the wound closure and modulated the

expression of two proteins which play a key role in cellular migration such as the focal adhesion kinase 1 (PTK2, also known as FAK) and the S100-A2 (S100A2).

Conclusions

In conclusion, the SWATH-MS proteomic analysis highlight that, LAB lysates could be useful to improve skin health. Indeed, the data obtained elucidated the molecular mechanism involved in the LAB effects on keratinocytes, and further highlights the importance of LAB lysates for preparation of skincare products based on probiotic lysates.

References

1. M. Egert, R. Simmering, and C.U. Riedel, *Clin Pharmacol Ther*, 102 (2017), pp. 62-69.
2. M.R. Roudsari, et al., *Crit Rev Food Sci Nutr*, 55 (2015), pp. 1219-40.
3. R. Knackstedt, T. Knackstedt, and J. Gatherwright, *Exp Dermatol*, 29 (2020), pp. 15-21.
4. J. Brandi et al, *J Am Soc Mass Spectrom*, 30 (2019), pp. 1690- 1699.

Energy metabolism and its role in neuroblast differentiation

M. Audano[1], S. Ligorio[1], S. Pedretti[1], M. Crestani[1], E. De Fabiani[1], D. Caruso[1] and N. Mitro[1]

[1]Dipartimento di Scienze Farmacologiche e Biomolecolari (DiSFeB), Università degli Studi di Milano, Milano,Italy.

Keywords: *metabolomics, fluxomics, neuro2a*

Introduction

Mitochondria are ubiquitous and multi-functional organelles involved in several cellular processes, such as energy production and synthesis of metabolites, hence regulating vital functions. During the developmental process, cells change their metabolic states to support cellular differentiation. Therefore, cells need a substantial amount of energy to cope with the newly established homeostasis that they have acquired. Generally, during differentiation cells shift to a more oxidative metabolism, thus mitochondrial function and biogenesis are boosted [1]. However, little is known about the driving role of energy metabolism during the last step involving the differentiation from neuroblast to mature neuron. In light of these premises, we investigated the role of central metabolism in the final step of neuron maturation.

Materials and Methods

Neuro2a (N2a) cells were used as model to study neuroblast differentiation. These cells can be differentiated using a medium supplemented with 1% of FBS. Steady state metabolomic analyses were performed with a liquid chromatography/tandem mass spectrometry (LC-MS/MS) on an API-4000 triple quadrupole mass spectrometer (AB Sciex) coupled with a HPLC system (Agilent). Quantification of different metabolites was performed using a C18 column (Biocrates) for amino acids, a Pursuit XRs Ultra 2.8 Diphenyl column (Varian) for acyl-carnitine and cyano-phase LUNA column (Phenomenex) for energetic metabolites, respectively. Metabolomic data were normalized by the sum of all detected ions in each sample [4]. For metabolic tracing analyses, N2a cells were exposed for 24h to [U-$^{13}C_6$]-Glucose 1 mM or [U-$^{13}C_5$]-Glutamine 2 mM or [U-$^{13}C_{16}$]-Palmitate 100µM. Metabolite isotopomer quantification was performed as described above. Statistical analysis of steady state metabolomics was obtained through MetaboAnalyst 4.0 webtool.

Results

In order to unravel the role of mitochondria and metabolism in Neuro2a (N2a) cell differentiation, we used a gene independent approach to alter mitochondrial function. N2a cells were treated for 30 days with a low dose of ethidium bromide (EtBr, 100ng/ml). As expected, EtBr-treated N2a exhibit impaired mitochondrial function associated to reduced mitochondrial DNA transcription and lower oxidative phosphorylation (Oxphos) protein expression. Given the tight relationship between mitochondria, metabolism, and cell differentiation, we then analyzed the intracellular metabolite levels. To capture early changes that may act as drivers of the observed phenotype, we conducted LC-MS/MS steady-state metabolomics in undifferentiated Wild-type and Oxphos-deficient N2a. Principal component analysis significantly discriminated the Wild-type cell population from that of N2a treated with EtBr, while steady-state measurements indicated that among 58 analyzed metabolites, 18 were significantly changed [fold change > 1.5; FDR < 0.1] in EtBr-treated neuroblasts compared to Wild-type cells. Specifically, reduced metabolites mainly belong to glycolysis, pentose phosphate pathway and tricarboxylic acid (TCA) cycle intermediates, while 6 out of 9 increased metabolites were acyl-carnitines. These data suggest that neuroblasts with dysfunctional mitochondria exhibit impaired glycolysis and amino acid metabolism. The increased levels of several carnitines strongly suggest a preferential use of fatty acids. Metabolic flux analysis confirmed that EtBr-treated cells depend on fatty acid oxidation and indicate a causal link between β-oxidation activity and the differentiation state of neuroblasts. To further confirm the tight relationship between energy metabolism and neuroblast differentiation, we treated N2a cells with metabolic inhibitors such as UK5099 (50µM), CB839 (4µM) and Etomoxir (20µM), targeting the mitochondrial pyruvate carrier, glutaminase I and carnitine-palmitoyl transferase 1a, respectively. LC-MS/MS steady state metabolomics and metabolic flux analyses confirmed that impaired fatty acid oxidation is associated to increased N2a differentiation state, while impaired mitochondrial pyruvate and glutamine metabolisms inhibited neuroblast maturation to neurons. Interestingly, flux analyses demonstrated that UK5099-treated cells compensated the metabolic deficiency by upregulating glutamine metabolism, while CB839-treated cells increased glucose consumption

to sustain energy metabolism. Nevertheless, either UK5099- or CB839-treated cells were unable to sustain the correct differentiation of N2a cells.

Discussion/Conclusions

In conclusion, our results demonstrate that *i)* mitochondria are key organelles for neuroblasts maturation to neurons, *ii)* that fatty acid β-oxidation is causally associated to an undifferentiated state of N2a cells and *iii)* that glucose and glutamine metabolisms cooperate to replenish the metabolic intermediates and to sustain the energy demand during the differentiation program.

References

1. M. Khacho, R. Harris, R.S. Slack, *Nat. Rev. Neurosci.* 20 (2019), pp. 34–48,
2. X. Zheng, L. Boyer, M. Jin, J. Mertens, Y. Kim, L. Ma, M. Hamm, F.H. Gage, T. Hunter, *Elife* 5 (2016)
3. M. Agostini, F. Romeo, S. Inoue, M. V Niklison-Chirou, A.J. Elia, D. Dinsdale, N. Morone, R.A Knight, T.W. Mak, G. Melino, *Cell Death Differ.* 23 (2016), *pp.* 1502–1514,
4. M. Audano, S. Pedretti, M. Crestani, D. Caruso, E. De Fabiani, N. Mitro, *FEBS Lett.* (2019).

Metabolomic approaches to investigate the role of the mitochondrial regulator Zc3h10 in adipocytes.

S. Pedretti[1], M. Audano[1], S. Ligorio[1], E. De Fabiani[1], M. Crestani[1], D. Caruso[1] and N. Mitro[1]

[1]Dipartimento di Scienze Farmacologiche e Biomolecolari (DiSFeB), Università degli Studi di Milano, Milano, Italy.

Keywords: *Metabolomic, Fluxomic, metabolism*

Introduction

We characterized the protein zinc finger CCCH-type containing 10 (Zc3h10) as a new mitochondrial regulator and we validated its role during myoblasts differentiation [1]. Mitochondria play a crucial role in many cellular processes and they are essential organelles for the health of the cell. Beyond their contribution to energy production, they are key regulators of tissue development and cell differentiation. The aim of this study is to validate the role of Zc3h10 during adipocytes differentiation.

Materials and Methods

C3H/10T1/2 cell line (mesenchymal stem cells) can be differentiated into white adipocytes using a specific adipogenic cocktail. Quantification of different metabolites was performed with a liquid chromatography/tandem mass spectrometry (LC-MS/MS) on an API-4000 triple quadrupole mass spectrometer coupled with a HPLC system using a C18 column for amino acids, Pursuit XRs Ultra 2.8 Diphenyl for acyl-carnitine and cyano-phase LUNA column for energy metabolites.

Results

Zc3h10 protein levels increase during C3H/10T1/2 differentiation. Zc3h10 depletion significantly reduce adipocyte differentiation and mitochondrial activity. To demonstrate that Zc3h10 impacts mitochondrial function and metabolism, we performed metabolomic analysis at two different stage of adipocytes differentiation (day 3 = early phase and day 9 = terminal phase). We evaluated the intracellular levels of by-products belonging to the main metabolic pathways: glycolysis, tricarboxylic acid (TCA) cycle, pentose phosphate pathway (PPP), amino acids and acyl-carnitines using LC-MS/MS. Steady-state metabolomics indicated that Zc3h10 depleted pre-adipocytes (day 3) showed decreased levels of PPP intermediates and of several TCA cycle metabolites, while various amino acids and acyl-carnitines were increased compared to control group. Zc3h10 silenced mature adipocytes (day 9) showed a more altered metabolic profile than pre-adipocytes characterized by decreased NAD^+/NADH ratio, reduced levels of acetyl-CoA, malate, citrate, and fumarate and increased levels of several acyl-carnitines and of glutamate. We also used metabolic tracers ([U-$^{13}C_6$]-glucose, [U-$^{13}C_{16}$]-palmitate or [U-$^{13}C_5$]-glutamine) to confirm that the flow of energy substrates into the TCA cycle is affected by Zc3h10 silencing at both considered time points.

Discussion/Conclusions

Our results indicate that Zc3h10 expression increases during murine white adipocyte differentiation. Furthermore, Zc3h10 silencing in white preadipocytes and adipocytes deeply impaired mitochondrial function, decreased adipogenic potential and altered metabolic profile.

References

1. M. Audano, S. Pedretti, G. Cermenati, E. Brioschi, G.R. Diaferia, S. Ghisletti, A. Cuomo, T. Bonaldi, F. Salerno, M. Mora, L. Grigore, K. Garlaschelli, A. Baragetti, F. Bonacina, A.L. Catapano, G.D. Norata, M. Crestani, D. Caruso, E. Saez, E. De Fabiani, N. Mitro, *EMBO Reports*, Mar 5 (2018), pii. e45531.

Multi-omics analysis of Panc-1 pancreatic cancer stem cells to investigate their metabolism

C. Di Carlo[1], J. Brandi[1], G. Ambrosini[2], E. Dalla Pozza[2], G. Fanelli[3], M. Manfredi[4,5], S. Rinalducci[3], M. Palmieri[2], I. Dando[2], E. Marengo[4,6] and D. Cecconi[1]

[1]Department of Biotechnology, University of Verona, 37134, Verona, Italy, [2] Department of Neurosciences, Biomedicine and Movement Sciences, University of Verona, 37134, Verona, Italy, [3] Department of Ecological and Biological Sciences, University of Tuscia, 01100, Viterbo, Italy, [4] ISALIT, Spin-off of Department of Sciences and Technological Innovation, University of Piemonte Orientale, Alessandria, Italy, [5] Center for Translational Research on Autoimmune & Allergic Diseases – CAAD, Novara, Italy, [6] Department of Sciences and Technological Innovation, University of Eastern Piedmont, Alessandria, Italy

Keywords: *pancreatic ductal adenocarcinoma; cancer stem cells; mass spectrometry.*

Introduction

Pancreatic ductal adenocarcinoma (PDAC) is the fourth leading cause of cancer-related death worldwide. This pathology is asymptomatic at early stages, so its promptly detection is fundamental to reduce mortality and to improve survival rate of patients. The high rate of PDAC is mainly due to the presence of a small subset of cells with very aggressive features, called pancreatic cancer stem cells (PCSCs), which are responsible to drive tumorigenesis and disease recurrence [1]. Hence, a great effort is being devoted to developing therapies targeting PCSCs in PDAC. It is known that PCSCs possess peculiar metabolic properties that distinguish them from the bulk of the tumour and that such biochemical features may constitute a basis for the development of new therapeutic strategies addressed to PCSC elimination. However, although many attempts have been made to delineate the metabolic features of PCSCs, it is not yet clear whether CSCs preferentially rely on a more glycolytic or oxidative metabolism in comparison to differentiated tumour cells [2]. We have previously shown that CSCs derived by the PDAC cell line Panc1 cultured for short periods preferentially rely on glycolysis, fatty acid synthesis, and mevalonate pathways [3]. In this study, a label free strategy based on SWATH-MS analysis was adopted to perform proteomic and metabolomic comparison between parental cells (P) and PCSCs derived from Panc1 PDAC cells, respectively. The investigation of CSCs proteome and metabolome alterations is extremely important to clarify the deregulated pathways involved in PDAC and possible to suggest new targets that can be useful for the development of novel strategies against PDAC.

Materials and Methods

The Panc-1 CSCs (at 2-, 4-, and 8-weeks subculture) and relative parental cells were grown and cultivated. Briefly, to investigate the proteomic and metabolomic profile of PCSCs as compared to parental cells LC-MS/MS analysis were applied, using a TripleTOF 5600 High Resolution Accurate Mass System (AB Sciex) instrument and Q Exactive™ HF Hybrid Quadrupole-Orbitrap Mass Spectrometer (Thermo Fisher Scientific) instrument, respectively. Bioinformatic analyses were performed for the integration of the omics datasets and detection of deregulated pathways of PCSCs. The dysregulated proteins and metabolites of PCSCs were analysed for assignment to KEGG and Reactome database and MetaboAnalyst 4.0, respectively.

Results

The results obtained indicated peculiar metabolic differences among the PCSCs grown for different weeks. We focused on the main energy metabolism-related pathways, including glycolysis, pentose phosphate pathway (PPP), tricarboxylic acid cycle (TCA) (i.e. citrate) and electron transport chain. Among the TOP 10 KEGG enriched pathways that characterized all the PCSCs (at 2-, 4- and 8-weeks of culture) it was possible to observe that the upregulated proteins were involved in oxidative phosphorylation and TCA cycle, while the downregulated proteins were mainly involved in glycolysis/gluconeogenesis. Reactome pathway enrichment analyses indicated an induction of proteins involved in respiratory electron transport in all PCSCs as compared to parental cells, with a dysregulation that increased from 2 to 8 weeks of culture. Interestingly, multi-omics analysis showed that TCA cycle (i.e. citrate; 2-oxoglutarate) and OXPHOS were particularly induced in PCSCs at 4

weeks as compared to PCSCs 2 and 8 weeks. Whilst, glycolysis/gluconeogenesis (i.e. glucose 6-phosphate; phosphoenolpyruvate) and PPP, resulted more induced in PCSCs at 2 weeks as compared to 4- and 8- weeks.

Discussion/Conclusions

The data integration suggested that long-term cultured PCSCs (8 weeks) diminished their metabolic requirements as compared to lower-term cultured PCSCs (2- and 4-weeks). In addition, PCSCs changed their metabolic arrangement as compared to parental cells, due the induction of OXPHOS and TCA metabolic pathways and a decrease of glycolysis intermediates. Accordingly, proteomics revealed an induction of proteins involved in respiratory electron transport in all PCSCs as compared to parental cells, particularly at 4 weeks. The multi omics data here obtained, imply that PCSCs at 2 weeks preferred a glycolytic metabolism, PCSCs at 4 weeks relied on a more oxidative metabolism, while PCSCs at 8 weeks had significant lower levels of metabolites and proteins, suggesting a more quiescent status.
Altogether these data suggested that, during progressive de-differentiation, PCSCs shift from a more glycolytic to a more oxidative metabolism, accomplishing at 8 weeks of culture a global reduced metabolism together with the acquisition of a quiescent status.
In summary, the dysregulated metabolites and proteins here identified add an important piece of knowledge for the comprehension of the metabolic features of PCSCs and may suggest potential targets for the development of new effective therapeutic approaches.

References

1. C. Di Carlo, J. Brandi, and D. Cecconi, *World Journal of Stem Cells*, 10 (2018).
2. I. Dando, E. Dalla Pozza, G. Biondani, M. Cordani, M. Palmieri, and M. Donadelli, *IUBMB Life*, 67 (2015), pp. 687–693.
3. J. Brandi et al., *Journal of Proteomics*, 150 (2017), pp. 310–322.

Food

LC-MS based metabolomic study of *Salvia officinalis* L. leaves treated with different bio-fertilizers and foliar applications of L-phenylalanine

M. R. Samani[1], G. D'Urso [2], P. Montoro[2], A. G. Pirbalouti[3] and S. Piacente [2]

[1]Medicinal Plants Department, Shahrekord Branch, Islamic Azad University, Shahrekord, Iran, [2] Department of Pharmacy, University of Salerno, Via Giovanni Paolo II, 84084, Fisciano, SA, Italy, [3] Research Center for Medicinal Plants, Shahr-e-Qods Branch, Islamic Azad University, Tehran, Iran

Keywords: *Salvia officinalis, metabolomics approach, bio-fertilizers*

Introduction

Sage leaves (*Salvia officinalis* L.) are commonly used as a condiment in food but mainly as a raw material in medicine and perfumery industries [1]. Nowadays, attention to biological fertilizer has been increasing due to the good features such as maintenance of soil health and reduction of environmental pollution promoting sustainable agricultural systems [2]. *Arbuscular mycorrhizal* fungi species and plant growth promoting rhizo-bacteria are considered as two important components of bio-fertilizers.
To determine the effects of bio-fertilizers and foliar applications of L-phenylalanine on specialized metabolites and biochemical characteristics of the sage leaves, a field experiment in a 2-year study (2016 and 2017) was carried out according to a combined design in Southwestern Iran. The treatment included herbage spray levels of L-phenylalanine and diverse bio-fertilizers, including control (C); inoculation of *Arbuscular mycorrhizal* fungi species (AM); inoculation of *Pseudomonas fluorescen*s (Pf); and combined inoculation of fungi and bacteria (AM + Pf) applied to plants under normal conditions.

Materials and Methods

A metabolomic approach was performed on the ethanolic extract of sage leaves by using Liquid Chromatography coupled with high-resolution mass spectrometry (LC-ESI/LTQOrbitrap/MS) followed by Multivariate Data Analysis and phytochemical characterization. After collection, *Salvia officinalis* leaves coming from different treatment of bio-fertilizers were freeze-dried and extracted with a mixture of ethanol / water (70: 30, v/v). Extracts were chromatographically separated on a Luna C18 5 µm (150x2.1mmm) (Phenomenex Aschaffenburg, Germany) column. The analyses were performed in negative ion mode by using a Linear Ion Trap-Orbitrap hybrid mass spectrometer (LTQ-Orbitrap XL, Thermo Fisher Scientific, Bremen, Germany) with electrospray ionization.

Results

Different specialized metabolites mainly belonging to organic acids, phenylpropanoids, flavonoids, diterpenes, salvianolic acid, and oxylipins were putatively identified by their accurate mass, fragmentation pattern and comparing data present in literature and databases. Multivariate Data Analysis by using the projection methods Principal Component Analysis (PCA) and Partial Least Square-Discriminant Analysis (PLS-DA) allowed us to classify the different treated samples.

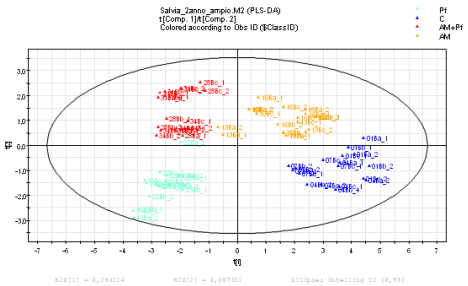

Fig. 4. Partial Least Square- Discriminant Analysis, Score Scatter Plot colored according to the treatment (Control (C), inoculation of Arbuscular mycorrhizal fungi (AM), inoculation of Pseudomonas fluorescens (Pf) and combined inoculation of fungi and bacteria (AM+Pf))

Discussion/Conclusions

In conclusion, with the present study it was possible to ascertain that foliar application of L-phenylalanine along with the inoculation of an equal mix of *Arbuscular mycorrhizal* fungi and *P. fluorescens* can improve production of phenolic metabolites of sage in biological and sustainable agriculture systems. Moreover, these results promote the use of bio-fertilizers in improving the specialized metabolites of *S. officinalis* to be used for pharmaceutical purpose.

References

1. E. Poulios, C. Giaginis, G. K.Vasios; *Planta Medica*, 86 (2020), pp 224-238.
2. M. Rahmani Samani, A. Ghasemi Pirbalouti, F. Moattard, A. Reza Golparvar*; Industrial Crops and Products*, 137 (2019), pp 1-8.

Arsenosugar phospholipids in marine algae extracts and their regiochemical assignment by regioselective hydrolase enzymes and LC-ESI tandem MS

D. Coniglio[1], C.D. Calvano[2,3], G. Ventura[1], I. Losito[1,3] and T.R.I. Cataldi[1,3]

[1]Department of Chemistry, University of Bari Aldo Moro, via Orabona 4, 70126 Bari, Italy; [2]Department of Pharmacy-Drug Sciences, University of Bari Aldo Moro, via Orabona 4, 70126 Bari, Italy; [3]SMART Inter-Departmental Research Center, 70126 Bari, Italy

Keywords: *algae, arsenosugar phospholipids, LC-MS*

Introduction

Aquatic algae are plant organisms that populate seas, rivers, lakes, and ponds around the world, often living on rocks and on damp soils. Tasty and rich in benefits, algae have been consumed since ancient times and have been the subject of numerous studies of both biological and chemical interest. Currently, there is a great demand for healthy and natural foods and edible algae represent an interesting answer. Edible marine algae are nowadays proposed as supplements to our daily diet or alternatively as an excellent ingredient for soups and salads, being toned, emollient, anti-infective and antioxidant, rich in minerals, vitamins, fibre, and proteins and because of their content of high quality lipids [1]. Herein we report the detailed characterization of a minor class of phospholipids (PL), known as diacylarsenosugar PL (As-PL, see Figure 1) along with their lyso-forms (LAs-PL) [2].

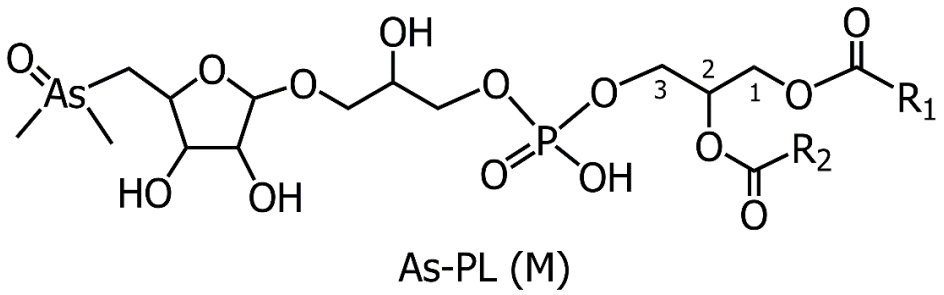

Figure 1. Diacylarsenosugar phospholipids (As-PL).

Materials and Methods

Four dried edible macroalgae samples were examined: Nori (*Porphyra spp*.), Wakame (*Undaria pinnatifida*), Dulse (*Palmaria palmata*) and Kombu (*Saccharina japonica*). Lipid fractions were firstly extracted from rehydrated specimens by the Bligh and Dyer protocol [3], then lipids were investigated by hydrophilic interaction liquid chromatography (HILIC) coupled with electrospray ionization (ESI) and mass spectrometry (MS) both at high and low resolution. Although As-PL have been previously investigated as protonated adducts, $[M+H]^+$ [4], we successfully applied an alternative paradigm operating in negative ESI mode on deprotonated molecules $[M-H]^-$ [5]. The search of As-PL in lipid extracts of marine algae was carried out by both HILIC-ESI(-)-FTMS for high-resolution/accuracy measurements using an Orbitrap analyser and HILIC-ESI(-)LIT MS for multistage collision induced dissociation using a linear ion trap instrument.

Results

Since As-PL are still not present in common online databases and commercially standards are not available, the identification in extracts of algal samples was attempted by comparing accurate *m/z* values provided by FTMS with the theoretically computed chemical formula of the $[M-H]^-$ ions. Each assigned *m/z* value as As-PL or LAs-PL was subjected to MS^n experiments, which showed a diagnostic class-related product ion at *m/z* 389.00 and several fragment ions arising from the fatty acyl groups. The additional use of *sn*-1 and *sn*-2 regioselective hydrolase enzymes (*i.e.*, phospholipases A1 and A2) provided further evidence for reliable regiochemical assignments on this class of phospholipids.

Discussion/Conclusions

The interplay between multistage MS and regioselective hydrolase enzymes enabled us to formulate three rules for regiochemical assignments on both As-PL and Las-PL occurring in all edible macroalgae samples investigated [6]. Up to 21 As-PL and 2 lyso-forms were successfully characterized; the comparison of As-PL and LAs-PL content in each sample showed a different composition both from a qualitative and quantitative point of view. Results are reported and discussed in this contribute.

References

1. P. Burtin; *Electronic Journal of Environmental, Agricultural and Food Chemistry*, 2 (2003), pp 498-503.
2. J. S. Edmond, M. Morita, and Y. Shibata; *Chemosphere*, 17 (1988), pp 1147-1152.
3. E. G. Bligh and W. J. Dyer; *Canadian Journal of Biochemistry and Physiology*, 37 (1959), pp 911-917.
4. A. Raab, C. Newcombe, D. Pitton, R. Ebel, and J. Feldmann; *Analitycal Chemistry*, 85 (2013), pp 2817-2824.
5. M. Pulfer and R. C. Murphy; *Mass Spectrometry Reviews* 22 (2003), pp 332-364.
6. D. Coniglio, C. D. Calvano, G. Ventura, I. Losito, and T. R. I. Cataldi; *Journal of the American Society for Mass Spectrometry*, 31 (2020) pp 1260-1270.

Structural characterization of *N*-acylphosphatidyl-ethanolamines (NAPE) in yellow lupin seeds by liquid chromatography coupledto mass spectrometry

***M. Bianco*[1], *C. D. Calvano*[1,2], *I. Losito*[1,2], *T. R.I. Cataldi*[1,2]**

[1]Dipartimento di Chimica and [2]Centro Interdipartimentale SMART, Università degli Studi di Bari Aldo Moro, Via E. Orabona 4, 70126 Bari

Keywords: *N-Acylphosphatidylethanolamines, lupin seeds, mass spectrometry.*

Introduction

N-Acylphosphatidylethanolamines (NAPE) are a minor class of membrane phospholipids (PL) that occur in both plant and animal tissues [1]. In plants, NAPE are involved in several functional roles such as to support the membrane structural integrity and to act as a precursor of lipid mediators known as *N*-acylethanolamines (NAE) [2]. Chemically, NAPE are modified phosphatidylethanolamines (PE) where the nitrogen on the polar head is linked to a fatty acid via amide bond. The molecular composition of NAPE in plants is complex due to the variation of length and number of double bonds in the three fatty acyl chains. In this study we focused on the NAPE composition of yellow lupin seeds. Lupin seeds can be considered as a nutraceutical food because they are known to reduce glycemic index and to play a key role in preventing obesity and alleviating diabetes and heart diseases [3]. Recently, we have characterized the major PL [4] and sphingolipid classes [5] in the lipid extracts of lupin seeds. Here we developed a strategy to characterize NAPE species based on liquid chromatography coupled to high and low resolution/accuracy mass spectrometers: Orbitrap Fourier-transform mass spectrometry (LC-ESI-FTMS) and linear ion-trap multiple-stage MS (LC-ESI-MS/MS and MS^3).

Materials and Methods

First, synthetic NAPE compounds were prepared following the method of Hansen et al. [6]. In the case of yellow lupin seeds, the lipid extraction was carried out following the Bligh-Dyer protocol [7]. Briefly, 800 µL of water and 3 mL of $CH_3OH/CHCl_3$ (2:1 v/v) were added to 1,5 g of lupin seed and vortexed. Then, 1 mL of water and 1 mL of chloroform were added and mixed again. After sample centrifugation for 15 minutes at 2000 g the organic phase was collected and dried under nitrogen. This lipid dried was dissolved in 200 µL MTBE/$CHCl_3$/CH_3COOH solution (98/2/0.05, v/v/v) and purified by a micro solid phase extraction (µSPE) [4]. The eluate was dried under nitrogen and then dissolved in 50 µL of propanol/$CHCl_3$/CH_3OH solution (90/5/5, v/v/v). The lipid extract was analysed using both hydrophilic interaction liquid chromatography (HILIC)-ESI-MS and reversed-phase (RP)LC-ESI-MS. MS analyses were carried out either on Q-Exactive (Q-Orbitrap) or VelosPro (Linear ion trap) spectrometer in negative ion mode.

Results

The total ion current (TIC) chromatogram by HILIC-ESI(-)-FTMS of a lupin seed extract showed several peaks corresponding to various lipid classes, namely hexosylceramides (HexCer), digalactosyldiacylglycerols (DGDG), phosphatidic acids (PA), NAPE, acyl-phosphatidylglycerols (Acyl-PG), phosphatidylinositols (PI), PE, lyso-PE, phosphatidylcholines (PC) and lyso-PC. Specifically, NAPE species were observed around 4-5 minutes. Extracted ion current (XIC) of synthetic NAPE compounds was used to confirm the retention time of this PL class. The preliminary identification of NAPE species in lupin lipid extract was achieved by searching the accurate m/z values on online databases. For future purposes of easy quantitation, the separation of NAPE was also performed by RPLC to avoid the signal suppression by co-eluting species such as acyl-PG and PA. To establish the fragmentation rules of fatty acyl chains, a few synthetic NAPE species were investigated by CID-MS and MS^3 experiments in negative ion mode [8]. Figure 1 shows the generic structure of deprotonated NAPE, $[M-H]^-$ (A) and a representative fragment with the *N*-linked fatty acyl chain observed by CID-MS (B). Moreover, the following product ions and the relative abundance (i.e. $[M-H-R_2COO]^-$ > $[M-H-R_1COO]^-$) from the sn-2 position relative to the sn-1 position of the glycerol backbone suggests a

preference for the loss of the sn-2 as a carboxylic acids and as ketenes. To ascertain the nature of *N*-linked fatty acyl chain it was necessary an additional fragmentation step on the ion B of Fig. 1. Following this approach, we have identified 32 NAPE species in yellow lupin seeds.

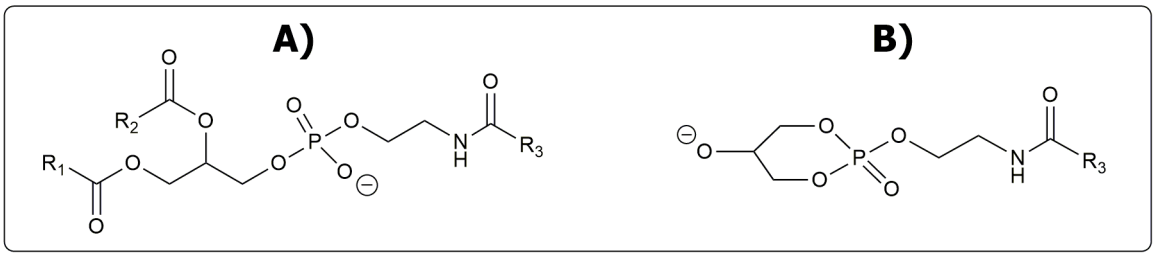

Fig. 5. Structures of deprotonated NAPE (A) and a representative fragment (B).

Discussion/Conclusions

The examination of lupin lipid extract was performed by combination of HILIC and RPLC separation coupled to ESI-FTMS and ESI-LIT MS in negative ion mode. The fragmentation pattern was established by CID multistage MS experiments accomplished on synthetized NAPE species, previously examined by ^{13}C-NMR on purified samples. Up to 32 NAPE species in the lipid extract of yellow lupin seeds were characterized including several isomeric species.

References

1. A. Kilaru, E. B. Blancaflor, B. J. Venables, S. Tripathy, K. S. Mysore, and K. D. Chapman, *Chemistry and Biodiversity*, 4 (2007), pp. 1933–1955.
2. H. H. O. Schmid, P. C. Schmid, and V. Natarajan, *Chemistry and Physics of Lipids*, 80 (1996), pp. 133–142.
3. M. Tapadia, R. Carlessi, S. Johnson, R. Utikar, and P. Newsholme, *Molecular and Cellular Endocrinology*, 480 (2019), pp. 83–96.
4. C. D. Calvano, M. Bianco, G. Ventura, I. Losito, F. Palmisano, and T. R. I. Cataldi, *Molecules*, 25 (2020), p. 805.
5. M. Bianco, C. D. Calvano, I. Losito, F. Palmisano, and T. R. I. Cataldi, *Food Chemistry*, 324, (2020), p. 126878.
6. H. H. Hansen, S. H. Hansen, I. Bøjrnsdottir, and H. S. Hansen, *Journal of Mass Spectrometry*, 34, (1999), pp. 761–767.
7. E. G. Bligh and W. J. Dyer, *Canadian Journal of Biochemistry and Physiology*, 37 (1959) pp. 911–917.
8. G. Astarita, F. Ahmed, and D. Piomelli, *Journal of Lipid Research*, 49 (2008), pp. 48–57.

Characterization of Natural Methylxanthines Oxidation Products By Mass Spectrometry: a mechanistic study

***R. Petrucci*,[1] *M. Bortolami*[1] *and P. Di Matteo*[2]**

[1]Dept. Basic and Applied Sciences for Engineering, Sapienza University of Rome, Via del Castro Laurenziano 7, 00161 Rome, Italy, [2]Dept. Chemical Engineering Materials Environment, Sapienza University of Rome, Via Eudossiana 18, 00184 Rome, Italy

Keywords: *ESI-MS/MS; caffeine; theophylline.*

Introduction

Natural methylxanthines as caffeine (CAF) and theophylline (TPh) (structures in the Figure) are alkaloids assumed with the diet *via* highly consumed beverages as coffee and tea. Their pharmacological potential has been recently reported [1], as well their use as bio-based and renewable starting materials in sustainable organic synthesis [2]. A deep discussion on their role as potential antioxidants towards oxidative damage was also reported [3]. We recently investigated the fate of CAF and TPh under oxidative conditions with the aim of gaining a deeper insight into their oxidative mechanisms and the involvement of radical species.

Materials and Methods

The electrochemical oxidation of CAF and TPh was carried out, in turn, in organic solvents and in aqueous organic medium [4, 5]. The electrolyzed mixtures were diluted with the mobile phase (A:B, 95:5, A=MilliQ and B=acetonitrile, 0.02% fromic acid) and analysed by using a High Performance Liquid Chromatography separation module coupled to a PhotoDiodeArray detector and a Tandem Mass Spectrometry system with an ElectroSpray Ionization source (HPLC-PDA-ESI-MS/MS, Waters). Spectral data of the mixtures were acquired in ES+ and ES- full scan. The main chromatographic peaks were then studied by direct infusion experiments, working in daughter mode on the selected parent ion, by optimizing the collision energy for the best fragmentation in ES+ and ES-.

Results

The oxidations products of TPh and CAF were well characterized on the base of spectral data in full scan and fragmentation, UV-vis spectra and elution order.
Five main oxidation products were found for TPh, four of which not previously reported: three dimeric compounds, the 4,5-diol derivative and a highly oxidized diol derivative.
Four main oxidation products were found for CAF: the 4,5-diol and the oxazolidin-2-one derivatives, as principal oxidation products, not previously reported with experimental evidence, and two highly polar degradation products. No dimeric compounds were found.

Discussion/Conclusions

The analysis of the spectral data of the main chromatographic peaks found for the electrolysed mixtures provided strong evidences for the proposed molecular structures of oxidation products of CAF and TPh, although they were not isolated from the reaction mixtures.
Dimeric compounds were found only for TPh, with prevalent formation in organic solvents, that can be considered a more friendly environment when radical species are involved in a reaction mechanism [4].
The 4,5-diol derivative was found for both TPh and CAF, in the case of CAF resulting the main product [5].
Spectral data for the TPh dimer and for the 4,5-diol derivative of CAF are shown in the Fig.1.
These data strongly support the oxidative mechanism previously proposed [3] for methylxanthines, starting from the primary oxidation of the olefinic bond and leading to the corresponding radical cation. A following fast deprotonation to the corresponding neutral radical is possible only for TPh, and dimeric compounds can be obtained by coupling reaction.

On the contrary, the radical cation of CAF cannot undergo deprotonation, reason why no coupling reactions may occur, while it may undergo easy nucleophilic attack by water, even when present in trace, leading to the oxygenated products.
The spectral analysis, combined with the electrochemical oxidation, provided strong evidences for a long discussed mechanism on the oxidation of natural methylxanthines (see a short scheme in Fig. 2), with an interesting new insight on the reactivity of the radical cation of the oxidized CAF, for useful synthetic applications and a better understanding of its behavior under oxidative stress conditions.

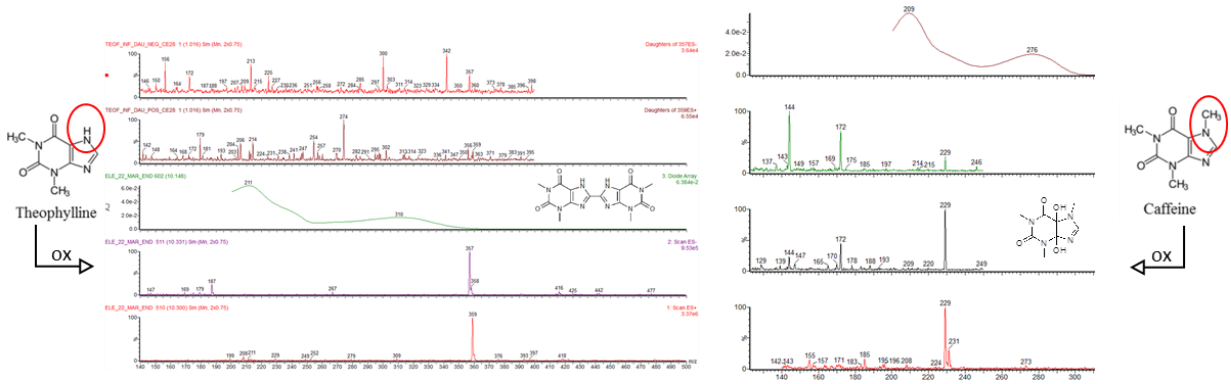

Fig.1 Spectral data of a representative dimeric oxidation product of TPh and a representative oxygenated derivative of CAF.

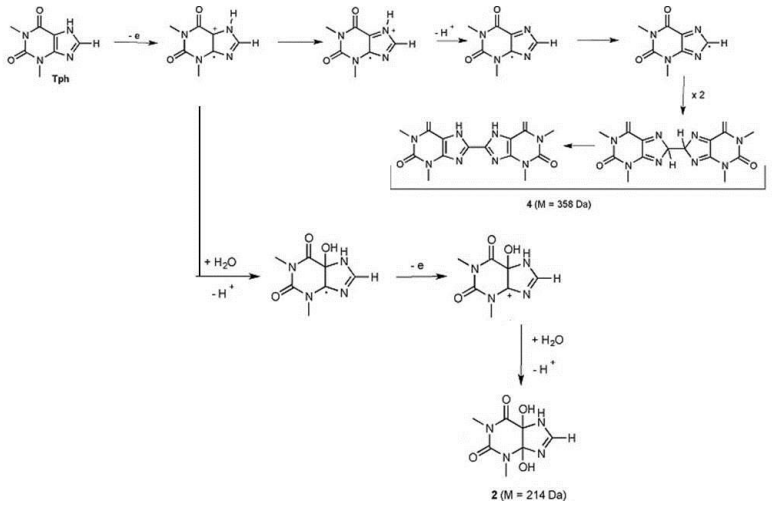

Fig. 2 Reactivity of the radical cation and the neutral radical of oxidized methylxanthines, reported for TPh.

References

1. J. Monteiro, M.G. Alves, P.F. Oliveira, B.M. Silva; *Critical Reviews in Food Science and Nutrition*, 59 (2019), pp 2597-2625
2. R. Petrucci, M. Feroci, L. Mattiello, I. Chiarotto; *Mini-Reviewes in Organic Chemistry*, (2020),
3. R. Petrucci, G. Zollo, A. Curulli, G. Marrosu; *BBA–General Subjects*, 1862 (2018), pp 1781-1789
4. I. Chiarotto, L. Mattiello, F. Pandolfi, D. Rocco, M. Feroci, R. Petrucci; *ChemElectroChem,* 6 (2019), pp 4511-4521
5. M. Feroci, M. Bortolami, I. Chiarotto, P. Di Matteo, L. Mattiello, F. Pandolfi, D. Rocco, R. Petrucci; *Electrochem*,1 (2020), pp 44-55

Identification of *Trichoderma* spp. volatile organic compounds (VOCs) by HS-SPME/GC-MS analysis

***V. Lazazzara*[1], *B. Vicelli*[1,2], *C. Bueschl*[3], *A. Parich*[3], *I. Pertot*[1,2], *R. Schuhmacher*[3] and *M. Perazzolli*[1,2]**

[1]Department of Sustainable Agro-ecosystems and Bioresources, Research and Innovation Centre, Fondazione Edmund Mach, Via E. Mach 1, 38010 San Michele all'Adige, Italy, [2]Center Agriculture Food Environment (C3A), University of Trento, Via E. Mach 1, 38010 San Michele all'Adige, Italy, [3]Institute of Bioanalytics and Agro-Metabolomics, Department of Agrobiotechnology (IFA-Tulln), University of Natural Resources and Life Sciences, Vienna (BOKU), Konrad-Lorenz-Straße 20, 3430 Tulln, Austria.

Keywords: *Trichoderma spp., volatile organic compounds, HS-SPME/GC-MS*

Introduction

Trichoderma spp. are among the most widespread soil microorganisms and have been widely used as biological control agents against numerous phytopathogens [1]. *Trichoderma* biological control mechanisms are based on the production of antimicrobial substances, lytic enzymes, competition with other microorganisms for nutrients and/or space, mycoparasitism, and plant resistance induction [2]. Moreover, *Trichoderma* spp. are known to produce numerous volatile organic compounds (VOCs) [3] that play crucial roles in the inter-kingdom communications and biological control mechanisms [4]. Three *Trichoderma* strains, such as *T. asperellum* T34 (T34), *T. atroviride* SC1 (SC1), *T. harzianum* T39 (T39) are well documented for their ability to cope with a broad spectrum of phytopathogens and are commercialised as biofungicides. Several studies highlighted the importance of *Trichoderma* spp. as an alternative strategy against grapevine pathogens [5], but no information is available on the possible biological control mechanism mediated by *Trichoderma* VOCs against grapevine downy mildew (caused by *Plasmopara viticola*). The aim of this study was to identify VOCs produced by T34, SC1 and T39 using headspace-solid-phase microextraction gas chromatography-mass spectrometry (HS-SPME/GC-MS) analysis.

Materials and Methods

Volatile-mediated effects of *Trichoderma* strains were assessed on grapevine leaf disks incubated with uninoculated potato dextrose agar (PDA) Petri dishes (Control) and dishes with PDA-grown T34, SC1 or T39 colonies without contact with leaf tissues. Leaf disks were inoculated with a suspension of *P. viticola* sporangia and downy mildew severity was assessed at six days post inoculation (dpi).
For headspace analysis of *Trichoderma* spp. VOCs, 20 µL of the conidial suspension of the respective *Trichoderma* strain were inoculated on PDA poured into sterile 20 mL-HS vials. VOCs produced by *Trichoderma* strains were measured using HS-SPME/GC-MS analysis at 48 or 72 h of incubation at 25°C. For compound identification, deconvoluted mass spectra were compared with an in-house library obtained with authentic reference standards. Compound annotation was achieved imposing a relative deviation of retention index (RI) value lower than 2% from the reference value published in the NIST14 database, and according to the mass spectrum similarity score set higher than 70%. Two independent experiments were carried out. Five of the identified VOCs were selected according to their emission profiles and pure compounds were tested against *P. viticola* by leaf disk assay.

Results

VOCs produced by T34, SC1 or T39 reduced downy mildew symptoms on grapevine leaf disks. HS-SPME/GC-MS analysis revealed a total of 26 and 21 *Trichoderma* VOCs found in the first and second experiments, respectively. *Trichoderma* VOCs included alkenes, ketones, pyrones, furanes and terpenes. Terpenes were successfully identified using manual inspection of extracted ion current (EIC) chromatograms at *m/z* 136 for monoterpenes, *m/z* 202 and 204 for sesquiterpenes, and *m/z* 272 for diterpenes. VOC profiles differed according to the *Trichoderma* strains and T39 was the highest producer of VOCs and terpenes compared to T34 and SC1. Five metabolite groups were identified according to changes in abundance among the three *Trichoderma* strains: VOCs with consistent changes

in both experiments at both (Group 1), or at one time point (Group 2); VOCs with different changes in abundance in both experiments (Group 3); VOCs detected only in the first (Group 4) or second (Group 5) experiment. Five VOCs (two sesquiterpenes, one alkene, one furan and one pyrone) were tested against *P. viticola* and each VOC was applied to a filter paper disk on the lid of the Petri dish without contact with leaf tissues. Three VOCs slightly reduced the development of downy mildew symptoms at dosages of 50 mg/L in air volume. Two pure VOCs significantly reduced downy mildew symptoms at the dosage of 10 mg/L in air volume.

Discussion/Conclusions

HS-SPME/GC-MS analysis is a powerful tool to detect and identify *Trichoderma* VOCs. VOC profiles differed in the three *Trichoderma* strains and T39 was the highest producer of terpenes, followed by T34 and SC1, indicating genotypic determinants of VOC production. Five VOCs (two sesquiterpenes, one alkene, one furan and one pyrone) reduced downy mildew symptoms on grapevine leaf disks. Preliminary results suggest that two most effective VOCs enhanced the grapevine defence responses against *P. viticola*. These results indicate that *Trichoderma* VOCs are promising molecules that could be further developed to naturally control grapevine downy mildew. Further transcriptomic and metabolomic studies are required to shed light on the grapevine defence mechanisms activated by *Trichoderma* VOCs against downy mildew.

References

1. G.E. Harman, C.R. Howell, A. Viterbo, I. Chet and M. Lorito; *Nature Reviews Microbiology*, 2 (2004), pp 43-56.
2. M. Lorito, S.L. Woo, G.E. Harman, E. Monte; *Annual Review of Phytopathology*, 48 (2010), pp 395-417.
3. F.K. Crutcher, A. Parich, R. Schuhmacher, P.K. Mukherjee, S. Zeilinger, C.M. Kenerley; *Fungal Genetics and Biology*, 56 (2013), pp 67-77.
4. Y. Guo, A. Ghirardo, B. Weber, J.-P. Schnitzler, J.P. Benz, M. Rosenkranz; *Frontiers in Microbiology*; 10 (2019), 00891.
5. A. Zanotto, M. Morroni and S. Compant, F. Mathieu editors, Mojor biocontrol studies and measures against fungal and oomycete pathogens of grapevine in "Biocontrol of major grapevine diseases: leading research", Boston (USA) (2016), pp 1-34.

LC-ESI/LTQ Orbitrap/MS/MS^n analysis highlights multi-class polar lipid and phenolic compounds in fresh and roasted hazelnut of Italian PGI product "Nocciola Piemonte

***A. Cerulli*[1], *A. Napolitano*[1], *M. Masullo*[1], *B. Olas*[2], *S. Piacente*[1]**

[1]Dipartimento di Farmacia, Università degli Studi di Salerno, via Giovanni Paolo II n. 132, 84084 Fisciano (SA), Italy,
[2]Department of General Biochemistry, Institute of Biochemistry, Faculty of Biology and Environmental Protection, University of Lodz, Pomorska 141/3, 90-236, Lodz, Poland

Keywords: *"Nocciola Piemonte" PGI fresh and roasted hazelnut, polar lipids, LC-ESI/LTQOrbitrap/MS/MS^n.*

Introduction

The Italian "Nocciola Piemonte", also known as "Tonda Gentile Trilobata" as well as "Tonda Gentile delle Langhe", is a labelled Protected Geographical Indication (PGI) hazelnut, known for intensity of its sweetness, the cooked-bread aroma and the low intensity of the burnt aroma [1].
With the aim to obtain a detailed and comprehensive characterization of the *n*-butanol extract of both fresh and roasted kernels of *Corylus avellana* cultivar "Nocciola Piemonte" the LC-ESI/LTQOrbitrap/MS/MS^n analysis, in negative and positive ionization mode, has been carried out. Furthermore, in order to unambiguously identify the phenolic compounds therein occurring, they were isolated from the *n*-butanol extract and characterized by 1D and 2D NMR experiments**.** Finally, the ability of the isolated compounds to inhibit the lipid peroxidation induced by H_2O_2 and H_2O_2/Fe^{2+} was determined by TBARS assay.

Materials and Methods

C. avellana fresh and roasted kernels were skinned by a knife, crushed and successively submitted to defatting with *n*-hexane, chloroform, and methanol at room temperature. After filtration, the MeOH extract was treated with *n*-hexane to remove the oily compounds. The derived MeOH extract was submitted to *n*-butanol-water partition to remove free sugars. Qualitative LC-ESI/HRMS analysis of *n*-butanol extract of both fresh and roasted hazelnuts was performed using an analytical system characterized by a quaternary Accela 600 pump and an Accela autosampler coupled to a LTQOrbitrap XL mass speworking in positive and negative electrospray ionization mode, according to a procedure previously reported[2]. 3 g of *n*-butanol extract of roasted hazelnuts were fractionated on a Sephadex LH-20 column, Fractions were chromatographed by semipreparative RP-RI/HPLC to yield phenolic compounds. Inhibitory effects on lipid peroxidation by phenolic compounds was assayed by measuring the concentration of TBARS using the same procedure previously reported [3].

Results

The analytical approach based on LC-ESI/LTQOrbitrap/MS/MS^n analysis highlighted in both fresh and roasted "Nocciola Piemonte" hazelnuts compounds belonging to phenolic and lipid classes. The careful analysis showed the occurrence of polar lipid compounds belonging to oxylipins and phospholipids, sphingolipids, and glycolipids as well as of phenolic derivatives. With the aim to unambiguously characterize the molecular structure of phenolic derivatives, the *n*-butanol extract of "Nocciola Piemonte" roasted hazelnuts was subjected to size-exclusion chromatography and to further separation by RP-RI/HPLC. By this way the occurrence of giffonin L, M, P and carpinontriol B, diarylheptanoids previously reported in other parts of *Corylus avellana* [4], along with flavonoid glycosides were determined. Moreover, the ability of the isolated compounds to inhibit the lipid peroxidation induced by H_2O_2 and H_2O_2/Fe^{2+} was determined by TBARS assay. Some phenolic compounds, particularly diarylheptanoids, at concentration of 10 μM, reduced both H_2O_2 and H_2O_2/Fe^{2+} induced lipid peroxidation more than the well-known diarylheptanoid curcumin.

Discussion/Conclusions

The results of this study highlight the occurrence of many classes of lipids, ranging from the small oxylipins and long chain bases to intact high molecular weight lipids such as phospholipids, sphingolipids, and glycolipids in Italian PGI hazelnut "Nocciola Piemonte". Moreover, diarylheptanoids, isolated from *n*-butanol fraction of roasted and fresh hazelnut extract showed a good antioxiodant activity. On the basis of the biological activities reported for lipid classes found in "Nocciola Piemonte" hazelnut kernels and their effects

on human health, these data support the use of hazelnuts in human nutrition as a food rich in different classes of bioactive and healthy lipids with beneficial effects.

References

1. Caligiani, J. D. Coisson, F. Travaglia, D. Acquotti, G. Palla, L. Palla, M. Arlorio; *Food Chemistry*, 148 (2014), pp 77–85.
2. A. Napolitano, A. Cerulli, C. Pizza, S. Piacente; *Food Chemistry*, 269 (2018), pp 125-135.
3. M. Masullo, A. Cerulli, B. Olas, C. Pizza, S. Piacente; *Journal of Natural Products*, 78 (2015), pp 17-25.
4. A. Bottone, A. Cerulli, G. D'Urso, M. Masullo, P. Montoro, A. Napolitano, S. Piacente; *Planta Medica* 85 (2019), pp 840–855

REE normalised distribution in soil/plant system as tool to discriminate the substrate origin of the *Vitis vinifera* plant

***M. Barbera*[1,2]**

[1]Università di Palermo, SAAF, Viale delle Scienze ed. 4, 90128, Palermo, Italy, [2] Sorbonne Université, METIS, 4 place Jussieu, 75005, Paris, France

Keywords: *Rare Earth Elements, Vitis Vinifera L., geographical origin*

Introduction

Geographical authentication of the foodstuffs is critical to quality control, food safety, and control adulteration. The establishment of an effective traceability method independent of paper records has become increasingly crucial. Therefore, the potential of multi-element analyses for distinguishing the geographical origin of food products was tested. In this work, we explore the possible tool of Rare Earth Elements as geographical tracer in food chain and plant physiological response to environmental stress in contaminated soils. Adopting controlled experimental conditions, we have investigated the effect of REE amount in the substrate during the *Vitis vinifera L* growth analysing the REE distribution in the different part of the plants.

Materials and Methods

Pristine plants one years old were put into polyurethane pots with 5 Kg of peat-gravel ratio of 2:3 w/w homemade. Two different growth conditions were investigated: one using the peat-gravel substrate (blank experiment) and another adopting the same substrate spiked with 2.5 µmol per Kg of each REE (spiked experiment).

Sampling was performed at five different growth stages selected according the different plant-life periods. For every sampling time, plants were separated in roots and aerial parts. The REE amounts in soil-plants system were detected by inductively coupled plasma mass spectrometry (ICP-MS).

The Translocation Factors (TF) was estimated by the ratio between the REE concentration in shoots and roots. The distribution of REE normalised patterns [REE]* was determined normalizing the REE value in the different part of the plants organ and native soil respect a lithological reference , Upper Continental Crust (UCC).

Results

We found that plant mass and amount of REE in leaves are not significantly influenced by the different REE enrichment of the substrate while roots are by one order of magnitude enhanced for three orders of magnitude REE enrichment of the soil substrate indicating that the soil enrichment does not significantly influence the amount of REE found in the aerial parts of *Vitis vinifera L.*

We found that TF, calculated for both experimental condition is lesser than one for all elements detected, meaning that REE accumulation is greater in roots in comparison with shoots. In particular, TF is by 3 to 15 times lower in the spiked experiment, compared to the blank one. Therefore, it appears that *Vitis Vinifera L.* limits the transfer of REE maintaining low levels in the aerial parts.

Figs. 1 show the distribution of REE normalised pattern in roots compared to the native soils and UCC for both blank and spike conditions. In blank experiment (fig 1a) the REE normalized spectra of the roots show a smooth trend reflecting the geochemical REE pattern of the native soil. This means that the roots have accumulated REE in proportion to the REE amount present in the native soil. In spike experiment the REE spectrum of roots does not correspond to the native soil, but shows a "Zig Zag" curve symmetrical to the UCC distribution (Fig 1b).

Figs. 2 show the distribution of REE normalised pattern in aerial part of the plant compared to the fine roots for both blank and spike conditions. For blank experiment (Fig 2a) aerial REE pattern show a smooth trend in agreement with the root pattern. For spiked experiment (Fig 2b) aerial part REE pattern is characterised by "zig zag" shape according to the pattern observed also in roots. For both experimental conditions we observe that despite the variable REE amount in plant organs, REE distribution pattern detected for plants organs keeps unaltered during the plant's growth. This means that *Vitis Vinifera L.* does not uptake any REE selectively. Therefore, we can suppose that the different normalised REE patterns for the two investigated system, can be related exclusively to the change in the substrate, the only variable present in the two experimental systems.

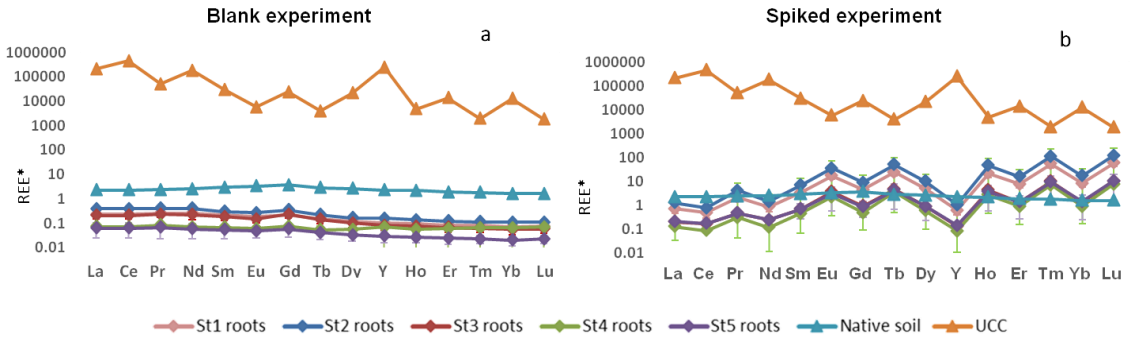

Fig. 1 Normalized REE patterns measured in roots and native soils and UCC during plant growth

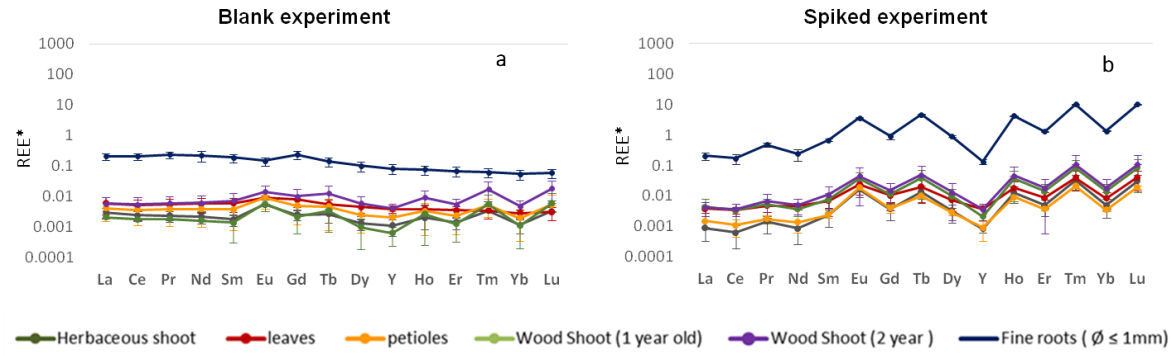

Fig. 2. Normalized REE patterns measured in fine roots and aerial part (8 month of growth)

Conclusions

We found that the transfer efficiency of REE from roots to leaves, evaluated by translocation factor, is lower in the spiked experiment, compared to the blank one, although, the total REE concentration in roots, for spiked experiment, is by one order of magnitude enriched in REE. This imply that eventual pollution of the soil by REE would not influence, significantly, the amount of the REE transfer into the aerial part of the plants and, consequently, grapevine products, obtained by *Vitis vinifera L.* plants, could show a very low REE amount.
We found that the normalized REE distribution pattern does not change during plant growth even if REE concentration may change during the plants' development. In the blank conditions REE distribution reflects the native soil, whereas under spiked substrate REE distribution mirror UCC, indicating that the REE transfer from soil through *Vitis vinifera L.* occur without significant fractionations. Therefore, we propose that the full REE normalized spectra is able to discriminate the substrate of *Vitis Vinifera L.* growth.

Environment and Miscellanea

Isotopic analysis of snow from Dome C indicates changes in the source of atmospheric lead over the last fifty years in East Antarctica

***S. Bertinetti*[1], *F. Ardini*[1], *M. A. Vecchio*[1], *L. Caiazzo*[2,3] *and M. Grotti*[1]**

[1]Department of Chemistry and Industrial Chemistry, University of Genoa, via Dodecaneso 31, 16146, Genoa, Italy, [2]Department of Chemistry Ugo Schiff, University of Florence, via della Lastruccia 3, 50019, Sesto Fiorentino, Italy, [3]INFN-Florence, via Sansone 1, 50019, Sesto Fiorentino, Italy

Keywords: *lead, isotopic ratios, snow.*

Introduction

Lead (Pb) is a toxic element whose natural biogeochemical cycle has been strongly affected by anthropogenic activities since ~5000 years ago [1]. Pb has been introduced into the atmosphere by mining and smelting activities, as well as by the use of leaded gasoline in the second half of the 1990's until its phases phases-out at the end of the XX century. These anthropogenic inputs overlap the natural ones due to rocks and soil dust, ocean salt and volcanic emissions. Lead associated to the fine particles can be transported over long distances by the atmospheric circulation, reaching the most isolated regions on the Earth, like Artic and Antarctica. Here, these particles are accumulated in the snow by dry and wet deposition processes, therefore their analysis in snow and ice samples can provide a proxy of historical changes of both natural and anthropogenic Pb input in the atmosphere. Moreover, the isotopic ratios of Pb of these samples con be used to investigate transport pathways and for source assessment [2]. In fact, there is a difference high enough to be detected in the relative abundance of the radiogenic Pb isotopes among various lead ore deposits. This difference is due to the different Pb, Th and U composition in the rocks at the moment of their formation and the elapsed time until the material was released in the environment.

In this work, a record of Pb isotope ratios and elemental concentration have been obtained by the analysis of 109 snow samples collected at Dome C, East Antarctica, in the framework of the project SIDDARTA (PNRA 14_00091, PNRA 16_00252) of the Italian National Program of Research in Antarctica. The aim of the work was: (a) providing updated information on the Pb pollution trend in the last fifty years, especially to discriminate between "steady-state" and "decreasing" trends in the last decade; (b) contributing to the source assessment of the atmospheric Pb reaching Antarctica, as a tracer of the mineral dust [3]; (c) evaluating the anthropogenic-to-natural Pb ratio and its temporal variation; (d) compare these data to similar estimations for other Antarctic sites.

Materials and Methods

The snow samples were collected from the wall of a 4 m deep hand-dug snow pit, covering the period from 1971 to 2017, by a 50 mL polypropylene graduate tubes horizontally inserted at about 3 cm intervals. Lead isotopic analysis was performed by ICP-DRC-MS (PerkinElmer Elan DRC II) using a previously reported method [4]. Briefly, the samples were melted in their closed tube and then, 20.0 g aliquots were acidified with 100 μL of concentrated HNO_3 and 100 μL of concentrated HF (both at ultrapure grade quality), left to stand for 24 hours and refrozen. Then, the samples were freeze-dried, redissolved in 200 μL of 0.05% HNO_3 solution and introduce into the ICP-MS spectrometer by using a home-made heated torch-integrated total consumption sample introduction system [5]. The sample volumes were, therefore, reduced from 20.0 to 0.200 mL, providing a 100-fold preconcentration of Pb. The instruments used is equipped with a dynamic reaction cell pressurized with neon to improve the precision of isotope ratios determination by collisional damping [6].

Instrumental mass bias was corrected applying the bracketing external correction method by measuring the NIST SRM 981 isotopic standard solution [7]. The quality of Pb isotopic and concentration measurements were systematically controlled by the analysis of the reference material IRMM CRM 482, for which Pb isotopic composition is available in literature.

Results

The Pb concentration found in the analysed samples was over than one order of magnitude higher than the natural background (0.2 pg g^{-1} in Holocene ice from Dome C [8]). However, Pb concentration shows a decreasing temporal trend from the early 1990s (median Pb concentration halved from 9.0 pg g^{-1} in 1970-1980 to 4.4 pg g^{-1} in 2010-2017), with an associated reduction of the anthropogenic contribution (from 61 ± 3 % in 1980-1990 to 49 ± 10 % in 2010-2017). Note that the 95%-confidence intervals reported are a measure of the date dispersion not the uncertainties of the estimate.
Lead isotopic ratios were much lower than the natural ratio measured at Dome C [8], highlighting the anthropogenic contribution to the Pb deposited in Antarctica over the last 50 years. The temporal trend of $^{206}Pb/^{207}Pb$ isotope ratios shows a sharp increase from the beginning to the end of the 1970s, with a subsequent drop to less radiogenic values during the 1980s, concomitantly with the Pb concentration peaks in that very periods. From the end of the 1980s, the Pb isotope ratio raised again for then stabilized during the last two decades.

Discussion/Conclusions

The Pb isotopic composition in the samples from 1970 to mid-1990s reflect the changes in the consumption of Pb-enriched gasoline in the South Hemisphere, showing a shift toward the natural isotopic signature from the 2000's. The measured ratios, compared to the isotopic signatures of the potential source areas, suggest that also Australia, jointly with South America, has acted as significant anthropogenic source in the last 50 years.
Finally, similitudes are observed between different sampling places at Antarctica, and the principal components analysis (PCA) highlighted that the altitude and the distance from the coast of this sites significantly affect their Pb concentration, but not their isotopic signature [9].

References

1. D. Weiss, W. Shotvk, O. Kempf; *Naturwissenschaften*, 86 (1999), pp 262-275.
2. F. Ardini, A. Bazzano, M. Grotti; *Environmental Chemistry*, 17 (2020), pp 213-239.
3. F.E. Grousset, P.E. Biscaye; *Chemical Geology*, 222 (2005), pp 149-167.
4. A. Bazzano, M. Grotti; *Journal of Analytical Atomic Spectrometry*, 29 (2014), pp 926-933.
5. M. Grotti, F. Ardini, J.L. Todolì; *Analytica Chimica Acta*, 767 (2013), pp 14-20.
6. D.R. Bandura, V.I. Baranov, S.D. Tanner; *Journal of Analytical Atomic Spectrometry*, 15 (2000), pp 921-928.
7. F. Vanhaecke, L. Balcaen, D. Malinovsky; *Journal of Analytical Atomic Spectrometry*, 24 (2009), pp 863-886.
8. P. Vallelonga, P. Gabrielli, K.J.R. Rosman, C. Barbante, C.F. Boutron; *Geophysical Research Letters*, 32 (2005) L01706
9. S. Bertinetti, F. Ardini, M.A. Vecchio, L. Caiazzo, M. Grotti; *Chemosphere*, 255 (2020).

Identification of Extracellular Polymeric Substances in Sea Ice Samples by a HPLC-ESI-MS/MS method

***D. Vivado*[1], *P. Rivaro*[1], *F. Ardini*[1], *M. Grotti*[1], *A. Salis*[2] and *G. Damonte*[2,3]**

[1]Department of Chemistry and Industrial Chemistry, University of Genoa, Via Dodecaneso 31, 16146, Genoa, Italy, [2]Centre of Excellence for Biomedical Research, Viale Benedetto XV 9, 16132, Genoa, Italy, [3]Department of Experimental Medicine, University of Genoa,Via Leon Battista Alberti 2, 16132, Genoa, Italy

Keywords: *sea ice, EPS, iron*

Introduction

Dissolved organic matter in sea ice is rich in extracellular polymeric substances (EPS) secreted by sea ice algae and bacteria [1] [2] [3]. EPS are complex macromolecules ranging from the dissolved phase through the colloidal and include lipids, nucleic acids, proteins and carbohydrates [4] [5]. Carbohydrates are the most abundant component of EPS and they may contribute to the Fe-binding organic ligand pool, increasing the residence time of bioavailable Fe in the euphotic zone when sea ice melts [3]. Despite the ecological importance of EPS and of their associated carbohydrates in particular, there is limited information in the literature regarding their chemical characterization, due to their heterogeneous composition, complex structures and low concentrations in a matrix with a high ionic strength [6]. Therefore, the objective of this work was the development of a suitable analytical method for the identification of dissolved EPS in sea ice. A new method is presented, using Solid Phase Extraction (SPE) column for the extraction and the pre-concentration steps and HPLC-ESI-MS/MS for the separation and identification of the analytes.

Materials and Methods

The method has been built up and optimized using composite samples obtained from pack-ice aliquots collected during winter 2012 in the framework of the activities of Australian-led Sea Ice Physics and Ecosystem eXperiment-2 (SIPEX-2) voyage. The solid phase extraction (SPE) was performed by treating 50 mL of acidified sample onto C18 SPE cartridges 500 mg, 3 mL (SupelcleanTM ENVITM – 18, Supelco®). The identification of organic ligands was carried out by a micro HPLC-ESI-MS/MS, using a HPLC 1100 series from Agilent Technologies (Santa Clara, California, USA) equipped with an autosampler and an Agilent Technologies XCT trap LC/MSD mass spectrometer, equipped with a high capacity ion trap. Verbascose (Merck, Darmstadt, Germany) standard solutions (2-10-20 ppm) were used for EPS quantification.

Results

The SPE allowed the use of only 50 mL samples, also reducing sample preparation time, as well as removing the salt of the matrix. Nine EPS with a mass lower than 1500 Da were identified by HPLC-ESI-MS/MS, characterized by a different number of glucose units making up the polymeric chain. The total estimated concentration, in agreement with spectrophotometric assay results, was about 46 ppb.

Discussion/Conclusions

HPLC-ESI-MS/MS proves to be a powerful technique for the separation and identification of EPS in sea ice samples. Despite its sensitivity, a SPE preconcentration is necessary for the detection of these compounds occurring in samples at ppb levels. Nevertheless, major advantages over previously published approaches include a smaller volume of the sample and the ability to obtain structural information on EPS. Nine EPS having a mass lower than 1500 Da were identified by HPLC-ESI-MS/MS, diversified by the number of glucose units making up the polymeric chain. The total estimated concentration was about 46 ppb, ranging from 0.4 to 23 ppb. Our method slightly opens a window to a better understanding of the iron biogeochemical cycle and speciation in the Antarctic sea ice. Obviously time series data and good resolution of EPS distribution along the sea ice core are required for this aim.

In this context, our optimized conditions can highly improve the resolution, since the ice sections could be thinner than the actual ones, because our method requires a small volume of sample.

References

1. C. Krembs and J. W. Deming, *Psychrophiles: from biodiversity to biotechnology*, (2008) pp. 247–264.
2. A. R. Juhl, C. Krembs, and K. M. Meiners, *Marine Ecology Progress Series*, 436 (2011), pp. 1–16.
3. C. S. Hassler, V. Schoemann, C. Mancuso, E. C. V Butler, and P. W. Boyd, *Proceedings of the National Academy of Sciences*, 108 (2011), 3, pp. 1076–1081.
4. N. C. A. Mancuso, S. Garon, J. P. Bowman, and G. Rague, *Journal of Applied Microbiology*, no. Alldredge (2000), pp. 1057–1066, 2004.
5. G. J. C. Underwood, S. Fietz, S. Papadimitriou, D. N. Thomas, and G. S. Dieckmann, *Marine Ecology Progress Series*, 404 (2010), pp. 1–19.
6. M. Gledhill and K. N. Buck, *Frontiers in microbiology*, 3 (2012), FEB, pp. 1–17.

SPME and LC-MS/MS as a toll for microplastic associated contaminants investigation

***F. Saliu*[1], *M. Lasagni*[1]**

[1]Earth and Environmental Science Department, University of Milano-Bicocca, piazza della Scienza 1, 20123 Milano- Italy

Keywords: *contamination, plasticizer, extraction*

Introduction

The impacts of microplastics (MP) on marine life are still larger unknown. Current studies focus on microplastics as carriers of a "cocktail of contaminants" that may display pronounced toxic effect. Evidences from lab feeding trials showed that microplastics may be ingested by marine organism and cause adverse effects. However, "on field" studies are still limited [1]. The main issues to collect significant data arise from the low concentration of microplastics and of the associated contaminants in the organisms living in the "real" marine environment, and from the widespread plastic contamination affecting the laboratories, that may cause uncontrolled background contamination, especially when the extractions are carried out by using organic solvents [2]. For this reason, we developed alternative analytical procedures based on the use of SPME and LC-MS/MS. that offered also the advantage to limit the impacts of the research on marine life, by working *in vivo*, even with sensitive species [3,4].

Materials and Methods

LC-MS/MS analyses were carried out with a TSQ Quantum Access Max (ThermoScientific) equipped with a UHPLC/HPLC chromatographic system, an ESI interface, and a triple quadrupole mass analyzer. A Thermo Scientific Accucore C-18 aQ column (100 mm x 2.1 mm, I.D. 2.6 µm) was used for the chromatographic separation. Elution was carried out at 0.6 mL/min with methanol and water and by applying gradient condition. Electrospray ionization (ESI) was performed in the positive ion mode with the following set up: spray voltage 3500 V, vaporizer temperature 350°C, capillary temperature 270°C, sheath gas pressure 50 AU, auxiliary gas pressure 15 AU, ion sweep gas pressure 2 AU. Mass spectrometric detection was carried out in the time segmented selected reaction monitoring mode (tSRM). Collision gas pressure was set up at 1.0 mTorr and cycle time 0.6 s. The selected MS/MS transition are were optimized by using reference standard. One qualifier and one quantifier were used for each analyte. Figure 1 reports a schematic illustration of the steps involved in the SPME procedure. Before the use, the fiber was preloaded with labelled internal standards to perform calibration under a kinetic approach [5].

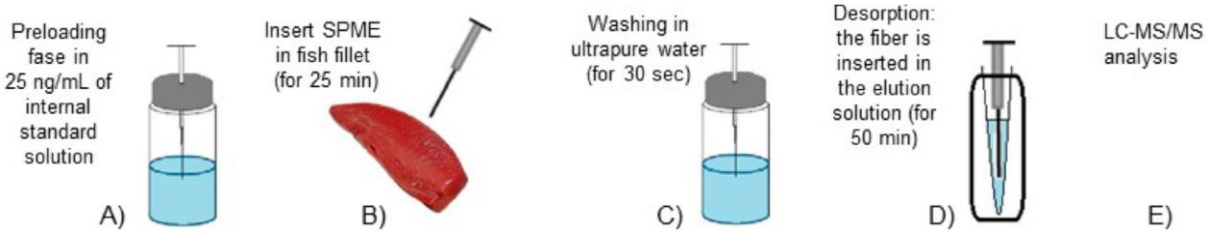

Fig. 6. The SPME procedure applied for the analysis of plasticizer.

Results

Linearity and limit of quantification were evaluated for several plasticizer using matrix-matched calibration curves and following the IUPAC recommendations, R^2 values ranged between 0.992 and 0.997 and MDLs from 0.8 to 3.7 ng/g, respectively. Low but consistent absolute recoveries, back-calculated through estimated concentration values, were also obtained (from 82% to 119%). Analysis of blanks showed that the method provided precise control of the background contamination and in most of the cases, the residual levels in the procedural blanks were beneath the instrument detection limit.

Average matrix factors determined by comparing the analytes responses in pure solvent with the response obtained in post-spiked SPME extracted samples indicated no significant matrix effects (Table 1)

Table 1. ESI-MS matrix effect measured from different marine invertebrates. Data indicates average matrix factor (MF) with RSD. For a given analyte in a specific extracted matrix, MF larger than 120% represents ionization enhancement, whereas values smaller than 80% represent ion suppression

Compound	*Porites* Lobata		*Petrosia* sp		*Tridacna* maxima	
	MF	RSD, *n*=5	MF	RSD, *n*=5	MF	RSD, *n*=5
MEHP	100	4	97	4	93	4
DMP	98	3	100	3	93	5
DEP	99	4	96	3	92	3
DBP	99	4	95	4	95	4
BBzP	100	3	96	4	94	3
DEHP	101	5	97	5	94	3

Discussion/Conclusions

In conclusion, we demonstrated that SPME and LC-MS/MS are applicable to quantification of the microplastic associated contaminants in marine organism. Satisfactory performance in terms of sensitivity were obtained within 15 minutes extraction time. Control of background contamination was enhanced compared to classical solvent extraction method, enabling the improvement of the quantitation limits. *In vivo* experiments with the mollusc *Tridacna* maxima did not show any negative effect on the health status, therefore the method may be applied for *non lethal* measurements on bioindicators.

References

1. A. L Andrady, *Marine Pollution Bulletin*, 62, (2011) pp 1596–1605
2. F. Saliu, S. Montano, B. Leoni, M. Lasagni,, P. Galli *Marine pollution Bulletin* 142, (2019). pp 234–241
3. F. Saliu, S. Montano, M. , Lasagni,, P. Galli *Journal of chromatography A*(2020)., 460852
4. F Saliu, S Montano, BW Hoeksema, M Lasagni, P Galli *Analytical Methods* 12 (2020), pp 1935-1942
5. J. Pawliszyn, Solid-Phase Microextraction—Theory and Practice, Wiley-VCH, New York, 1997.

Structural investigations on "green" alkyl ether sulfates by direct injection mass spectrometry

***M. A. Acquavia*[1,2], A. Onzo[1], T.R.I Cataldi[3], M. Ligonzo[1], D. Coviello[1], R. Pascale[1], G. Martelli[1], M. Bondoni[2], L. Scrano[4] and G. Bianco[1]**

[1]Università degli Studi della Basilicata, Dipartimento di Scienze, Via dell'Ateneo Lucano 10, 85100, Potenza, Italy, [2]ALMAGISI s.r.l, Corso Italia, 27, 39100, Bolzano, Italy, [3]Università degli Studi di Bari Aldo Moro, Dipartimento di Chimica, via E. Orabona 4, 70126, Bari, Italy, [4]Università degli Studi della Basilicata, Dipartimento delle Culture Europee e del Mediterraneo: Arch., Ambiente, Patrimoni Culturali, Via Lanera, 20, 75100 Matera, Italy.

Keywords: *Green surfactants, sodium coceth sulfate, tandem mass spectrometry*

Introduction

Alkyl ether sulfates (AESs) represent one of the major class of anionic surfactants used in soaps and detergent formulations [1]. Due to their favorable physicochemical characteristics, they are currently employed also in many fields of technology and research, such as for the enhancement of active ingredients' efficacy in pharmaceutical and agricultural formulations, or in biotechnological and industrial processes. Like all the surfactants, after their use AESs as well as their products, are mainly discharged into sewage treatment plants and then dispersed into the environment, through effluent discharge into surface waters and sludge disposal on lands [2]. As such, they are among the most relevant organic pollutants of anthropogenic origin which cause eutrophication and acidification of rivers and lakes [3]. Besides, the use of detergent-contaminated water for cultivation reduces the photosynthetic rate and chlorophyll content in plants [4]. Due to the growing awareness of environmental issues related to the extensive use of tensioactives and to the increasing consumer demand for products that are both more biocompatible and efficient, milder and biodegradable, the use of "green surfactants" has recently being proposed [5,6]. Green surfactants are defined as bio-based amphiphilic molecules obtained from renewable raw materials and whose synthesis results in a less CO_2 liberation compared to the production of conventional petrolchemicals-based compounds [7]. Several renewable raw materials could serve as starting compounds for surfactant synthesis, such as fatty acids, carbohydrate sources and organic acids; clearly fatty acids or sterols contribute to the hydrophobic part of green tensioactives while sugars and amino acids contribute to the hydrophilic moiety [7]. Fatty acids could be recovered from a wide range of vegetable oils; as example, fatty acids deriving from coconut, palm, and palm kernel oils are used to obtain substantial yields of hydrophobic surfactants. Anyway, regardless of their derivation source, different oleochemical transformations, hydrogenation, hydrolysis, trans-esterification as well as certain specific modifications of fatty acids to yield various surfactants and surfactant precursors are needed.

Coconut oil is the base ingredient of the surfactant sodium coceth sulfate (CES), i.e. an alkyl ether sulfates mixture added in a lot of cleaning products and detergents defined as non-aggressive and biodegradable, and it is obtained as the sodium salt of the sulfate esters of the polyethylene glycol ether of coconut alcohols [8].

To date, no structural investigations on green alkyl ether sulfates constituting CES have been made. The length of their alkyl chains and the degree of ethoxylation in their chemical formula ($C_xH_y(OCH_2CH_2)_nOSO_3Na$) remain still unknown, therefore making difficult their identification in products that are marketed with the "eco-frindly" label. Thus, in this work a structural characterization of coceth sulfate was performed, for the first time, by direct-injection ESI(-)-LTQ-MS and MS/MS technique.

Materials and Methods

A methanolic solution of commercial coceth sulfate raw material was analysed by direct-injection into the ESI-LTQ-MS instrument, in order to investigate the structure of the green alkyl ether sulfates constituting it. Full-scan MS experiments were performed in the range *m/z* 100–1500 and negative ion ESI-MS was used for the detection of the intact AESs of CES. To identify the alkyl chain length "*x*" and the degree of ethoxylation "*n*" of all the species corresponding to the *m/z* signals occurring in the

MS spectrum of CES, an in-house database of putative molecular formulae, written in RStudio software (https://www.r-project.org/), was used. For confirming the proposed structures, tandem mass spectrometry (MS/MS) analyses were performed on single members of CES MS spectrum. Tandem mass spectrometry experiments were conducted by using Collision Induced Dissociation (CID) as fragmentation technique and the collision energy was optimized for each precursor ion, between 0.9-1.5 eV of applied electrical potential.

Results

ESI(-)-LTQ-MS analysis of commercial CES revealed a well-defined and asymmetric molecular weight distribution. There were apparently two ion series with 44 Da apart within the series and 28 Da apart between the series. Thus, the presence of two alkyl homologues, whose the alkyl chain differed for a ethylene (C_2H_4) moiety, with a variable number of monomeric ($-CH_2CH_2O-$) units was suggested. Starting from the existing data reported in literature about alkyl ether sulfates and by using an in-house dedicated database of putative molecular formulas, alongside with MS/MS experiments, it was possible to characterize the alkyl chain composition and the number of ethylene oxide units of the anionic species occurring in CES raw material. Two series of oligomeric species characterized by a C12 and C14 alkyl chain, i.e. $[C_{12}H_{25}(OCH_2CH_2)nOSO_3]^-$ and $[C_{14}H_{29}(OCH_2CH_2)_nOSO_3]^-$ with *n* comprised between 0 to 7, were successfully ascertained.

Discussion/Conclusions

Direct-injection mass spectrometric and tandem mass spectrometric analysis were used to conduct, for the first time, a detailed investigation on the structure of biodegradable alkyl ether sulfates constituting sodium coceth sulfate. Due to its desirable ecological profile and to its good compatibility with eyes, skin and mucous membranes, CES is used in a wide variety of consumer products in which viscosity building and foam characteristics are of importance. Therefore, the definition of its characteristic *m/z* signals is remarkably useful for its detection in green labelled detergents. Direct-injection mass spectrometry turned out to be a simple and low-cost technology to that purpose, as it allowed to quickly define the *m/z* signals pattern of the CES, ensuring its identification in commercial products.

References

1. N.J. Turro, M. Grätzel, A.M. Braun; *Angewandte Chemie International Edition in English*, 19 (1980), pp 675-696.
2. G. G. Ying; *Environment international*, 32 (2006), pp 417-431.
3. S. González, D. Barceló, M. Petrovic; *TrAC Trends in Analytical Chemistry*, 26 (2007), pp 116-124.
4. B. R. Jovanic, S. Bojovic, B. Panic, B. Radenkovic, M. Despotovic; *health*, 5 (2010), pp 395-399.
5. K. Holmberg; *Current Opinion in Colloid & Interface Science*, 6 (2001), pp 148-159
6. T. Benvegnu, J. F. Sassi; *Carbohydrates in Sustainable Development I*, (2010), pp 143-164.
7. S. Rebello, A. K. Asok, S. Mundayoor, M. S. Jisha; *Environmental chemistry letters*, 12 (2014), pp 275-287.
8. S. Paria, K. C. Khilar; *Advances in colloid and interface science,* 110 (2004), pp 75-95.

Forensic

Molecular Networking: a useful tool for new psychoactive substances identification in seizures by LC–HRMS

C. Montesano[1], F. Vincenti[1,2], F. Di Ottavio[3], A. Gregori[4], D. Compagnone[3]and M. Sergi[3]

[1]Department of Chemistry, Sapienza University of Rome, Rome, Italy, [2]Department of Public Health and Infectious Disease, Sapienza University of Rome, Rome, Italy, [3]Faculty of Bioscience and Technology for Food, Agriculture and Environment, University of Teramo, Teramo, Italy, [4]Department of Scientific Investigation (RIS), Carabinieri, Rome, Italy

Keywords: *new psychoactive substances; LC–HRMS; molecular networking*

Introduction

New Psychoactive Substances (NPS) are a global concern because they are spreading at an unprecedented rate [1]; even if their commerce is still limited when compared to traditional illicit drugs the identification of NPS in seizures may represent a challenge because of the variety of possible structures. A number of proprietary or open software and platforms exist for the analysis of complex raw data from untargeted LC-HRMS analysis, however they only allow the annotation of known compounds, through library search [2]. Molecular Networking (MN) is a computational strategy that may aids visualization and interpretation of the complex data arising from MS analysis. MN is able to identify potential similarities between all MS/MS spectra within the dataset and to propagate annotation to unknown but related molecules [3].

Materials and Methods

Two seized samples (A and B) collected during investigative operations by RIS between September 2017 and December 2018 were extracted with 1 mL of methanol and analysed with an untargeted data-dependent acquisition approach by LC–HRMS. The obtained data were analysed using the MN workflow within the Global Natural Product Search (GNPS). Data of seizures were analysed along with raw files of standard mixtures containing synthetic cannabinoids and fentanyls; standard spectra were used to establish a representative network for both molecular classes. Library annotations were obtained from the comparison between the MS/MS spectra with several spectral libraries, including GNPS, NIST17, HMDB, and Massbank; at least 6 fragment ions should match the MS/MS spectra contained in those libraries with a cosine score of 0.7.

Results

All synthetic cannabinoids in the mixture were linked together in a molecular network despite exhibiting different fragmentation spectra. However, no synthetic cannabinoids were found in the seizures by using the MN-based screening method. For what concerns fentanyls, only drugs with the typical 188.143 and 105.070 fragments were combined in a network. By exploiting the networks obtained with standard solutions two unexpected fentanyls (m/z 393.197 and m/z 351.243) were found in the analyzed seizures (fig. 1): they were putatively identified as para-fluorofuranylfentanyl and (iso)butyrylfentanyl. Other m/z ratios in the seizures were compatible with fentanyl derivatives however they appeared to be minor constituents and even if it was not possible to assign a possible structure for all these compounds at this stage, the detection of possible impurities is a tool for investigations since they may might be an important marker for its source and are likely to be specific for a particular synthesis site or wholesaler.

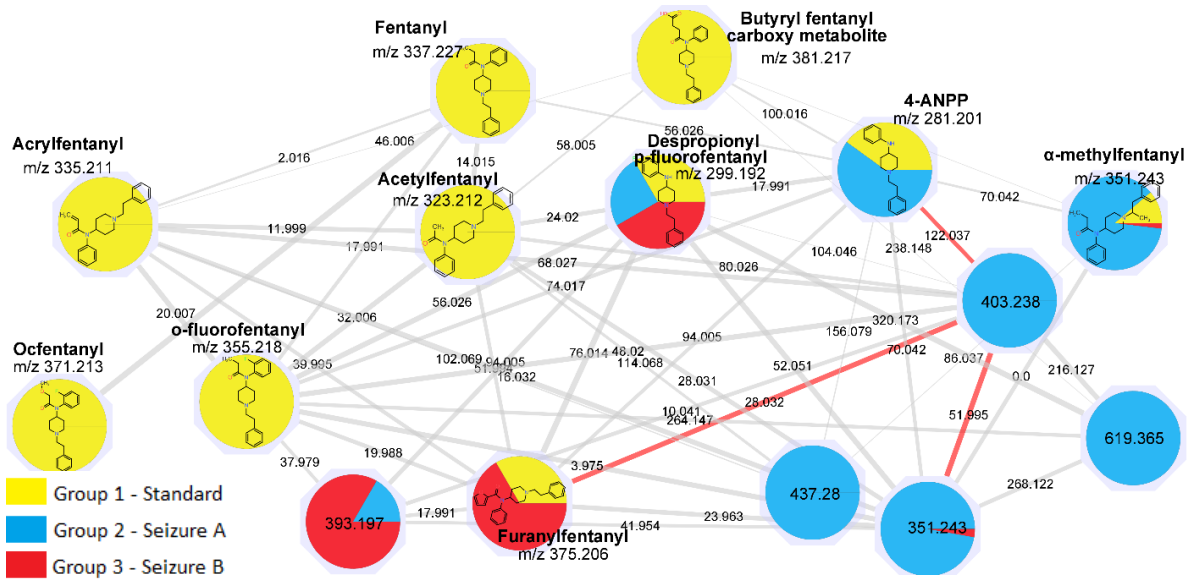

Fig. 7. Fentanyl network

Discussion/Conclusions

Results show the utility of the GNPS in the forensic field and especially for NPS analysis. In fact, on the one hand library matching with crowdsourced databases may allow the annotation of unexpected compounds, on the other hand MN allows to connect unknown compounds to "standard networks", simplifying the annotation of new drugs. As a proof of concept, two unexpected fentanyls were found in the analyzed seizures; they were putatively identified as para-fluorofuranylfentanyl and (iso)butyrylfentanyl by connection to a fentanyl standard network. It was also showed that structurally related compounds that do not share common fragments, such as some synthetic cannabinoids, form an integrated network.

This study demonstrates that GNPS is a very useful tool in forensic investigations especially for identification of new drugs and metabolites. In future, MN could represent an important tool in the forensic field, but to reach its full potential public sharing of data is needed.

References

1. A. M.Weinstein, P. Rosca, L. Fattore, and E. D. London, *Front. Psychiatry* 8 (2017), n. 156
2. L. L.Hohrenk, F. Itzel, N. Baetz, J. Tuerk, M. Vosough, and T. C. Schmidt, *Anal. Chem* 92 (2020), pp. 1898–1907
3. M. Wang, J. J. Carver, V. V. Phelan, L. M. Sanchez, N. Garg, Y. Peng, et al. *Nat. Biotechnol.* 34 (2016), pp. 828–837.

Analytical identification of some nootropics

M. Visentin[1], M.V. Picci[1], C. Guillou[2] and F. Reniero[2]

[1]Regional Forensic Science Police Office of Milan, [2]European Commission Joint Research Centre Ispra (Va)

Keywords: *case study, nootropics*

Introduction

In the last few years, seizures of substances not easily recognisable as drugs of abuse have increasingly been spreading.

New Psychoactive Substances (N.P.S.) and smart drugs analysis represents a challenge for forensic scientists due to the continue evolution in their development.

Here we report a case of a seizure of various powders following a sudden illness of a person. The use of different analytical techniques was necessary to characterize the seized materials.

Materials and Methods

At first sight, we supposed that the seizure consisted of eight types of different evidences. Firstly, we evaluated the characteristics of the powders with preliminary tests.

Then, we processed the samples in order to make them suitable to be analysed by gas-chromatography. We evaluated some extraction/dissolution solvents and the solutions were analysed by GC equipped with a DB5ms Ultra Inert column coupled to a single quadrupole mass detector.

Both mass spectra processing with NIST library and fragmentation studies did not immediately allow the recognition of the molecules but just gave little information about their structure. Other specialized mass spectral databases such as SWGDRUG mass spectral library [1] and Cayman Chemical Compounds Database [2] narrowed the field to a pharmaceutical class of molecules just for some samples.

For this reason, we involved in this study the Joint Research Centre of Ispra (VA) that supported us with NMR experiments.

Samples were dissolved in DMSO-d6 and ^{1}H, ^{13}C, ^{15}N spectra were recorded using a 600MHz NMR equipment. Moreover, 2D-NMR correlation experiments COSY, TOCSY, HMBC and HSQC were performed.

Results

Both preliminary information obtained from GC/MS analysis and NMR experiments have made possible to name seized substances.

Seven different molecules were identified: four nootropics i.e. mitragynine, noopept, phenibut and phenylpiracetam and three selective androgen receptor modulator (SARM) i.e. ibutamoren, ligandrol and RAD140. The former group is particularly interesting because some nootropics are considered drugs of abuse by Italian legislation [3].

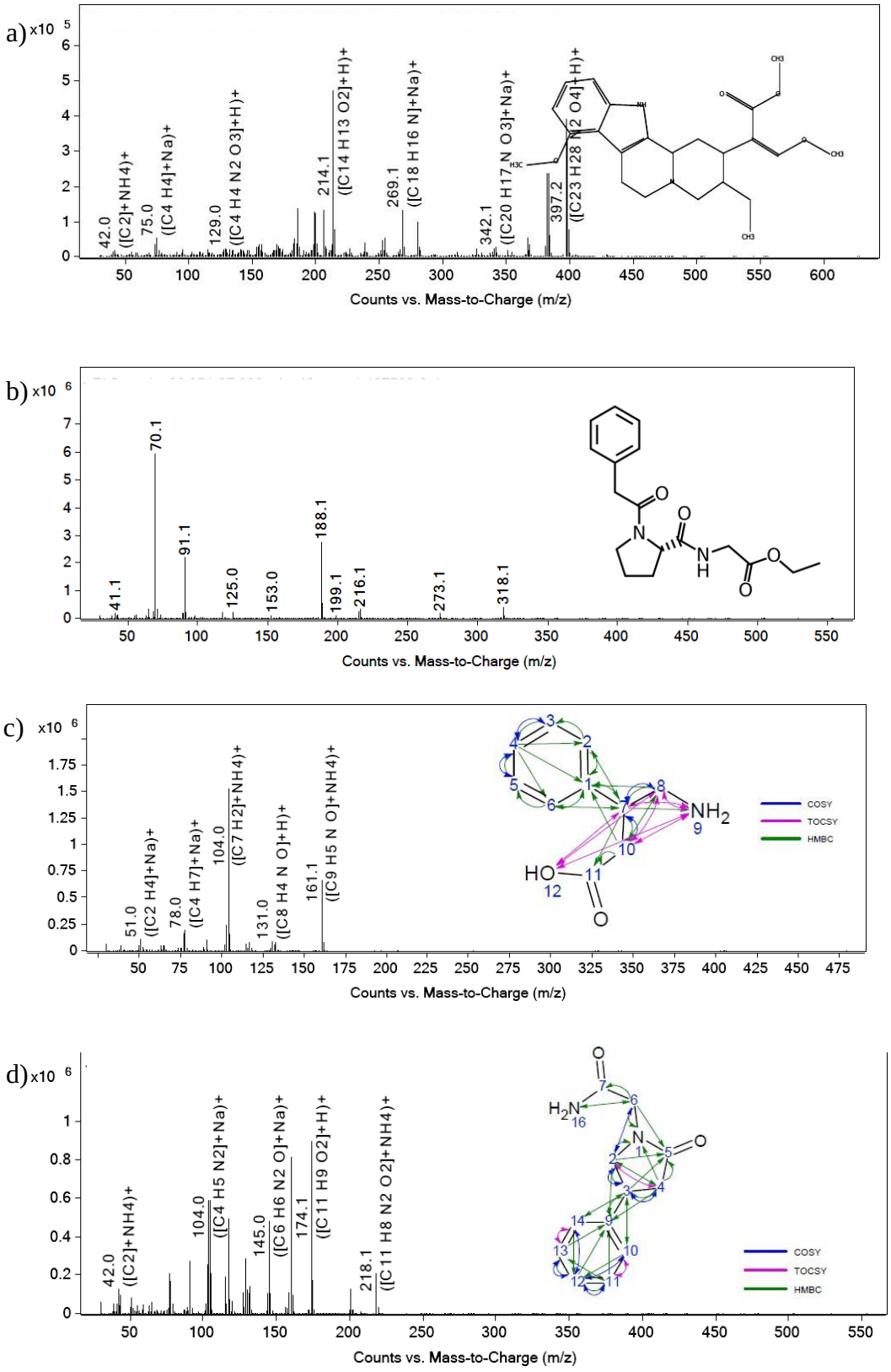

Fig. 1. The identified nootropics: a) and b) mass spectra and formula of mitragynine and noopept; c) and d) mass spectra and formula of phenibut and phenylpiracetam with 2D-NMR experiments interactions among atoms.

Discussion/Conclusions

DPR 309/90 categorizes only one out of four nootropics (i.e. mitragynine) as drug of abuse. To our knowledge, noopept, phenibut and phenylpiracetam have already been reported to EMCDDA from some European countries but they had not been documented in Italy yet.
This work highlights that mass spectrometry is a very useful technique for the identification of smart drugs and N.P.S. Nonetheless, the use of other analytical techniques to have a complete characterization of the molecules of interest is almost mandatory, especially for isomers recognition.

References

1. http://www.swgdrug.org/ms.htm
2. https://www.caymanchem.com/StructureDefinitions
3. D.P.R. 9 ottobre 1990, n. 309, *Testo unico delle leggi in materia di disciplina degli stupefacenti e sostanze psicotrope, prevenzione, cura e riabilitazione dei relativi stati di tossicodipendenza.*

Identification of 1-cP-LSD in stamps by UHPLC-HRMS and in silico fragmentation: a new LSD derivative

***C. D'Alfonso*[1], G. De Sangro[1], S. Napoletano[1], S. Detti[1], R. Scarpone[2], G. Migliorati[2] and M. Sergi[3]**

[1]Servizio Polizia Scientifica – Direzione Centrale Anticrimine – Dipartimento di PS – Ministero dell'Interno
[2]Istituto Sperimentale Zooprofilattico (IZS) di Teramo, [3]Facoltà di Bioscienze e Tecnologie Agroalimentari e Ambientali, Università degli Studi di Teramo

Keywords: *1-cP-LSD, HRMS, NPS*

Introduction

New Psychoactive Substances (NPS) phenomenon is constantly evolving and every year a great number of new molecules are placed on the illicit market to satisfy the requests of "customers" and to elude controls by law enforcement. The difficulties associated with the identification of NPS are well known, such as the absence of analytical standards and reliable analytical methods, and as a consequence non-targeted approach is needed by using sophisticated techniques, such as high resolution mass spectrometry (HRMS) with specific software for data mining [1,2].
Here we report the identification by HRMS supported by in silico fragmentation of a new lysergic acid diethylamide (LSD) derivative, 1-cyclopropionyl-d-lysergic acid diethylamide (1-cP-LSD; Fig. 1). The substance was extracted from stamps with the inscription "1cP-LSD" printed on one side and the correspondent molecular structure printed on the other side. Preliminary analysis by HPLC-TQ suggested the presence of this LSD derivative.

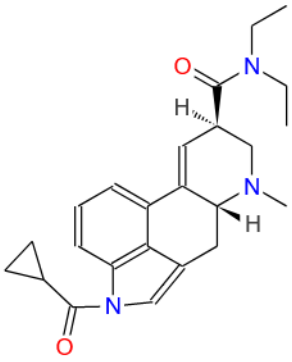

Fig. 1: Molecular formula of 1-cyclopropionyl-d-lysergic acid diethylamide (1-cP-LSD)

Materials and Methods

Preliminary analysis carried out in HPLC-TQ allowed to detect the ion at 392 m/z ascribable to the protonated 1-cP-LSD together with the m/z 69 fragment correspondent to the specific functionalization.
Sample has been extracted with a methanolic solution and analyzed by UHPLC Dionex UltiMate 3000 (RSLC) (Thermo Fisher Scientific) coupled with HRMS Q Extractive orbital trap (Thermo Fisher Scientific) equipped with HESI source.
Chromatographic separation has been carried out at 32°C, on Accucore aQ column (2.1 x 100 mm) with 2.6 µm particles using 5 mM ammonium formate in water and 5 mM ammonium formate in methanol containing 0.1% formic acid at a constant flow rate of 0.400 ml/min.
Mass spectrometer has been set in FullScan-ddSM2 acquisition mode which allows to set up MS/MS experiments on the ions above noise in order to have both a high resolution spectrum and the ions fragmentation in absence of any preliminary information.
The *in silico* fragmentation analysis has been carried out by means of Mass Frontier software.
Spectra resulting from analysis have been compared with on-line databases running on Compound Discoverer 2.0, Sieve and ChemSpider.

Results

Spectrum associated to the main chromatographic peak presents the same fragmentation pattern of 1-cP-LSD resulting from *in silico* fragmentation: 349.19-291.15-74.10-69.03 m/z fragments deriving from m/z 392.93 ion, ascribable to the protonated 1-cP-LSD (Fig. 2).

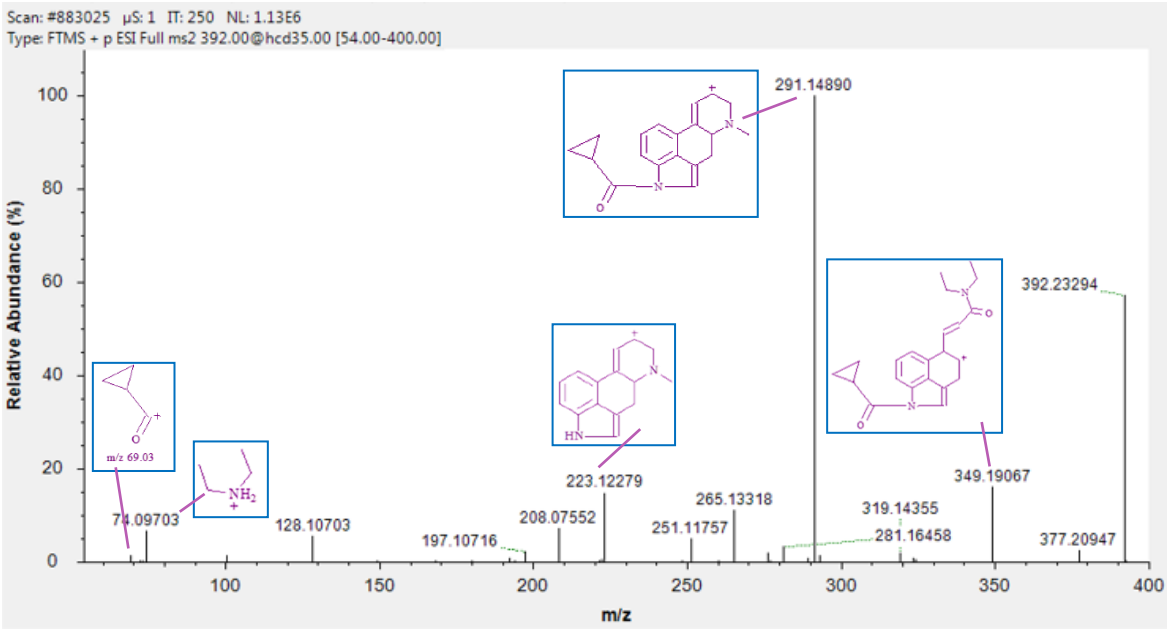

Fig. 2: Fragmentation spectrum of *392 m/z ion acquired in FullScan-ddSM2 acquisition mode.*

Discussion/Conclusions

Fragmentation spectra obtained by MS/MS experiments match with those resulting from *in silico* calculations on 1-cP-LSD. The exact identification is also the result of on-line databases consulting by means of Compound Discoverer 2.0, Sieve and ChemSpider. Nevertheless, third level identification is not possible due to the absence of 1-cP-LSD molecule in the databases.
Finally, the second level identification is the result of exact mass data on molecular peak (elemental composition) and the correspondence of in silico calculations with experimental fragmentation.

References

1. C. Montesano, G.Vannutelli, F.Fanti, F.Vincenti, A.Gregori, A.R.Togna, I.Canazza, M. Marti, M. Sergi; *Journal of Analytical Toxicology*, 41 (2017), pp 688-697
2. N. Fabresse, I.A. Larabi, T. Stratton, R. Mistrik, G. Pfau, G. Lorin de la Grandmaison, I. Etting, S. Grassin Delyle, J.-C Alvarez; *Drug Testing and Analysis*, 11 (2019), pp 697-708

Pharma

A direct measurement of serum carnosinase activity for the discovery of competitive inhibitors

E. Gilardoni[1], A. Artasensi[1], L. Fumagalli[1], A. D'Amato[1], M. Carini[1], G. Aldini[1] and Luca Regazzoni[1]

[1] Department of Pharmaceutical Sciences, Università degli studi di Milano, via Mangiagalli 25 20133 Milan Italy

Keywords: *LC-MRM; carnosinase; inhibitors*

Introduction

Serum carnosinase (CN1; EC. 3.4.13.20) is a M20 family metalloprotease produced in the brain that reaches the blood through the cerebrospinal fluid. It is the main enzyme involved in carnosine metabolism in humans [1]. Carnosine has several properties, such as metal chelating, buffering and carbonyl scavenging. Therefore, carnosine has potential mitigating effects in oxidative stress-based diseases such as metabolic syndrome, diabetes, and atherosclerosis [2]. The pharmacological effects of carnosine are well established in animal models with no serum CN1, although in humans carnosine is less effective owing to carnosinase-dependent metabolism.

In the past years, several strategies were developed to enhance carnosine availability, by the development of derivatives stable to carnosinase [3]. Only recently a new strategy tackling carnosinase inhibition have been explored [4]. Although carnosine metabolism has risen lot of attentions in the scientific community, methods aiming to study it and its action were poorly investigated.

Materials and Methods

An Exion LC-100 coupled to an API4000 mass spectrometer system (AB-Sciex) were used for the analysis. Serum samples were diluted in saline phosphate buffer (pH 7.4) and incubated with carnosine and/or other natural peptides for a determined time. The reaction was stopped by protein precipitation at 4 °C with 9 volumes of acetonitrile containing the internal standard carnosine ($^{13}C_3$) at a fixed concentration. After centrifugation, the supernatant was injected in LC system where the analytes were separated with a HILIC chromatography. Elution was achieved with a gradient method increasing the percentage of ammonium formate solution (100 mM pH = 3) over time. The triple quadrupole analyser worked in MRM mode for the quantification of the analytes.

Results

The system developed allows us to determine the serum hydrolytic rate of carnosine and its main natural analogues (i.e. homocarnosine, balenine and anserine) (Table 1).

Table 1: Histidine dipeptides serum hydrolytic rate

Histidyl-dipeptide	Substrate concentration (µM)	Serum hydrolytic rate (nmol/µL/h)
Carnosine	50	1.33 ± 0.032
Homocarnosine	50	0.018 ± 0.003
Anserine	50	0.45 ± 0.057
Balenine	50	0.0501±0.008

Moreover, the maximum hydrolytic rate and the K_m of the serum on carnosine was determined (i.e. V_{max} = 2.513±0.14 nmol/µL/h K_m = 169.3±29.04 µM). Several competition experiments were carried out to identify putative hit as carnosinase inhibitors. (Figure 1)

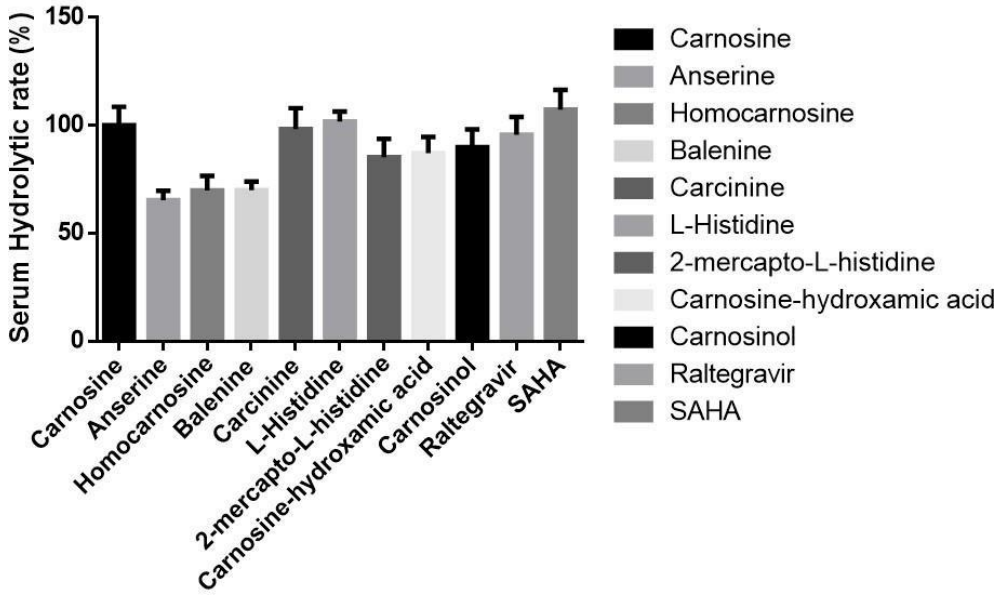

Fig.1: residual serum hydrolytic rate of carnosine (%) in presence of putative inhibitors

Discussion/Conclusions

We developed a direct and accurate method for the evaluation of serum hydrolytic rate of histidine dipeptides. Histidine dipeptides have quite different hydrolysis rates based on their structures with the following descending order: carnosine > anserine > balenine > homocarnosine. The maximum serum hydrolytic rate for carnosine and the K_m are comparable to the one determined on the pure carnosinase enzyme in literature, thus indicating that carnosinase is the main enzyme responsible for carnosine hydrolysis in serum. Several compounds have been tested to identify putative hits as carnosinase inhibitors. Only anserine, balenine and homocarnosine have shown a good activity even if they are not able to completely compete with carnosine degradation. These experimental data were used for the development of a virtual screening model and molecules identified are currently being synthetized for further evaluation as putative carnosinase inhibitors.

References

1. M. Teufel, V. Saudek, J-P. Ledig, A. Bernhardt, S. Boularand, A. Carreau, N. J. Cairn, C. Carter, D. J. Cowley, D. Duverger, A. J. Ganzhorn, C. Guenet, B. Heintzelmann, V. Laucher, C. Sauvage, T. Smirnova; *The Journal of Biological Chemistry*, 278 (8) (2003), pp. 6521-6531
2. A. A. Boldyrev, G. Aldini, W. Derave; *Physiological Review*, 93 (2013), pp 1803-1845
3. E. J. Anderdon, G. Vistoli, L. A. Katunga, K. Funai, L. Regazzoni, T. B. Monroe, E. Gilardoni, L. Cannizzaro, M. Colzani, D. De Maddis, G. Rossoni, R. Canevotti, S. Gagliardi, M. Carini, G. Aldini; *The Journal of Clinical Investigation*, 128 (12) (2018), pp. 5280-5293
4. J.Qui, S. J. Hauske, S. Zhang, A. Rodriguez‐Niño, T. Albrecht, D. O. Pastene, J. van den Born, H. van Goor, S. Ruf, M. Kohlmann, M. Teufel, B. K. Krämer, H‐P Hammes, V. Peters, B. A. Yard, A. Kannt; *Amino Acid*, 51 (2019), pp. 7-16

A two-quartet G-quadruplex topology of human KIT2 is conformationally selected by a perylene derivative

***S. Ceschi*[1], *E. Largy*[2], *V. Gabelica*[2], *C. Sissi*[1]**

[1]Department of Pharmaceutical and Pharmacological Sciences, University of Padova, v. Marzolo 5, 35131, Padova, Italy [2]Laboratoire Acides Nucléiques : Régulations Naturelle et Artificielle, Université de Bordeaux, Inserm & CNRS (ARNA, U1212, UMR5320), IECB, 2 rue Robert Escarpit, 33607 Pessac, France

Keywords: *Native ESI-MS, G-quadruplex, perylene ligands*

Introduction

Guanine-rich DNA/RNA sequences may arrange into tetra-helical secondary structures called G-quadruplexes (G4s). G-quadruplexes are promising targets for innovative anticancer therapy. Indeed, they are enriched in the promoters of several oncogenes and for many of them a role in the downregulation of the gene expression has already been demonstrated. Hence, many efforts are being made to find ligands that selectively bind to and stabilize them. Drug design is often based on the available high-resolution structures, obtained for the thermodynamically stable forms. However, the complexity of the G-quadruplex folding landscape has clearly emerged in recent years, with the discovery of intermediate conformations that persist on the second to the minute time scale.[1] This is the case of the KIT2 G-quadruplex forming sequence, found within human *c-KIT* promoter, for which we recently identified a long-lived folding intermediate, characterized by guanine stacking in alternating orientation (as determined by circular dichroism).[2] Given the rate of transcriptional processes, a physiological role of this arrangement should not be excluded.

Materials and Methods

In the present study, we applied native electrospray mass spectrometry (ESI-MS), circular dichroism (CD) spectroscopy, and electrophoretic mobility shift assays (EMSA). Native electrospray mass spectrometry (ESI-MS) separates the different G-quadruplex scaffolds according to the number of the DNA strands that are involved, and the number of K^+ ions that are selectively coordinated in the structure, which reflects the number of consecutive G-quartets.[3],[4] Thus, it can be exploited to investigate ligand binding to polymorphic G4 forming oligonucleotides, such as KIT2.

Results

Native ESI-MS experiments performed at low K^+ concentration, allowed us to detect and characterize the kinetically favoured G-quadruplex topology of KIT2 by means of K^+ binding stoichiometry. Interestingly, the presence of a single specifically coordinated K^+ ion, revealed its two-quartet scaffold.
Furthermore, we identified the perylene derivative K20 as able to drive the conformational selection of this topology, against the more thermodynamically stable three-quartet one.

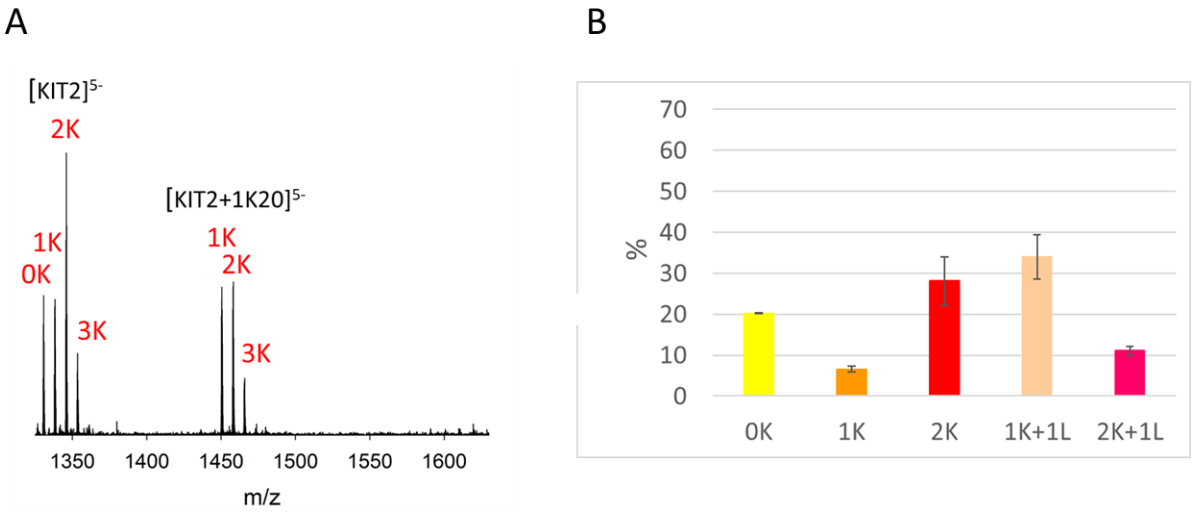

Fig. 1. A) ESI-MS spectra of 10 µM KIT2 in 100 mM TMAA, 3 mM KCl, after incubation with one equivalent of K20, zoomed on the 5-charge state. B) Reconstructed relative distribution of specific K^+ adducts. Error bars are obtained from standard deviation of three replicates.

Discussion/Conclusions

The present study paves the way to the evaluation of the physiological role played by the KIT2 folding intermediate and hopefully to the resolution of its structure, with the final aim to design selective ligands that can be exploited for the regulation of *c-KIT* expression.

References

1. A. Marchand, V. Gabelica, *Nucleic Acids Res.* 44 (2016) 10999–11012.
2. R. Rigo, W.L. Dean, R.D. Gray, J.B. Chaires, C. Sissi, *Nucleic Acids Res.* 45 (2017) 13056–13067.
3. A. Marchand, V. Gabelica, *J. Am. Soc. Mass Spectrom.* 25 (2014) 1146–1154.
4. J. Gros, F. Rosu, S. Amrane, A. De Cian, V. Gabelica, L. Lacroix, *Nucleic Acids Res.* 35 (2007) 3064–3075.

The Knoevenagel condensation catalyzed by task-specific ionic liquids: a gas-phase study to highlight the reaction mechanism

C. Salvitti[1], A. Troiani[1], I. Chiarotto[2] and G. de Petris[1]

[1]Dipartimento di Chimica e Tecnologie del farmaco, Università di Roma "Sapienza", P.le Aldo Moro 5-00185 Roma (Italy); [2]Dipartimento di Scienze di Base e Applicate per l'Ingegneria, Università di Roma "Sapienza", via del Castro Laurenziano 7-00161 Roma (Italy); chiara.salvitti@uniroma1.it

Keywords: *Ionic liquids, reaction monitoring, gas-phase chemistry*

Introduction

Ionic liquids (ILs) represent a fascinating class of stable compounds that, owing to their recyclability and ignorable vapour pressure, are commonly used as green solvents in a variety of chemical reactions [1]. The possibility to incorporate suitable functional groups into the cationic or anionic scaffold allows one to implement their catalytic properties and design task-specific derivatives for synthetic applications [2]. In particular, the Knoevenagel condensation between an aldehyde and an activated methylene compound can be considered an archetypal reaction widely used in various fields, such as in pharmaceutical chemistry, for the formation of carbon-carbon bonds. In this regard, some examples are the syntheses of the antimalarial Lumefantrine [3] and a series of tyrosine kinase inhibitors called trifostintins [4]. According to these important implications, the employment of a well-designed basic catalyst can be useful to optimize the selectivity of the process. Likewise, the elucidation of the reaction mechanism is essential to finely design the features of the catalytic system, although it is often hindered by the instability of the elusive intermediates that prevents their isolation and characterization. To this end, the high sensitivity and speed of the electrospray ionization mass spectrometry (ESI-MS) have been exploited in this study to efficiently intercept the ionic reactants, intermediates and products of the Knoevenagel condensation, characterize them by collision-induced dissociation (CID) experiments and highlight the action mechanism of the ionic liquid 1-methyl-3-carboxymethylimidazolium chloride (MAI.Cl) as reaction catalyst.

Materials and Methods

1-methyl-3-carboxymethylimidazolium chloride (MAI.Cl) was synthesized according to the literature procedure [5] and loaded in catalytic quantity (10% mol) into a room temperature-stirred mixture of an aromatic aldehyde (1.0 mmol) and an activated methylene compound (1.0 mmol). All the reagents were purchased from Sigma-Aldrich Ltd (St. Luis, MO, USA) and used without further purification.

The progression of the condensation was monitored over the time by sampling at regular intervals 2 μL of the reaction blend and diluting them in acetonitrile to a concentration of 10^{-4} M.

Full scan mass spectra were acquired by using an LTQ-XL linear ion trap (Thermo Fisher Scientific) equipped with an atmospheric pressure ion source (ESI and APCI) and operating in the positive/negative ion mode.

MS^n experiments were performed by isolating the reactant, intermediate and product ions with a width of 1 *m/z* and subjected them to dissociation in the presence of helium as collision gas.

All the displayed spectra were processed by using Xcalibur 2.0.6 software supplied with the instrument.

Results

The task-specific activity of the MAI.Cl ionic liquid was verified towards two model substrates, C-H acid $CN(CH_2)CO_2Et$ and *p*-metoxybenzaldehyde, in the absence of solvents. Under these reaction conditions, excellent yields (> 90%) of the corresponding condensation product were obtained and characterized by H- and ^{13}C-NMR spectroscopy.

According to previous studies [6,7] and following the deprotonation of the acid cyano-methylene compound by the basic catalyst, the reaction proceeds through a nucleophilic attack of the catalyst [6] or of the deprotonated substrate [7] to the aldehydic carbonyl group leading to two different intermediates and consequently to two possible reaction pathways (Figure 1).

To shed light on the actual mechanistic picture, the reaction mixture was sampled after different prefixed times and analysed by electrospray ionization mass spectrometry in both polarities. In the presence of the MAI.Cl catalyst, ionic reagents, intermediates and products are simultaneously detected and subjected to collision induced dissociation to gain structural information.
To understand the role played by the chloride anion or by the acetate moiety on the MAI cation in the deprotonation of the methylene compound, the synthetic procedure was extended to different catalysts and the reproducibility evaluated on several substrates, also varying the C-H acidity of the methylene species.
Each reaction was therefore monitored by ESI-MS to establish the current mechanistic path and define the kinetic efficiency of the catalyst employed.

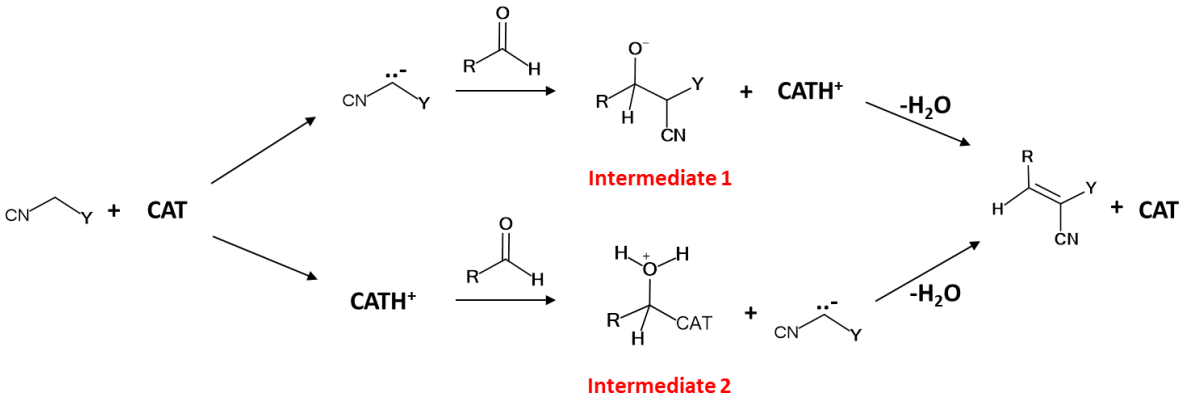

Fig. 8. Two suggested pathways for the Knoevenagel condensation.

Conclusions

The mechanism of the Knoevenagel condensation performed by the MAI.Cl catalyst was investigated by ESI- and CID- mass spectrometry at room temperature and under solvent-free conditions. The role of the anion and cation in deprotonating the cyano-methylene substrate was evaluated and the reaction intermediate structurally characterized. Accordingly, a possible mechanistic picture was highlighted and experimentally verified for different substrates and catalysts.

References

1. S. K. Singh, A. W. Savoy; *Journal of Molecular Liquids*, 297 (2020), p 112038.
2. R. Giernoth; *Angewandte Chemie Int. Ed.*, 49 (2010), pp 2834-2839.
3. U. Beutler et al., *Organic Process Research & Development*, 11 (2007), pp 341-345.
4. a) M. L. Lyall et al., *Journal of Biological Chemistry*, 264 (1989), pp 14503-14509; b) M. Z. Dieter et al., *Biochemical Pharmacology*, 61 (2001), pp 215-225.
5. F. F. Oliveira, M. R. dos Santos, et al.; *Journal of Organic Chemistry*, 76 (2011), pp 10140-10147.
6. P. Dell'Orco, J. Brum, et al.; *Analytical Chemistry*, 71 (1999), 5165-5170.
7. A. R. Moosavi-Zare, M. A. Zolfigol, et al.; *Chemical Engineering Journal*, 248 (2014), pp 122-127.

Characterisation of the pre-processing in MALDI-MSI mass spectra analysis to build sensitive classification models for therapy assessment in thyroid cancer

***G. Capitoli*[1], *I. Piga*[2], *F. Clerici*[2], *M. Petrosino*[1], *F. Pagni*[3], *F. Magni*[2], *S. Galimberti*[1]**

[1] Bicocca Bioinformatics Biostatistics and Bioimaging B4 Center, School of Medicine and Surgery, University of Milano - Bicocca, Monza, Italy, [2] Proteomics and Metabolomics Unit, School of Medicine and Surgery, University of Milano - Bicocca, Vedano al Lambro, Italy, [3] Pathology, School of Medicine and Surgery, University of Milano - Bicocca, San Gerardo Hospital, ASST Monza, Italy

Keywords: *pre-processing, MALDI-MSI, thyroid carcinoma*

Introduction

Before the construction of a classification model from MALDI-MSI mass spectra, data need pre-processing in order to smooth the intra and inter-sample variability in intensities and *m/z* localisation due to technical variations as sample preparation and mass spectrometric instrumentation. Pre-processing is recognized as a standard procedure, but in the context of biomarkers research, no guidelines exist.

The motivating clinical context is represented by thyroid cancer where the actual gold standard to exclude the malignant nature of thyroid nodules in the clinical routine is defined by thyroid Fine Needle Aspirations (FNAs) biopsies [1]. Approximately the 20-30% of cases have an indeterminate for malignancy final report, but after surgery the 80% of these thyroid nodules are benign. This overtreatment has of course important consequences in the quality of life of the patients and high healthcare costs [2]. A clinical study was conducted with the aim to build a diagnostic model for the characterization of malignancy thyroid nodules based on proteomic data.

Materials and Methods

Mass spectrometry is one of the most important analytical tools able to obtain information regarding the molecular composition of a sample. Statistical analyses of these data were based on a considerable number of Region of Interests (ROIs), according to the morphological triage performed by the pathologist. The mass spectra of each ROI represents the proteomic signature of benign and malignant thyrocytes cells that were investigated through the comparison of *m/z* signals. The whole data-set was partitioned into two groups, i.e. the training set and the validation set, with the aims of building a classification model and confirming the findings, respectively. The pre-processing phase is generally divided in five steps: baseline subtraction, smoothing, normalisation, alignment and peak picking. The baseline noise, related to electrical noise and chemical impurities in the sample, is estimated and subtracted from the original spectrum, bringing all the intensities to start from zero. Smoothing process removes false positive peaks corresponding to artefacts, smooth out fluctuations and highlight the shape of the spectrum. Normalization is indispensable to bring all the spectra to the same intensity range in order to compare spectra not only within the same analyses but also among different ones. Slightly differences in *m/z* values have be recognized as the same and aligned with the same *m/z* names, so peaks in different spectra that represent the same protein species have to be aligned to be matched. Finally, peaks detection identifies peaks in the mass spectrum. Peak picking extracts the information regarding the only true informative peaks to be retained for the statistical analyses.

We proposed here a strategy of pre-processing that performs, for the two groups in the training set (benign vs malignant thyroid lesions), a separate pre-processing with intra- and inter-patients filters in the training set that are suggested before performing the logistic regression model with a Lasso regularization method. Subsequently, baseline subtraction, smoothing, normalisation were performed separately for each patients in the validation set and in a final step they were aligned to the training model.

Specifically, peak peaking was performed considering peaks present in at least the 25% of the training spectra within sample and between benign and malignant spectra, were retained for statistical purpose.

m/z values of the relevant peaks in the training set, present in a tolerance window of ±4 Da were converged to the same names value and validation sets were realigned to them.

Results

In the application of the workflow we proposed to the motivating clinical study, a considerable number of ROIs was used. For the two groups in the training set (45 benign vs 36 malignant ROIs), a separate pre-processing step with intra- and inter-patients filters was conducted, and the Lasso method selected twenty features as the most discriminant to correctly distinguish benign and malignant training samples. The model was further validated on a median of 11 ROIs for each patient, using the overall average spectra of all the analysis, the spectra from each ROI and a pixel by pixel approach using all the single spectra of the MALDI-MSI analysis. Successful results were obtained, with the correct classification of different types of thyroid lesions being achieved (73.3% for the overall average spectra and 86.6% in the ROIs and pixel-by-pixel analyses) [3].

Discussion/Conclusions

The choice of the pre-processing process puts the basis for the construction of a sensitive classification model. Traditionally, when the aim of a MALDI-MSI analysis is a classification model, data are divided in a training and a validation subgroup, but nobody seems to consider this aspect in the pre-processing framework. We developed a unified strategy for the pre-processing of the training and validation set that allowed the construction of a performing classification model able to successfully discriminate benign and malignant thyroid lesions based on proteomic data. The direct consequences of successful results could be the use of MALDI-MSI proteomics and a correct statistical framework, as a complementary approach for the pathologist diagnosis of indeterminate for malignancy thyroid nodules. This could reduce the number of unnecessary thyroidectomies, healthcare costs and potential need for a lifelong hormone replacement therapy for patients.

References

1. G. Russ, SJ. Bonnema, MF. Erdogan, C. Durante, R. Ngu,L. Leenhardt; *European Thyroid Journal*, 6 (2017), pp 225-237.
2. S. Trombetta, G. Attinà, G. Ricci, P. Ialongo, and P. Marini. *International Journal of Surgery*, 28 (2016), pp S59– S64.
3. G. Capitoli, I. Piga, S. Galimberti, D. Leni, AI. Pincelli, M. Garancini, F. Clerici, A. Mahajneh, V. Brambilla, A. Smith, F. Magni, F. Pagni; *Cancers*. 11 (2019), p 1377.

Premio Sindona

A non-targeted high-resolution mass spectrometry approach for the assessment of the geographical origin of durum wheat

***D. Cavanna*[1,2], *C. Loffi* [1,2], *C. Dall'Asta* [2], *M. Suman*[1]**

[1]Advanced Research Laboratory, Barilla G. e R. Fratelli S.p.A., Via Mantova 166-43122 Parma (Italy)
[2]Department of Food and Drug, University of Parma, Parco Area delle Scienze 95/A-43124 Parma,(Italy)

Keywords: *wheat, geographical origin, non targeted mass spectrometry*

Introduction

The declaration of durum wheat geographical origin, sometimes claimed on pasta labels, represent an added value to the commodity, especially if it is made only with wheat coming from a specific nation or region (i.e. "100% Italiano").
The chemical composition of wheat, indeed, is partially related to the cultivation soil and to the climate conditions, that are different by geographical areas and that can affect the quality and subsequently the commercial value of this raw material [1].
For these reasons, the false origin declaration of this commodity or the creation of fraudulent mixtures of wheat coming from different countries could represent an illegal economical gain for wheat sellers and this is the reason why the attention of pasta producers in the development of methods able to assess the geographical origin of wheat largely increased in the last decade [2].
The aim of this work was the development of a non-targeted Liquid Chromatography–High Resolution Mass Spectrometry study for the detection of new chemical markers responsible of the geographical origin of wheat and able to discriminate if the raw material comes from Italy, Europe or Extra Europe.

Materials and Methods

Authentic samples coming from different Italian, European and Extra European regions were collected during two years of harvesting, 2016 and 2018: the 2016 campaign was used for the model creation and for markers selection, while the 2018 campaign was used for model and markers validation.
91 samples were collected during the 2016 campaign (56 from Italy, 21 from other European countries and 14 from Extra European countries) and 49 samples were collected during the 2018 campaign (11 from Italy, 21 from other European countries and 17 from Extra European countries).
Samples were extracted with a mixture of Methanol:Water in the ratio 50:50 (v/v), subsequently shaken, centrifuged, and lastly filtered in HPLC vials.
UHPLC analysis was carried out with a reverse phase analytical column with a gradient elution. Mass spectrometry analysis was performed with a Thermo® Q-Exactive Orbitrap analyser equipped with an ESI ionization interface.
Raw data were processed with the Compound Discoverer software (Thermo Scientific) and chemometric data analysis was performed with SIMCA software (Umetrics).
A predictive OPLS-DA model was created and, subsequently, a new multivariate data elaboration study was executed in order to select markers responsible of the "Italian", "European" or "Extra European" origin of wheat [3].

Results

The predictive OPLS-DA model (figure 1) was able to correctly classify 100% of the samples used for its creation and approximately 80% of the samples of the test set.

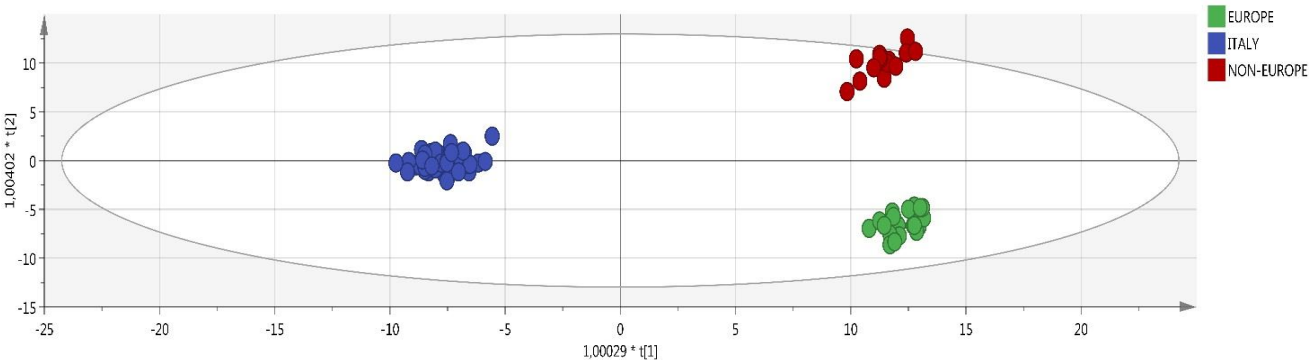

Fig. 9. ESI + OPLS-DA scores plot of 2016 wheat samples. Green dots: European samples; blue dots: Italian samples; red dots: Extra European samples;. R^2X (cum): 0.532 R^2Y (cum): 0.981 Q^2(cum): 0.900.

25 chemical compounds were selected and classified as "Italian" or "Not Italian" depending on whether they were present only or mostly in the Italian or in the not Italian samples; in addition, two molecules were selected as discriminant markers for the "Extra European" geographical origin of wheat; subsequently, a group of these molecules was putatively identified.

All the selected features were searched in the 2018 wheat samples and their presence or absence, together with their trends across the different geographies, were evaluated and compared with the results obtained with the 2016 samples used for the model creation. Comparable results were obtained between the two years. As example, table 1 shows the comparison of the area values of Vanillylactic acid (an "Italian" marker) across the different regions for the 2016 samples and for the 2018 ones.

Table 1 comparison of the mean area values (+/- Standard Error) of VanIllylactic Acid in the three geographical areas between the 2016 and the 2018 campaigns. First bar, "European wheat"; second bar, "Extra-European wheat"; third bar, "Italian wheat"

NAME	2016 CAMPAIGN	2018 CAMPAIGN
Vanillylactic acid	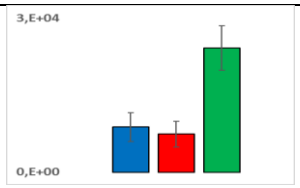	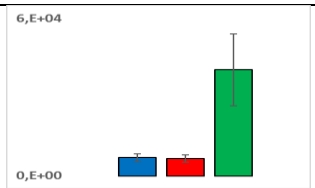

Discussion/Conclusions

The current study reported, for the first time, the possibility to discriminate the geographical origin of durum wheat samples based on a HRMS non targeted approach, assessing its origin as 100% Italian, European or Extra European.

The study was designed using a real scenario approach and increasing the variability by including a wide geographical diversity.

Therefore, the markers presented herein can be regarded as generally robust markers, not related to specific geographical area.

Further improvements should lead to the development of target methods focused on the detection of these specific molecules, that could be easily applied in quality control laboratories.

References

1. H. Zhao, B. Guo, Y. Wei, B. Zhang, S. Sun, L. Zhang, J. Yan ; *Journal Of Agricultural and Food Chemistry*, 59 (2011), pp 4397-4402.
2. J. Morin, P. Vermeulen, E. Maestri; J. Morin and M. Lees editors, *FoodIntegrity Handbook. A guide to food authenticity issues and analytical solutions*. Nantes 2018, pp. 101-114.
3. D. Cavanna, C. Loffi, C. Dall'Asta, M. Suman; *Food Chemistry*, 317 (2020), 126366

Proteomics and metabolomics strategies for biomarker discovery in Multiple Sclerosis: research of a molecular cross-talk between cerebrospinal fluid and tears

I. Cicalini[1], M. C. Cufaro[1], P. Lanuti[1], C. Rossi[1], D. Pieragostio[1], P. Del Boccio[1]

[1]*Center for Advanced Studies and TechnologyResearch (CAST)"G. d'Annunzio" University of Chieti-Pescara, Chieti, Italy*

Keywords: *Proteomics, Metabolomics, Multiple Sclerosis*

Introduction

Multiple Sclerosis (MuS) is a complex pathology whose physiopathological mechanisms are still unknown [1]. Therefore, the purpose of the following project was to investigate and to characterize the molecular repository of various biofluids, starting from the CSF, to highlight possible alteration of biological relevance. These aims were pursued by high throughput analysis such as Lipidomics and Proteomics application based on mass spectrometry.

Materials and Methods

CSF and Tears lipidomics approach, focusing on the acquisition on phosphatidylcholines and sphingomyelin was carry out for the comparison between MuS patients vs other neurological disorder patients and healthy controls. Flow cytometry analysis was used to sort and purify 106 Extracellular Vesicles (EVs) from untouched CSF and tears of MuS patients and healthy subjects. Purified EVs were analyzed with shotgun proteomics analysis.

Results

Using a lipidomic approach, we observed low levels of several sphingomyelins in CSF of MuS patients compared to other inflammatory neurological diseases. Starting by this result, we investigated the sphingomyelinase activity, showing a significantly higher enzyme activity in MuS and a high number of acid sphingomyelinase-enriched exosomes correlated to enzymatic activity. Furthermore, we shifted our attention to more peripheral biological fluids, carrying out lipidomics investigations in tears, in order to identify specific molecular pattern able to distinguish MuS patients from both healthy people and patients with similar symptomatology. Tears lipidomics highlighted 30 phospholipids significantly modulated and, notably, all the differential sphingomyelins resulted lower in MuS. These data suggested that the metabolic profiling of tears appears to reflect the pathological conditions of the CNS [2]. Finally, assuming that the communication between CSF and tears could be based on EVs, here we applied an optimized flow cytometer for the identification, subtyping and sorting of EVs from CSF and tears. We found, for the first time, microglia-derived and neural-derived EVs in tears. Purified EVs were analysed with shotgun proteomics, revealing that EVs from both CSF and tears of MuS patients conveyed similar proteins [3].

Discussion

Surprisingly more than 70% of the biological functions highlighted by proteomics analyzes are in common between CSF and tears, and only in the pathological condition. Tear "omics" investigation demonstrate that lacrimal fluid may represent an interesting source for molecular alteration in MuS diagnosis. According to our results tears seem to reflect the CNS pathological conditions, highlighting a molecular cross-talk with CSF, probably mediated by EVs. Finally, EVs in MuS carry a specific inflammatory, angiogenetic and immunological message, not only in the CSF but also in tears, opening the way to the identification of new potential biomarkers of MuS.

References

1. B. Macchi et al; *JNeuroimmunol*, 287 (2015), pp 80-7.
2. I. Cicalini et al; *Int J Mol Sci*. 1265 (2019).
3. D. Pieragostino; *J Proteomics*, 204 (2019).

POSTER PRESENTATIONS

Omics

Metabolomics applied to modelling an ageing metabotype by targeting senescence metabolism

D. Berardi[1] ***and N. J.W. Rattray***[1]

[1]University of Strathclyde

Keywords: *Ageing, Senescence, Metabolomics*

Introduction

Ageing is a complex and multifactorial process that significantly extends beyond biology and exerts a huge influence on public and economic aspects of society[1,2]. Therefore, understanding its mechanisms and how to regulate and/or repair them is a major challenge that can have huge implications on the health and life-span of an individual.

The past 80 years of ageing research has focused primarily on the identification of ageing phenotypes that exist during the lifespan of several organisms. For example, several studies have focused on chronic senescence, the stress response contributing to the gradual deterioration of cellular functions during the ageing process [3]. However, no reliable chemical biomarkers have been identified that can predict age-dependent decline [4]. In vitro studies with senescence induced cells could serve as an advantageous strategy for this purpose. Accordingly, scientists are trying to optimize X-ray senescence induction depending on the cell-type of interest [5,6], to enable a prompt, stable and effective cellular model of ageing. In recent years, metabolomics has gained attention within the biogerontology community as a powerful omics discipline for the identification of bioactive metabolites. The challenge of using metabolomics for ageing research is that it needs to be understood in the context of interactions with the genetic, transcriptional and protein levels – developing an integrative analytical approach [7,8].

Materials and Methods

In this context, we present an untargeted metabolomics approach used to understand a range of different cellular senescent metabolic phenotypes [9], induced by a range of x-ray sources [10]. Molecular Biology assays have been used to assess some of the known hallmarks of senescence including β-Galactosidase (β-Gal) activity, senescence-associated heterochromatin foci (SAHF), apoptosis resistance and metabolic reprogramming.

Results

X-ray irradiated cells (normal and tumour fibroblasts) showed senescence-like hallmarks especially at higher radiation dose: increased β-Gal expression (Fig. 1), the appearance of SAHF in their nuclei, decrease of apoptosis-dependent cell death and accelerated metabolism.

Untargeted metabolic analysis of irradiated cells revealed the partitioning of metabolic features depending on the delivered radiation dose and cell type (Fig. 2).

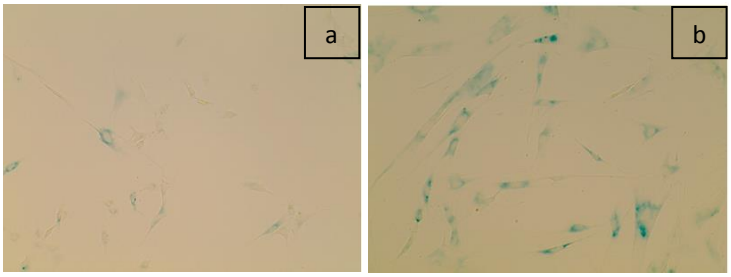

Fig. 10. β-Gal expression in the control (a) and cells irradiated at 6 Gy (b).

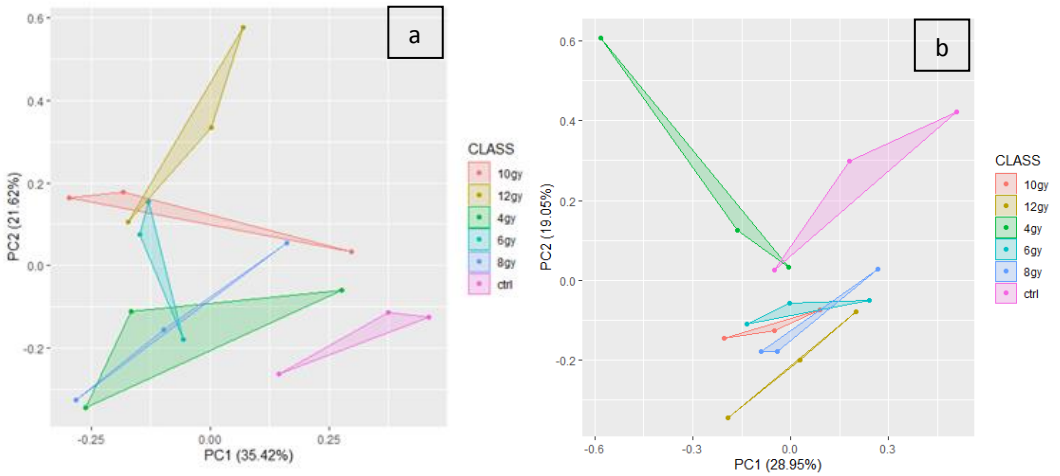

Fig. 2. Untargeted metabolic analysis of normal (a) and cancerous fibroblasts (b) in different classes of X-ray irradiation dose

Discussion/Conclusions

This study confirms that, upon certain radiation dose, cells are induced to senescence. Furthermore, senescence cells of different types have a peculiar metabolic content, which also depends on the amount of radiation dose received. These data need further validation. Then, they will be used to generate a constraint-based model of ageing metabolism using a Human Genome-Scale Metabolic Model[11]. This approach will allow us to integrate the orthogonal cell datasets together and explore how the global combination of cell metabotypes are modulated within the ageing cell models. Candidate age-cell linked molecular markers will then be identified.

References

1. J. Campisi, *et al. Nature* 571, (2019), pp 183–192.
2. A. Kalache, & A. Gatti, *Adv. Gerontol.* 11, (2003), pp 7–18.
3. J. Campisi, & L. Robert, *Aging Facts Theor.* 39, (2014), pp 45–61.
4. C. D. Wiley, & J. Campisi, *Cell Metab* 23, (2016), pp 1013–1021.
5. S. Marthandan, *et al. Biol. Res.* 49, (2016), pp 1–16.
6. A. M. Aliper, M. E. Bozdaganyan, P. S. Orekhov, A. Zhavoronkov, & A. N. Osipov, *Aging (Albany. NY).* 11, (2019), pp 2378–2387.
7. C. López-Otín, L. Galluzzi, J. M. P. Freije, F. Madeo, & G. Kroemer, *Cell* 166, (2016), pp 802–821.
8. N. J. W. Rattray, *et al. Nat. Commun.* 10, (2019), pp 1–12.
9. A. Hernandez-Segura, , J. Nehme, & M. Demaria, *Trends Cell Biol.* 28, (2018), pp 436–453.
10. N. V. Petrova, A. K. Velichko, S. V. Razin, & O. L. Kantidze, *Aging Cell* 15, (2016), pp 999–1017.
11. J. L. Robinson, P. Kocabas, P. E. Cholley, A. Nilsson, & H.Wang https://github.com/SysBioChalmers/Human-GEM#human-gem-the-generic-genome-scale-metabolic-model-of-homo-sapiens.

An Application of Variable Selection Methods in Omics Data obtained by GC-MS and LC-MS for the study of Non-Alcoholic Fatty Liver Disease

***S. Sabatini*[1], *C. Saponaro*[1], *M. Gaggini*[1], *F. Carli*[1], *C. Rosso*[2], *E. Bugianesi*[2] *and A. Gastaldelli*[1].**

[1]Institute of Clinical Physiology, CNR Pisa, Italy, [2] Division of Gastroenterology and Hepatology and Lab. of Diabetology, Dept. of Medical Sciences, University of Turin, Turin, Italy

Keywords: *NAFLD, supervised classification, variable selection.*

Introduction

In recent years, omics technologies have been widely exploited in the study of metabolic diseases. One of the main goals of these studies is the identification of metabolites (or genes) relevant in the discrimination among different conditions. In a typical omics experiment, the features are highly inter-correlated, and their number usually greatly exceeds the number of samples, making hard the analysis and interpretation of the results. Variable selection methods are therefore necessary to deal with multicollinearity and overfitting.

NAFLD is a complex liver disorder, that ranges from liver steatosis to non-alcoholic steatohepatitis (NASH) and cirrhosis [1]. It is known that NAFLD is associated with alterations of glucose and lipid metabolism and that one of major risk factors of NAFLD is obesity [2]. However, the exact role of obesity (BMI) and fat accumulation in the outbreak and progression of NAFLD remains mostly unclear. In this study, two sparse classification methods able to perform features selection, Elastic Net (EN) [3] and Sparse Partial Least Square Discriminant Analysis (SPLS-DA)[4], were proposed and compared to evaluate the impact of BMI on glucose and lipid metabolism in NAFLD subjects.

Materials and Methods

34 non-diabetic subjects, with biopsy proven NAFLD (11 lean, 12 overweight and 12 obese) and 8 controls (CT) were enrolled for the study. We measured non esterified fatty acids (FFA) and aminoacid plasma composition by GC-MS, and target lipidomics (Ceramides, PC, LysoPC, PE, DG and TG composition) by LC-QTOF. In vivo fluxomic analysis was performed by stable isotope tracer infusion; tracer enrichment was measured by GC-MS and lipolysis and endogenous glucose production (EGP) were obtained from modelling analysis of tracer turnover. We calculated desaturation index (SCD1=palmitoleic/palmitic acid) and unsaturated-to-saturated fat ratio (UFA/SFA), IR in the periphery (HOMA), adipose tissue (Lipo-IR, Adipo-IR) and liver (Hep-IR).

We applied EN and SPLS-DA as classification methods, in order to make a discrimination based on the metabolic profile between CT and NAFLD subjects, between CT and lean (BMI≤25) NAFLD subjects and between lean and obese (BMI>30) NAFLD subjects. In latter classification, variables were expressed as fold-changes with respect to the median of the controls ($\log_2$(-/median CT)).

Hyper-parameters were tuned through repeated cross-validation and permutation tests were used to assess the statistical significance of the classifications.

Results

In the controls versus NAFLD and controls versus lean NAFLD subjects' discriminations (fig. 1a), both EN and SPLS-DA were able to discriminate between the classes with very high accuracy measures (≥89%). The two methods brought out a recurrent group of relevant discriminant factors: insulin resistance indexes (HOMA, Lipo-IR and Hep-IR), AAs (alanine, threonine, methionine and aromatic AA), UFA/SFA and several lipidomic species (Cer, LysoPC and TG, mainly).

The two classification methods were also able to discriminate lean vs obese NAFLD subjects (fig. 1b), even if EN showed a better accuracy in predictions (Table 1), selecting less variables. Both models selected insulin resistance's indexes (HOMA and Adipo IR), amino acids (serine, aromatic AA) and FFAs (margaric fatty acid, UFA/SFA) as main discriminating factors.

Discussion/Conclusions

This study shows that insulin resistance, amino acids, FFAs and lipids (TG, Cer, LysoPC, mainly) are relevant to distinguish non-NAFLD from NAFLD subjects, even when they have similar BMI. On the contrary, when comparing lean versus obese NAFLD subjects the main discriminator factors are insulin resistance in adipose tissue and periphery, amino acids and FFAs.
The two classification methods considered here show similar performances, although the sparsity of EN is greater.

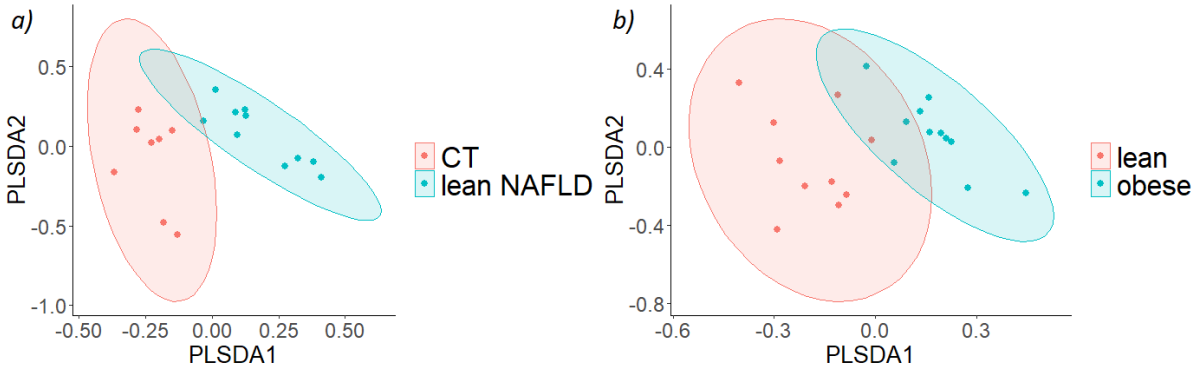

Fig. 11. Scores plots of SPLS-DA between non-NAFLD and lean NAFLD subjects (panel a) and between lean and obese NAFLD subjects (panel b).

Table 2. Accuracy and number of selected features in three classification performed for both EN and SPLS-DA methods.

	EN		SPLS-DA	
	Accuracy	**Selected Features n.**	**Accuracy**	**Selected Features n.**
CT vs NAFLD	97.5%	40	92%	85
CT vs Lean NAFLD	89%	45	92%	51
Lean vs Obese NAFLD	82%	13	70%	18

References

1. A. Gastaldelli, K. Cusi; *JHEP Reports*, 1(4) (2019), pp. 312-328.
2. M. Gaggini, M. Morelli, E. Buzzigoli, R. A. DeFronzo, E. Bugianesi, A. Gastaldelli, *Nutrients*, 5(5) (2013), pp. 1544-1560.
3. H. Zou ,T. Hastie; *J. R. Statist. Soc. Series B*, 67, Part 2 (2005), pp. 301–320.
4. H. Chun, S. Keleş; *J. R. Stat. Soc. Series B*, 72(1) (2010), pp. 3–25.

Comparison between data- dependent analysis and data- independent analysis in EPS-urinary proteomics

L. E. Prestagiacomo[1], C. Gabriele[1], M. A. Rota[2], S. Alba[2], G. Cuda[1], R. Damiano[1]and M. Gaspari[1]

[1]Università degli Studi Magna Graecia di Catanzaro, Catanzaro, Italy; [2] Romolo Hospital, Rocca di Neto (KR), Italy

Keywords: *Prostate cancer biomarker discovery, data dependent acquisition, data independent acquisition*

Introduction

Prostate cancer (PCa) is the second lethal cancer in men with 606.520 cancer deaths recorded in the United States in 2020 [1]. This pathology is silent and non-aggressive in some patients while in others shows a fast evolution and metastasis onset. Prostate cancer diagnosis, to date, is based on serum dosage of prostate specific antigen (PSA) and on digital rectal exam (DRE). Nevertheless, PSA has low specificity and does not help in discriminating between nonaggressive and aggressive disease.
In the effort of analysing urinary expressed prostatic secretion (EPS-urine) [2] to identify prostate cancer associated proteins, we tested two different label-free, MS-based approaches: data-dependent and data independent analysis.

Materials and Methods

Sample collection
Urine samples were collected after DRE from patients with PCa (n = 48) and from patients with benign prostatic hyperplasia (BPH) (n= 30). After collection EPS-urine samples were centrifugated within 2 hours of collection at 2100 rcf for 10 minutes at RT to remove cellular debris. The supernatant was stored at -80°C until use.

Protein digestion
EPS-urinary proteins were digested using on-filter digestion (FASP) [3] on Microcon-10 Centrifugal Filter Units (Millipore) suggested by the manufacturer with minor modifications. Proteins were digested overnight at 37°C after adding 200 ng of trypsin.
Peptide mixtures were purified by sequential strong cation exchange (SCX) and C_{18} StageTips before LC-MS/MS analysis.

LC condition
Peptides were separated using a linear gradient of 140 minutes at a flow rate of 230 nl/min on a 15 cm, 75 µm ID in house made column packed with 3 µm C18 silica particles. The binary gradient was performed using mobile phase A (0.1% formic acid, 2% ACN) and mobile phase B (0.1% formic acid and 80% of ACN). Gradient elution was obtained increasing mobile phase B from 3% B to 25% in 90 minutes, from 25% to 40% in 30 minutes and from 40% to 100% in 8 minutes.

DDA analysis
DDA analysis was performed by a top-12 method where the 12 most intense ions were selected for MS/MS events. MS full scan range was 350-1800 m/z and resolution 70.000. Mass window for precursor ion isolation was 1.6 m/z and resolution 35.000. Raw files for label-free quantification was processed by MaxQuant while statistical analysis was performed in Perseus.

DIA analysis
We have developed a DIA method to minimize the problem of missing values typical of DDA. Each cycle DIA was based on full scan range 350-1200 m/z at resolution of 17.500 and DIA scans with resolution of 35.000. In details, total windows of our method were 26 with 20 windows of 20 m/z isolation width, 5 windows of 50 m/z isolation width and 1 window of 200 m/z isolation window.

For library generation, a pool of tryptic peptides from 22-EPS urine samples was fractionated by high-pH reversed phase (10 fractions) and analysed in DDA mode. Data analysis was carried out by Spectronaut 13.0.

Results

DDA analysis led to the identification of 954 proteins in 42 samples (20 PCa and 22 BPH). The list of identified proteins was compared to a panel of 135 prostate cancer-specific and tissue enriched proteins obtained from BioGPS (www.biogps.org) and Protein Atlas (www.proteinatlas.it); this comparison has shown that there were only 36 proteins common (Fig.1).

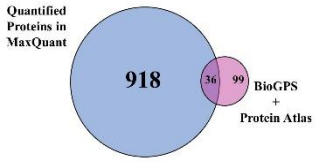

Fig. 1 The comparison between the quantified proteins in MaxQuant and the panel of 135 proteins

DIA analysis has cumulatively quantified 1961 proteins in 80 samples showing a greater percentage of matches to the list of 135 proteins. In fact, more than 50% (72 proteins) of these prostate cancer-specific proteins were quantified in DIA analysis (Fig.2)

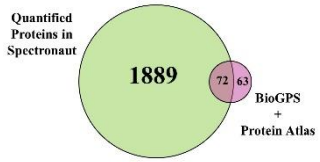

Fig. 1 The comparison between the quantified proteins in Spectronaut and the panel of 135 proteins

Discussion/Conclusions

To date, this work has shown that the DIA method is a promising approach to obtain a rich proteomic map of EPS-urine. This is demonstrated by the ability of DIA analysis to detect the majority of proteins known to be associated with PCa. The advantage of DIA is that each peptide is detected by MS/MS event; this ultimately allows, wider proteome coverage and lower incidence of missing values. The increase in the number of protein identifications could raise the probability to detect cancer-associated proteins of potential interest.

References

1. R. Siegel, K. Miller, A. Jemal; *Cancer Journal for Clinicians*, 70 (2020), pp 7-30.
2. Y. Kim, J. Jeon, S. Mejia, C.Q. Yao, V. Ignatchenko, J.O. Nyalwidhe, et al; *Nature Communication*, 7 (2016), pp 1-10.
3. J. R. Wisniewski, A. Zougman, N. Nagaraj, M. Mann; *Nature Methods*, 6 (2009), pp 359-362

New insights in lipids MALDI MS imaging in FFPE tissue: Antigen retrieval and its effect on positive ion species

V. Denti[1], I. Piga[1], S. Guarnerio[2], F. Clerici[1], M. Ivanovaa[1], C. Chinello[1], G. Paglia[1], F. Magni[1] and A. Smith[1]

[1]Clinical Proteomics and Metabolomics Unit, Department of Medicine and Surgery, University of Milano-Bicocca, Vedano al Lambro, Italy, [2]*Biomolecular* Sciences Research Centre, Sheffield-Hallam University, City Campus, Howard Street, Sheffield, UK

Keywords: *MALDI imaging; lipids; FFPE;*

Introduction

MALDI-MS imaging (MSI) is a unique technology that enables the in-situ detection of a wide range of biomolecules, including lipids [1]. However, this could be challenging when analysing formalin fixed paraffin-embedded (FFPE) tissues, the main source of clinical tissue, given that many lipids species are depleted during tissue processing. Nevertheless, several solvent-resistant lipids remain but their extraction could be impeded by the cross-link between proteins [2]. Hence, an antigen retrieval step could enable the extraction of a greater number of lipids and may provide information that is complementary to that which can be obtained from other biomolecules, such as proteins. Here we aim to address the effect of performing antigen retrieval prior to MALDI-MSI of lipids in FFPE tissue.

Materials and Methods

Consecutive tissue sections from five FFPE blocks of clear cell Renal Cell Carcinoma (ccRCC) were prepared using a protocol without an antigen retrieval step (A) and with an antigen retrieval step (B). Two additional cases of ccRCC tissue, characterised by more intricate histopathological features, were then analysed with the latter protocol (B).

For both protocols (A and B) a matrix solution containing equimolar quantities of aniline and 10 mg/ml α-cyano-4-hydroxycinnamicacid (ANI-CHCA) dissolved in a 70% methanol solution with 0.1%TFA was deposited using the HTX TM-Sprayer™. All analyses were performed using a rapifleXTM MALDI TissuetyperTM mass spectrometer equipped with a Smartbeam™ 3D laser. All mass measurements were acquired in positive ion reflectron mode in the m/z range of 420 to 820.

For on tissue MALDI MS/MS a single precursor ion was selected by using the smallest precursor ion selector (PCIS) window possible and dissociated using LID-LIFT™ technology, with the laser energy being set within a range of 40–70%.

Results

When performing an antigen retrieval step, we observed that an improved number of lipid signals could be detected and, the signals detected using this approach (protocol B) enabled the tissue to be segmented into the tumoural and non-tumoural regions indicated by the H&E staining, with these signals not being detected when using protocol A.

Additionally, a further two specimens, with more complex histological environments, were analysed to assess the capability of protocol B to define the tissue on the basis of its lipidomic content. In these instances, the tumoural, cortical, necrotic and haemorrhagic regions could all be spatially resolved on the basis of individual m/z signals and was in accordance with those regions that could be defined using H&E staining.

In order to understand which phospholipids classes are more accessible with AR, on-tissue MALDI-MS/MS was performed on the key signals whose distribution was in agreement with the histology of the tissue. In brief, a number of different lipid species were identified, including phosphatidylcholine (PC), as well as their lyso variants (LPC), and sphingomyelin (SM), with these lipid species already been reported to be readily detected in fixed tissue [3, 4]

Discussion/Conclusions

The greater number of signals detected when using protocol B may have derived from lipid species that are known to be implicated in the lipid-protein crosslinking that is formed because of formalin fixation. Moreover, the region-specific signatures confirmed also in the samples with more complex histological features were also evident in the average profiles generated from these regions of interest and supports the proposal that it could be possible to still detect clinically relevant lipid species in FFPE samples, despite the loss of a large proportion during tissue processing. Human ccRCC tissue was used as a proof of concept to determine whether using the detected lipid signals were also able to highlight the histopathological regions that were present.
These preliminary results indicate that it may be possible to detect relevant alterations in the spatial lipidome of FFPE tissue, opening up new possibilities for spatial omics investigations of disease.

Acknowledgements

This work received funding from the 2019 Gilead Fellowship Program and Regione Lombardia POR FESR 2014-2020. Call HUB Ricerca ed Innovazione: ImmunHUB**.**

References

1. S.A.Schwartz, M.L. Reyzer, R.M. Caprioli, *J. Mass Spectrom*. 38, (2003), pp 699–708.
2. D.R.N. Vos, A.P. Bowman, R.M.A. Heeren, B. Balluff, S.R. Ellis, *Int. J. Mass Spectrom*. 446, (2019) 116212.
3. G. Stubiger, E. Pittenauer, G. Allmaier, *An al. Chem*. 80, (2008) pp 1664–1678.
4. A. Wojakowska, Ł. Marczak, K. Jelonek, K. Polanski, P. Widlak, M. Pietrowska, *PLoS One*. 10, (2015), pp 1–13.

High fat-high sucrose diet induced hepatic accumulation of lipotoxic compounds without hepatic mitochondrial dysfunction

***S. Guerra*[1,2], *I. Mateus*[3], *F. Carli*[1], *V. Lenoir*[3], *C. Prip-Buus*[3] and *A. Gastaldelli*[1,2]**

[1] National Research Council, Institute of Clinical Physiology, Pisa, Italy, [2]Sant'Anna School of Advanced Studies, Institute of Life Sciences, Pisa, Italy, [3]INSERM U1016-CNRS UMR 8104-University Paris Descartes, Institute Cochin, Paris, France

Keywords: *lipidomics; fatty liver; mitochondrial function*

Introduction

Excess fat and sugar in the diet promote lipid synthesis/accumulation and the deterioration of glucose metabolism likely through gluco- and lipo-toxicity, associated with impaired mitochondrial function[1, 2]. However, the effect of high fat–high sucrose (HFHS) diet on liver mitochondria lipid composition has not been fully elucidated. LC-MS QTOF lipidomic of plasma, hepatic tissue and isolated liver mitochondria of mice fed HFHS vs standard (SD) diet and studied the relationship with hepatic mitochondrial function and glucose tolerance.

Materials and Methods

Male adult C57BL/6J mice were fed HFHS (n=7) or SD (n=8) diet for 20 weeks with oral glucose tolerance test (OGTT) and histological analysis of liver tissues. LC-MS QTOF target lipidomics was performed in plasma, liver, and isolated liver mitochondria. Oxygen consumption was measured with an oxygraph (Oroboros) using isolated liver mitochondria in respiration buffer in the presence of glutamate/malate or succinate plus rotenone.

Results

HFHS increased body and adipose tissue (AT) weight compared to SD-diet, worsen glucose tolerance, and resulted in higher hepatic accumulation of lipotoxic lipids. Among active lipids, PC 34:1, and CER (18:1/20:0) were decreased and increased, respectively, similarly in plasma, liver, and mitochondria and hepatic CER (18:1/20:0) was correlated with glucose concentrations during OGTT. Despite an increase in plasma and liver TAGs and CER after HFHS, hepatic mitochondrial TAG accumulation and mitochondrial function (given by oxygen consumption and respiratory control ratio) were unchanged while we observed lower accumulation of sphingomyelins (SM) and phosphatidylglycerols (PG).

Discussion/Conclusions

HFHS-diet is associated to hepatic fat accumulation, but until TAG and ceramides do not accumulate into the mitochondria the oxidative capacity of the cell remains unaltered.

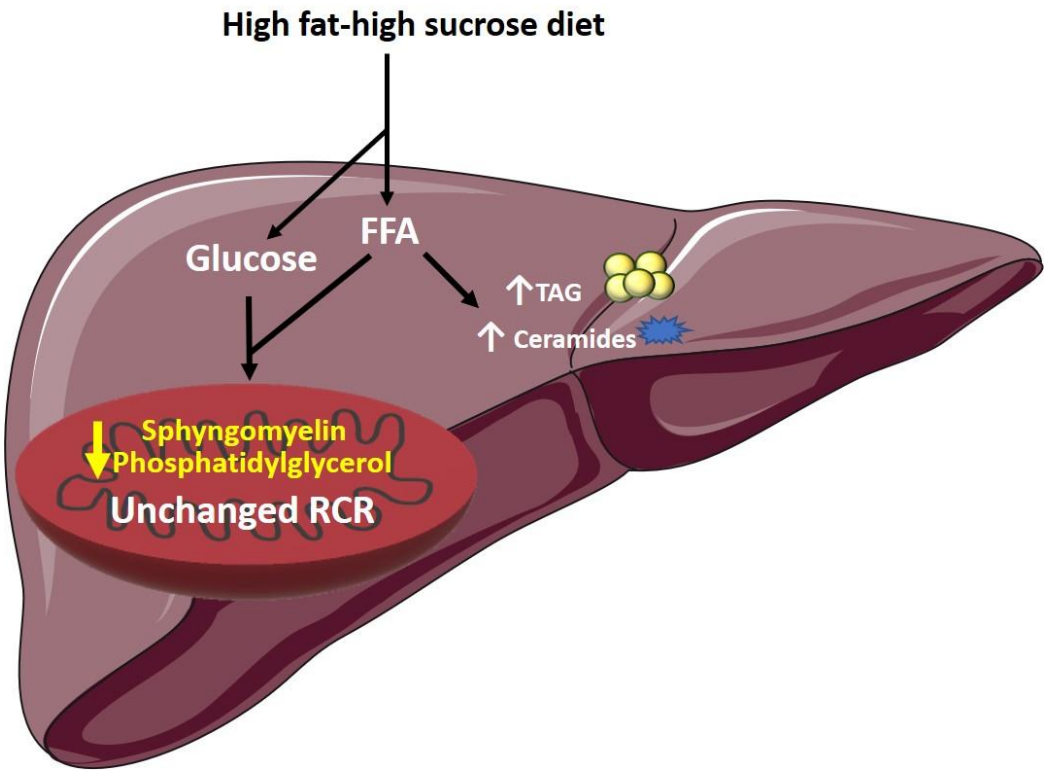

Fig. 12. High fat-high sucrose diet induces hepatic accumulation of lipotoxic compounds and variations on mitochondrial lipidome without any impairments on mitochondrial respiratory control (RCR).

References

1. K.Y. Peng, et al.; *Journal Lipid Research*, 59(10), (2018), pp 1977-1986.
2. K. Chella Krishnan, et al.; *Cell Systems*, 6(1), (2018), pp 103-115 e7.

Proteomic and glycoproteomic approaches based on nLC-ESI MS/MS for exploring cancer matrisome: explorative study

L. Pagani[1], C. Chinello[1], A. Mahajneh[1], F. Clerici[1], F. Facchinetti , G. Pollaci[2], L. Roz[2] and F. Magni[1]

[1]*Department of Medicine and Surgery, University of Milano-Bicocca, Clinical Proteomics and Metabolomics Unit, Vedano al Lambro, Italy,* [2]*Department of Research, Fondazione IRCCS Istituto Nazionale dei Tumori, Tumor Genomics Unit, Milan, Italy*

Keywords: *matrisome, proteomics, glycoproteomics*

Introduction

The matrisome is defined as the whole proteins which compose the extracellular matrix (ECM) of biological samples [1]. ECM plays an important structural role and it is involved in many physiological processes. Matrisome proteome show furthermore an high level of glycosylation which is implicated in protein-protein interactions and in the binding with other soluble growth factors. That's why alterations in ECM proteins and dysregulation in matrisome glyco-features are reported to correlate with the development of several human diseases [2-4]. However, the characterization of the matrisome has been shown as dramatically challenging, due to the nature of ECM typical proteins: large, highly glycosylated and insoluble [5]. The goal is to develop a feasible and effective method to evaluate proteomic and glycoproteomic features belonging to cancer matrisome.

Materials and Methods

Proteomic and glycoproteomic characterization of de-cellularized extracellular matrix (dECM), derived from Cancer Associated Fibroblasts (CAF) isolated from a surgical specimen of non-small cell lung cancer and immortalized with human Telomerase Reverse Transcriptase (LT154 CAF hTERT), will be performed by liquid chromatography coupled with tandem mass spectrometry. Matrisome samples will be enzymatically digested and consequently enriched in glycopeptides using various approaches for each sample preparation step. Then, they will be analyzed with nLC-UHRTOF using a label-free strategy. Protein identification, relative quantification and glyco- characterization will be performed through Mascot database search and PEAKS studio X+ platform.

Results

The different approaches to prepare and enzymatically digest the sample in order to maximize the identification power are currently under comparison. In particular, samples treated with FASP protocol [6], MS-compatible surfactant aided in-solution digestion or multi-enzyme digestion (LysC before trypsin) are used.

More than 800 proteins have been so far identified and annotated in their biological roles, with the purpose of evaluating the quality of the digests also in terms of enriched pathways and functions associated to ECM related proteome and the specific CAF line.

In addition, different methods to explore the glycoproteome, such as the lectins- functionalized tips (TopTips) [7] and N-Glyco-FASP method [6] will be compared.

Discussion/Conclusions

Shotgun analysis and label-free quantification allow to characterize the proteins and glycoproteins present in dECM derived from CAFs. The comparison between diverse strategies provides useful keys to identify an optimized method for describing ECM proteome and glyco-proteome and the possible alterations that occur in cancer micro-environment.

Acknowledgments

The research leading to these results has received funding from the FAR 2014–2018, from Fondazione Gigi & Pupa Ferrari Onlus and Regione Lombardia POR FESR 2014-2020. Call HUB Ricerca ed Innovazione: ImmunHUB**.** Italian Ministry of Health (Grant No. RF-2016-02362946).

References

1. A. M. Socovich, A. Naba, *Seminars in cell & developmental biology*, 89 (2019), pp 157-166.
2. I. N. Taha, A. Naba *Exploring the extracellular matrix in health and disease using proteomics*, 63 (2019), pp 417-432.
3. R. Raghunathan, M. K. Sethi, J. A. Klein, et al., *Essays in Biochemistry*, 18 (2019), pp 2138-2148.
4. B. Deb, K. Patel, G. Sathe, et al., *Journal of clinical medicine*, 8 (2019), p 1303.
5. L. Krasny, A. Paul, P. Wai, et al., *Biochemical Journal*, 473 (2016), pp 3979-3995.
6. L. Santorelli, G. Capitoli, C. Chinello, et al., *Cancers*, 12 (2020), p 239.
7. Y. Zhang, E. P. Go, H. Desaire. *Analytical chemistry* , 80 (2008), pp 3144-3158.

Proteomic monitoring by label-free nLC-MS/MS of human platelet lysates for a standardized and optimized production

L. Pagani[1], A. Bianchetti[2], F. Re[3], A. Mahajneh[1], F. Clerici[1], S. Bernardi[3], C. Almici[2], D. Russo[3], F. Magni[1] and C. Chinello[1]

[1]*Department of Medicine and Surgery, University of Milano-Bicocca, Clinical Proteomics and Metabolomics Unit, Vedano al Lambro, Italy,* [2]*Immunoematology and Transfusion Medicine service, ASST Spedali Civili of Brescia, Italy,* [3]*Unit of Blood Diseases and Stem Cell Transplantation, DPT of Clinical and Experimental Sciences, Brescia University, ASST Spedali Civili Brescia, Italy*

Keywords: *human platelet lysate, cell culture, proteomics*

Introduction

Human platelet lysate (hPL) is a cell-free blood product obtained from lysis of human blood platelets, that has been emerged as a xeno-free possible substitute of FBS (foetal bovine serum) for ex vivo expansion of MSCs (mesenchymal stem cells) [1-2]. Indeed, the relatively easy and inexpensive production, the abundance of growth factors and the significant beneficial effects on cells growth make hPL the gold standard for cell therapies. However, hPL has currently not yet been standardized both for platelet sources and production protocol. A plethora of hPL preparation methods have been described in literature bringing to a wide heterogeneity of the final products and consequently of their effects on cell biology and performances [3]. To this end, great efforts are currently applied in this direction in order to standardize the manufacture process of hPL production and to establish common guidelines [4]. Therefore, the possibility of exploring the proteomic content of hPL and to compare it between different preparations and batches could offer a precious support for evaluating the quality of this human blood derivative and better understanding the molecular basis of its efficacy in cell culture.

Materials and Methods

Plasma from 54 healthy donors belonging to transfusional blood bank were divided into 3 groups (18 donors in each one) and used for hPL production. From each group, hPL batches were prepared following two protocols of lysis involving a different number of freeze/thaw cycles: the basic method (hPLbasic) and the plus one (hPLplus), which demonstrated a greater mitogenic effect in MSCs *in vitro* models. Three samples populations (hPLbasic, hPLplus and the related platelet poor plasma) for each donors' group (n=9) were subjected to proteomic analysis via albumin and IgG depletion, followed by enzymatic digestion based on FASP protocol [5]. Then, they were injected in triplicates into nLC-UHR-TOF and data were submitted to PEAKS studio X+ platform for protein identification and label-free quantification.

Results

In order to evaluate the variability between batches, outcome obtained from PEAKS analysis were filtered with three different levels of stringency, using parameters more and more conservative. Independently from the filtering setup, hPLbasic showed a greater variability than hPLplus. More in detail: at poor, mild and high stringency, hPLbasic displayed a variability of 30%, 31% and 21% respectively, while hPLplus of 15%, 10% and 14%. In addition, *in vitro* studies of cells propagation confirmed this lower variability of *plus* preparation than the *basic* one (data not reported). This observation suggests a correlation between an increase stability of hPLplus preparation and its beneficial action in cell culture propagation. Moreover, the list of proteins, which emerged from the comparison between the two methods, is likely to contain possible candidates responsible of the favourable effect seen *in vitro*.

Discussion/Conclusions

Proteomic characterization and quantification through mass spectrometry analysis could be used to monitor the quality of different preparation protocols of hPLs, even in terms of batch-to-batch variability. Furthermore, the comparison between different preparations at diverse efficacy levels

provides useful keys to decode the protein actors that drive the growth and differentiation processes in *in vitro* models for regenerative medicine.

Acknowledgments

The research has received funding from the FAR 2014–2018, from Fondazione Gigi & Pupa Ferrari Onlus and Regione Lombardia POR FESR 2014-2020. Call HUB Ricerca ed Innovazione: ImmunHUB. Italian Ministry of Health (Grant No. RF-2016-02362946). 2019 Gilead Fellowship Program

References

1. K. Bieback, B. Fernandez-Muñoz, S. Pati, R. Schäfer. *Cytotherapy*, 21(9), (2019), pp 911-924.
2. Burnouf T, Barro L, Nebie O, Wu YW, Goubran H, Knutson F, Seghatchian J. *Transfusion and Apheresis Science*, 58(6), (2019), p 102674.
3. Schallmoser, R. Henschler, C. Gabriel, M. B. C. Koh, and T. Burnouf. *Trends in biotechnology*, 38(1), (2020), pp 13-23.
4. Bohonek M, Kutac D, Acker JP, Seghatchian J. *Transfusion and Apheresis Science*. 59(2), (2020), p102754.
5. Chinello C, Stella M, Piga I, et al. *Journal of proteomics*. 191 (2019), pp 29-37

Characterization of non-small cells lung cancer heterogeneity with high spatial resolution mass spectrometry imaging

F. Clerici[1], G. Panarello[1], MM. Bolognesi[2], M. Jaconi[3], A. Smith[1], G. Cattoretti[2], F. Magni[1], I. Piga[1]

[1]Clinical Proteomics and Metabolomics Unit, University of Milano-Bicocca, Department of Medicine and Surgery, Vedano al Lambro, Italy, [2]Department of Pathology, Istituto Nazionale per lo Studio e la Cura dei Tumori, Milan, Italy, [3]School of Pathology, University of Milan, Milan, Italy.

Keywords: *MALDI-MS imaging, tumor microenvironment (TME)*

Introduction

Lung cancer is the leading cause of cancer-related mortality and non-small cells lung cancer (NSCLC) is the most common form. The majority of patients with NSCLC are diagnosed with advanced disease because in early stages NSCLC doesn't cause any symptoms, hence the 5-years survival rates with metastatic tumours is less than 20%. Therefore, it is evident the need of more accurate and sensitive prognostic and diagnostic biomarkers to guide clinical decision-making [1]. Tumor microenvironment (TME) has a central role in the initiation and development of *de novo* lung carcinoma as well as in the support of metastasis, and can become an interesting target for NSCLC early detection and treatment with novel anticancer strategies [2].

MALDI-MS imaging can be a useful tool in obtaining proteomic information together with high spatial distribution information for a better understanding of tumor growth and development as well as to investigate the influence of the tumour microenvironment.

Materials and Methods

In this study 19 patients with NSCLC (n = 9 adenocarcinoma, n = 1 pleomorphic, n = 1 mucoepidermoid carcinoma, n = 2 squamous cell carcinoma, n = 4 adenocarcinoma metastasis, n = 1 squamous cell carcinoma metastasis and n = 1 mucoepidermoid carcinoma metastasis) were included. A total of 61 FFPE tissue microarray (TMA) sample cores of NSCLC and 1 core from tonsil donor (2 mm of diameter) were investigated. From each FFPE tissue, multiple cores from the central area of the tumor, from the peripheral area and from healthy tissue were taken. Finally 2 TMA were prepared and section of 4 µm were placed on ITO glass slides for MALDI-MSI analysis.

Samples were trypsin-digested and then MALDI-matrix CHCA (10mg/ml in 70% ACN and 1% TFA) was uniformly deposited. The analysis was performed with a RapifleX MALDI Tissuetyper™ mass spectrometer equipped with a SmarbeamTM 3D laser. All spectra were acquired using a raster setting of 20 µm in the mass range 700 to 3000 *m/z*. After the MALDI-MSI analysis, the matrix was removed and the slides stained with haematoxylin and eosin. Finally, after digital acquisition, the images were coregistrated with the MSI datasets. TME, cancer, necrosis and healthy regions of interests were histologically annotated in each core by the pathologist. Data analysis was performed onSciLs Lab2019 software.

Results

For an explorative analysis we compared adenocarcinoma (ADC) vs non-adenocarcinoma (healthy non-ADC) specimens spectra. The unsupervised principal component analysis (PCA) proved a division between the two populations and the receiver operating characteristic (ROC) analysis identified 24 discriminant peaks with AUC ≥ 0.70 (2↑ in ADC and 22↓ in healthy samples non-ADC). Confronting ADC and TME spectra of the same samples 4 peaks resulted indicative for the adenocarcinoma specimens. Interestingly in a further comparison of tumor microenvironment from adenocarcinoma vs the one from other NSCLC samples, the analysis identified 23 peaks more representative for the ADC TME. With samples from the tissue microarray cores, we then built a training set composed of adenocarcinoma and healthy tissue samples. The generated set was validated on all the border cores which were correctly assigned in their different structures, as benign or malignant areas. Interestingly even the other non-small cells lung cancer and metastases cores were properly predicted based on their histological features.

Discussion/Conclusions

This preliminary work highlights the potential of spatially resolved MALDI-MSI to discriminate differential features in lung adenocarcinoma, the specific proteomic signature of the TME and the possibility to predict the malignant nature of other NSCLC (both primary tumour and metastatic). This approach thus opens new windows for a better understanding of tumor growth, development and of the interplay between tumor cells and adjacent immune cells within the tumor microenvironment.

Acknowledgements

This work received funding from Regione Lombardia POR FESR 2014-2020. Call HUB Ricerca ed Innovazione: ImmunHUB.

References

1. M. K. Mayekar & T. G. Bivona. *Clin. Pharmacol.Ther*. 102 (2017), pp 757–764.
2. N K. Altorki, G J. Markowitz, D Gao, J L. Port, A Saxena, B. Stiles, T. McGraw, V. Mittal, *Nat Rev Cancer*, 19 (2019), pp 9–31.

Food

Analysis by LC-ESI/LTQ Orbitrap/MS/MS of polar lipid fraction from *Portulaca oleracea*

***C. Cannavacciuolo*[1,2], *A. Napolitano*[1] *and S. Piacente*[1]**

[1]Department of Pharmacy, University of Salerno, via Giovanni Paolo II n. 132, I-84084 Fisciano, SA, Italy, [2]PhD Program in Drug Discovery and Development, University of Salerno, via Giovanni Paolo II n. 132, I-84084 Fisciano, SA, Italy.

Keywords: *Portulaca oleracea*, *lipidomic*, *functional food*

Introduction

The growing awareness of prevention and wellness promotes a healthy lifestyle mediated by equilibrate diet and physical activity, in order to maintain a good state of health and contribute to the reduction of metabolic disorders and pathologies. A key role in the new healthy trend is the integration in everyday diet of poly-unsaturated fatty acids (PUFAs) [1-3].

In this overview, the spontaneous herb *Portulaca oleracea* L., better known as purslane, is a promising resource of PUFAs. Previous studies have reported an amount of α-linolenic acid (ALA) in its leaves five times higher than other leafy plants [4], along with a good content of long-chain PUFAs, eicosapentaenoic acid (EPA) (20:5, ω-3) and docosahexaenoic acid (DHA) (22:6, ω-3) [4]. Furthermore, an increasing amount of DHA has been measured in the plant grown under conditions of saline stress [5]. Generally, in leafy plants the most abundant species are chloroplast membrane glycolipids. Several classes of glycolipids vary for the nature of head group and for the fatty acid unsaturation degree and composition. However, focus on the abundant and nutritionally important leaf lipids is still elusive. Notwithstanding this, in literature no data are available about *P. oleracea* polar lipid composition despite diet intake of mentioned class of lipids is generally associated with significant biological activities [6].

Thereby, the analysis of the polar extracts obtained from leaves and stems of a wild Italian *P. oleracea* species has been carried out by using liquid chromatography coupled to electrospray ionization and multiple-stage linear ion-trap and orbitrap high-resolution mass spectrometry (LC-ESI/LTQOrbitrap/MS/MS). By considering both their molecular formulae and diagnostic fragmentation pattern, in comparison with literature data, several metabolites belonging to different classes of complex polar lipids such as phospholipids, glycolipids, oxylipins and cerebrosides were identified.

Materials and methods

The edible parts (leaves and stems) of *P. oleracea*, wildly grown in a field of Salerno (Italy), were separately freeze-dried and then submitted to maceration with solvents of increasing polarity. Thus obtained methanol extracts of leaves and stems were fractionated on an analytical chromatographic C-18 cartridge by using CH_3CN/H_2O (v/v) in different ratio, in order to obtain lipid enriched fractions. Both methanol extracts and lipid enriched fractions were analysed by LC-ESI/HRMS using a quaternary Accela 600 pump and an Accela autosampler coupled to a LTQOrbitrap XL mass spectrometer (ThermoScientific, San Jose, CA), operating in both negative and positive electrospray ionization mode. Data were collected and analysed using the software provided by the manufacturer. Each sample was submitted to two different HPLC separation conditions using different columns RP-C18 and RP-C4, linear increasing solvent gradient consisting of a combination of water and organic solvents, and a flow rate of 0.2 mL/min. For ESI source, the experimental conditions were adopted depending from the polarity selected. In order to obtain tandem mass (MS/MS) spectra, data-dependent scan experiments were performed.

Results

The preliminary results obtained by LC-(-)ESI/LTQOrbitrap/MS/MS analysis of methanol extracts obtained from both the edible parts of *P. oleracea* (data not shown) guided the subsequent analytical steps aimed at obtaining lipid enriched fractions permitting a more detailed and comprehensive multi-class polar lipid analysis. By using two different types of chromatographic columns (RP-C18 and RP-C4) allowing the analysis

of lipids differing by size and polarity, a wide range of peaks corresponding to metabolites ranging from oxylipins and long chain bases to intact high molecular weight lipids, such as phospholipids, sphingolipids (mainly cerebrosides), and glycolipids, could be detected in both leaves and stems. Qualitative difference between the two edible parts could be appreciated by observing the respective LC-HRMS profile of lipid enriched fraction obtained by analytical chromatographic cartridge **(Fig.1)**.

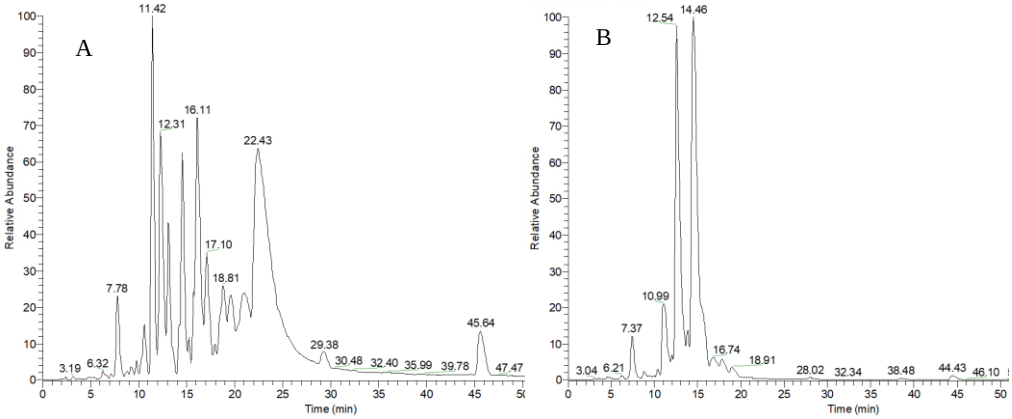

Fig.1. LC-(-)ESI/HRMS profile showing differences in metabolites between P. oleracea stems (A) and leaves (B) lipid enriched fractions.

Discussions/conclusions

The results obtained by the described analytical approach highlight, for the first time, the occurrence in *P. oleracea* L. of several polar lipids, supporting a revalued use of the vegetable in human nutrition as a food rich in different classes of bioactive and healthy lipids with beneficial effects [6]. Among the several detected classes, notable is the report of an unusual glycolipid class, previously reported in bacteria, fungi and in some species of algae, but whose occurrence in higher plants was established only in recent times [7]. Finally, the abundance of bioactive lipids suggests the use of the *P. oleracea* as functional food. Moreover, the high occurrence of cerebrosides in ripe stems suggests for them alternative uses, e.g. as new matrices in cosmetic formulations.

References

1. R.Ayerza, W. Coates, *Ind Crops Prod*, 34 (2011), pp 1366-1371.
2. G. Cumberford, A. Hebard, *Lipid Technol*, 27 (2015), pp 207-210.
3. V. Venkateshwari, A. Vijayakumar, A. K. Vijayakumar, L. P. A. Reddy, M. Srinivasan, R. Rajasekharan, *Planta*, 248 (2018), pp 347-367.
4. A. P. Simopoulos, H. A. Norman, J. E. Gillaspy, J. A. Duke, *J Am Coll Nutr*, 11 (1992), pp 374-382.
5. A. AnastáCio, I. S. Carvalho, *Int J Food Sci Nutr* 64 (2012), pp 235-242.
6. A. Napolitano, A. Cerulli, C. Pizza, S. Piacente, *Food Chemistry*, 269 (2018), pp 125-35.
7. Y. Okazaki, H. Otsuki, T. Narisawa, M. Kobayashi, S. Sawai, Y. Kamide, M. Kusano, T. Aoki, M. Yokota Hirai, & K. Saito *Nat. Commun*, 4 (2013), p 1510.

Non-Targeted Mass Spectrometry Approaches for the Detection of Food Frauds: a proposed Harmonization Workflow

D. Cavanna[2], C. Dall'Asta[2] and M. Suman[1]

[1] Barilla G. & R. Fratelli S.p.A., Advanced Research Labs – via Mantova 166, 43122 Parma, Italy , [2] University of Parma, Department of Food and Drug - Parco Area delle Scienze 95/A, 43124 Parma, Italy

Keywords: *Non-Targeted Mass Spectrometry, food frauds, workflow*

Introduction

Detecting and measuring food fraud is a challenging analytical task since a very wide range of food ingredients may be adulterated by numerous potential adulterants, many of which are yet unknown. This problem could be faced with the use of non-targeted mass spectrometric studies, and this is the reason why the number of these applications increased dramatically in this decade.
Unfortunately, a harmonized approach does not exist up to now, especially for the validation of the results obtained, so their robustness is not always certified.

Materials and Methods

Taking inspiration from a recently published Scientific Opinion, a proposed harmonization workflow for the validation of non-targeted approaches will be presented, with a specific focus on the industrial perspective of the topic.
Three studies concerning different raw materials (eggproducts, extra virgin olive oils and wheat) will be used as examples during the discussion of the validation steps.

Results

Despite the inevitable differences through the three subjects (due to the intrinsic nature of raw materials and to the different target frauds) all the studies exhibited the same criticality (i.e. use of authentic samples) and strengths, but at the end have proved to be fit for the purpose.
Predictive models were developed, but above all, new chemical markers were detected as responsible of the adulterations; their robustness was certified with the analysis of external /commercial samples and in one case also with an inter-laboratory study.

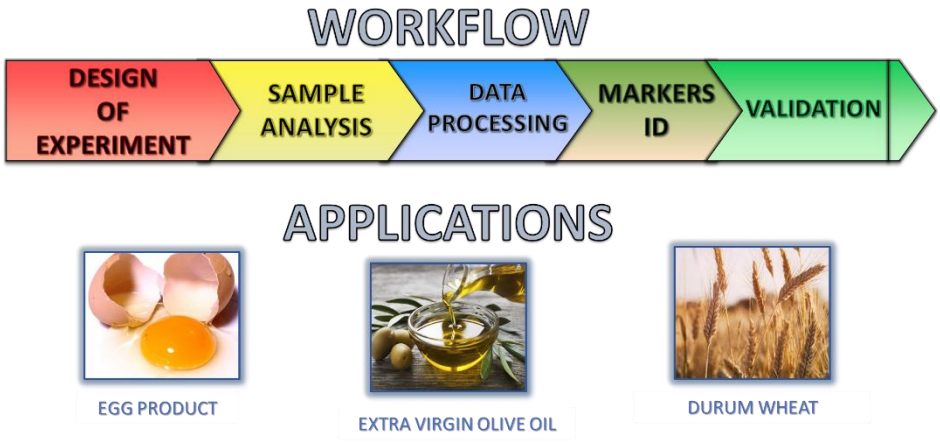

Fig. 13. A harmonized Non-Targeted MS Workflow applied to different food integrity needs

Discussion/Conclusions

The three studies certified that, following the same validation workflow, similar robustness in the results can be achieved, despite the differences in raw materials and frauds investigated.
This work would like to stimulate the debate between public and private institutions and increase their efforts in order to finalize a shared approach, able to guide the development of robust non-targeted methods for food fraud detection using mass spectrometric techniques.

References

1. D. Cavanna, D. Catellani, C. Dall'Asta, M. Suman; *Journal of Mass Spectrometry*, 53 (2018), pp 849-861.
2. D. Cavanna, L. Righetti, C. Elliott, M. Suman; *Trends in Food Science & Technology*, 80 (2018), pp 223-241.
3. D. Cavanna, C. Loffi, C. Dall'Asta, M. Suman; *Food Chemistry*, 317 (2020).
4. D. Cavanna, K. Hurkova, Z. Dzuman, A. Serani, M. Serani, C. Dall'Asta, M. Tomaniova, J. Hajslova, M. Suman, *ACS Omega*, in press.

LC-ESI/LTQOrbitrap/MS metabolomic analysis of Fennel waste (*Foeniculum vulgare Mill.*) as a byproduct rich in bioactive compounds. A preliminary study

***M. A. Crescenzi*[1,2], *G. D'Urso*[1], *S. Piacente*[1] *and P. Montoro*[1]**

[1]Department of Pharmacy, University of Salerno, Via Giovanni Paolo II, 84084, Fisciano, (SA) Italy, [2]PhD Program in Drug Discovery and Development, University of Salerno, via Giovanni Paolo II n. 132, I-84084 Fisciano, SA, Italy.

Keywords: *fennel waste, LC-ESI-FT-MS analysis, bioactive compounds.*

Introduction

Food industries produce high amount of waste every year. These wastes may be rich of bioactive compounds that can be used to produce cosmetic and nutraceutical products [1]. Fennel (*Foeniculum vulgare Mill.)* is a Mediterranean aromatic plant belonging to the Umbelliferae (Apiaceae) family. It is rich in bioactive compounds such as polyphenols that have anti-inflammatory, antioxidant, immunomodulatory properties [2]. As fennel industrial processes yield a large amount of byproducts, in this study the possibility to retrain this waste food as potential source of bioactive metabolites was investigated. In particular, the metabolite profiles of different parts (fruit, leaves, stems and little stems) of *F.vulgare* waste were investigated by LC-ESI/LTQOrbitrap/MS analysis and a Multivariate Data Analysis approach was developed to discriminate the different fruit parts.

Materials and Methods

The freeze-dried vegetable waste was extracted both with water decoction and with sonication with a solution of water/ethanol (80:20). The extracts were analysed by a Thermo Scientific Liquid Chromatography system constituted of a quaternary Accela 600 pump and an Accela autosampler, connected to a linear Trap-Orbitrap hybrid mass spectrometer (LTQ-Orbitrap XL, Thermo Fisher Scientific, Bremen, Germany) with Electrospray Ionization (ESI). Separation was performed on a Phenomenex Luna C18 5µm (150x2.00 mm) column [3]. The mass spectrometer operated in negative ion mode. Xcalibur software version 2.2 was used for instrument control, data acquisition and data analysis. For fragmentation study Data Dependent Scan was performed. The data obtained were studied with a multivariate statistical analysis approach, using PCA and PLS-DA, projection methods.

Results

LC-ESI/LTQOrbitrap/MS and MS^n analysis allowed to identify different metabolites mainly belonging to hydroxycinnamic acid derivatives, flavonoid glycosides, flavonoid aglycons, phenolic acids, iridoid derivatives and lignans. Identification of compounds was based on retention times, accurate mass measurements, MS/MS data, exploration on specific metabolites database (Knapsack, Mass Bank) and comparison with data reported in the literature for the species *F. vulgare* [3]. Moreover, the presence of different oxylipins was relieved, that were for the first time identified in fennel.

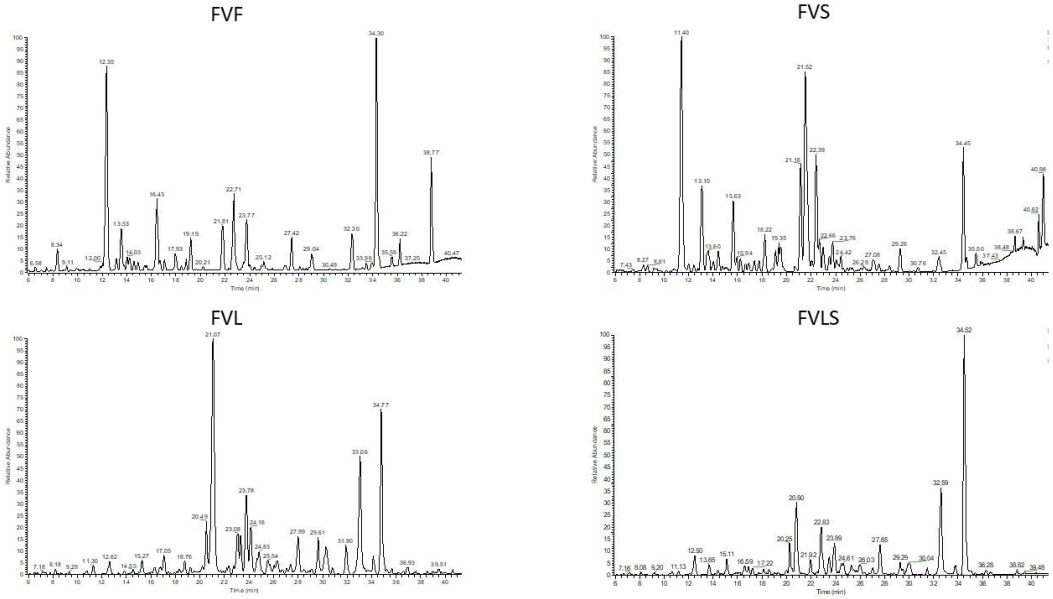

Fig. 1 Negative ion mode profiles of F. vulgare waste ethanolic extracts obtained by LC-ESI/LTQ/Orbitrap MS: FVF (Foeniculum Vulgare Fruit), FVS (Foeniculum Vulgare Stem), FVL (Foeniculum Vulgare Leaf) and FVLS (Foeniculum Vulgare Little Stem).

Discussion/Conclusions

The present study allowed the identification of many bioactive compounds in the waste products of fennel, suggesting their possible use in nutraceutical and cosmetic industries. Therefore, it will be necessary to evaluate their biological activities with cell metabolomics. The cells will be exposed to the various extracts and the alterations in the various cellular pathways will be studied [4,5].

References

1. N. A. Sagar, S. Pareek, S. Sharma, E. M. Yahia, M. G. Lobo; *Comprehensive Reviews in Food Science and Food Safety*, 20 (2018), pp 512-531.
2. S. B. Badgujar, V. V. Patel, A. H. Bandivdekar; *BioMed Research International*, 2014.
3. I. Parejo, O. Jauregui, F. Sànchez-Rabaneda, F. Viladomat, J. Bastida, C. Codina; *Journal of Agricultural and Food Chemistry*, 52 (2004), pp 3679-3687.
4. Z. Leòn, J. Garcia-Canaveras, M. T. Donato, A. Lahoz; *Electrophoresis Journal*, 34 (2013), pp 2762-2775.
5. A. Zhang, H. Sun, S. Qiu, X. Wang; *Journal of Integrative Biology*, 17 (2013), pp 495-501.

Development and validation of a multiclass method for over 60 antibiotics in eggs by LC-HRMS/MS

F. Paoletti[1], S. Sdogati[1], C. Barola[1], D. Giusepponi[1], S. Moretti[1] and R. Galarini[1]

[1]Istituto Zooprofilattico Sperimentale dell'Umbria e delle Marche "Togo Rosati", Via Salvemini 1-06126 – Perugia, Italy

Keywords: *Eggs*; *antibiotics; liquid-chromatography high resolution mass-spectrometry (LC-HR-MS/MS); validation study*

Introduction

The European Union requires the member states to implement yearly monitoring plans to assess the presence of antibiotic residues in food. This surveillance is mainly aimed to verify the sample compliance with the Maximum Residue Limits (MRLs) fixed in Regulation (EC) No 37/2010 [1]. Some years ago, our group developed multi-class methods for the simultaneous determination of over 60 antibiotics in meat and milk applying liquid chromatography coupled to high resolution mass spectrometry (LC-Q-Orbitrap) [2,3]. The aim of this work was to extend these procedures to other food matrices collected within Italian Residue Control Plan. Therefore, a multi-class method has been developed and validated to screen and confirm 64 antibiotics belonging to ten different families in eggs.

Materials and Methods

The sample preparation was that proposed by Moretti et al. (2016) [2] with slight modifications. The analytical determination was carried out using a Thermo Ultimate 3000 Ultra High Performance Liquid Chromatography system coupled with a Thermo high resolution Q-Exactive mass spectrometer (Thermo Scientific, San Jose, CA, USA). The instrumental analysis was performed in positive ionization mode (ESI+) using FullMS-ddMS^2 as acquisition mode. The method was validated according to Commission Decision 2002/657/EC [4] in the range 3.3-3333 µg/kg performing four replicates (n=4) at each validation level repeated on three separate occasions [5]. Seven concentrations were tested for a total of 84 experiments.

Results

Recovery factors were in the range 70-100 % for the majority of analytes, whereas coefficients of variation (CV%) evaluated both in repeatability and intra-laboratory reproducibility conditions were lower than 15 %. The limits of detection (LODs) and quantification (LOQs) were 3.3 µg kg^{-1} and 10 µg kg^{-1}, respectively. The only exception was cefacetrile, which was detected starting from 100 µg/kg. In Figure 1 the LC-HRMS chromatograms of five representative antibiotics in a blank eggs sample and in the same spiked at 3.3 µg/kg are shown.

Discussion

The procedure demonstrated suitable performance characteristics in terms of selectivity, linearity, precision, recovery, decision limits (CCαs), detection capabilities (CCβs), LODs and LOQs. In addition, since several antibiotics are not authorized in laying hens [1], the achievement of LODs lower than 10 µg/kg is fundamental to control abuses in farm. Finally, the method development time has been short (two weeks) confirming one of the characteristics of multiclass methods, that is their flexibility.

Conclusions

Although the advantages of multiclass methods are well-known, they are fully realizable only if all the matrices included in the official control plans are analysed with this kind of methods enabling the elimination of single-class procedures with different sample preparation protocols and equipments. For this purpose, experiments are in progress to further extend this approach also to other food involved in food safety monitoring programmes for antibiotic residues (e.g. honey).

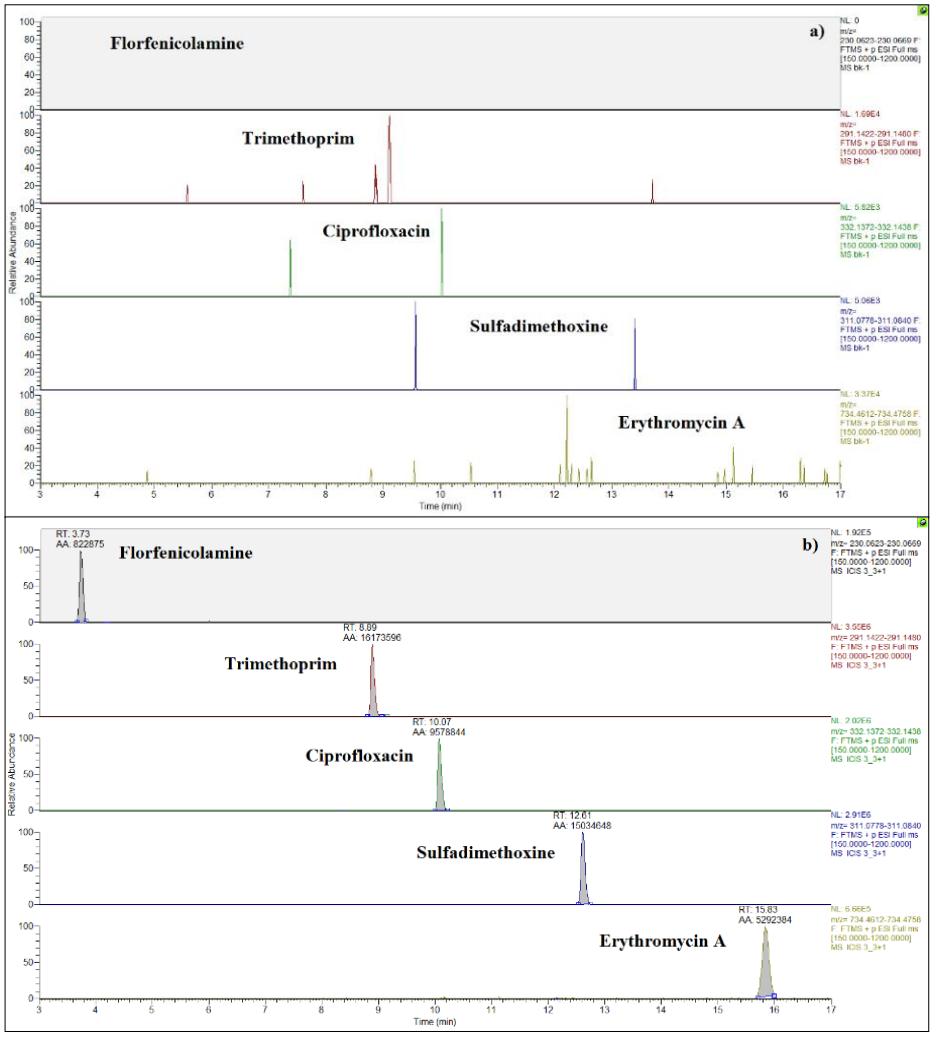

Fig. 1. Chromatograms of a blank (a) and a spiked egg sample (b) at 3.3 µg kg^{-1}

Acknowledgements

The authors gratefully acknowledge financial support from the Italian Health Ministry (Project code: IZSUM RC0032019 "Multiclass method for antibiotic residues in food. Closing the circle: eggs and honey")

References

1. The Commission of the European Communities, Commission Regulation (EU) No 37/2010 of 22 December 2009 on pharmacologically active substances and their classification regarding maximum residue limits in foodstuffs of animal origin, *Off. J. Eur. Communities*, L15 (2010) pp 1-72.
2. S. Moretti, G. Dusi , D. Giusepponi, S. Pellicciotti, R. Rossi, G. Saluti, G. Cruciani, R. Galarini; *Journal of Chromatography A*, 1429 (2016) pp 175–188.
3. S. Moretti, G. Cruciani, S. Romanelli, R. Rossi, G. Saluti, R. Galarini; *Journal of Mass Spectrometry*, 51 (2016) pp 792–804.
4. European Commission, Commission Decision (2002/657/EC) of 12 August 2002 implementing Council Directive 96/23/EC concerning the performance of analytical methods and the interpretation of results, *Off. J. Eur. Communities*, L221 (2002) pp 8-36.
5. A .Kaufmann, *Analytica Chimica Acta*, 637 (2009) pp 144-155.

Environment and Miscellanea

A minimally invasive approach for the identification of proteinaceous binders in works of art by mass spectrometry

C. D. Calvano[1,2], E. C. Rigante[3], R. A. Picca[3], D. Coniglio[3], T. Cataldi[1,3] and L. Sabbatini[3,4]

[1]Dipartimento di Farmacia-Scienze del Farmaco, [2]Centro Interdipartimentale SMART, [3]Dipartimento di Chimica, [4]Centro Interdipartimentale "Laboratorio di ricerca per la diagnostica dei Beni Culturali", Università degli Studi di Bari Aldo Moro, via Orabona 4, 70126 Bari (Italy)

Keywords: *mass spectrometry, works of art, proteomics*

Introduction

Proteinaceous paint binders are responsible of both film formation and adherence of micrometer-sized pigments to the substrate. The recognition of the binders employed can provide useful information on the historical period and artist's preferences. Moreover, the medium identification may be useful to better evaluate conservation and restauration on the artwork itself [1]. Among the oldest binders employed in paintings, there are animal protein-based media such as animal glues, casein and whole egg or white and yolk [2]. Currently, one of the most widespread mass spectrometry (MS) based approaches devoted to identify the proteinaceous binders rely on removing small amounts of specimen and analysing them through a classic bottom-up proteomic approach [3]. When very precious samples are under investigation, the absence of invasiveness represents an undeniable advantage; in fact, non-invasive techniques have been the main purpose of recent research in the field of the cultural heritage [4,5].

Materials and Methods

A simple method is introduced for a quasi-non-invasive analysis of proteinaceous binders in artworks based on the use of a very small (3 mm × 3 mm) poly (2-hydroxyethyl methacrylate)/poly (vinylpyrrolidone) (pHEMA/PVP) hydrogel previously loaded with trypsin and applied onto the objects' surface for less than 30 minutes for the *in-situ* digestion of proteins. The released peptides from the paint layers of paintings were recovered from the gel and identified by either matrix-assisted laser desorption/ionization (MALDI) time of flight (ToF) MS or reversed-phase liquid chromatography (RPLC) coupled to electrospray ionization (ESI) using a linear ion trap (LIT) MS [6,7]. Both analytical approaches allowed us to recognize the proteinaceous binders of investigated paintings.

Results

Firstly, the protocol was assessed by comparing the MALDI mass spectrum of an *in-situ* digested model standard solution (*i.e.*, bovine serum albumin, BSA) with that obtained by conventionally digesting BSA to evaluate the activity of trypsin in the chosen hydrogel. The efficacy of the loaded hydrogel was corroborated by collecting peptide mass fingerprinting (PMF) of paint models composed of chicken egg yolk, different types of animal glue (collagen), and caseins from cow milk mixed with various pigments, carrying out the proposed *in situ* protocol (Figure 1). Database search allowed us to assign the main peptides of paint replicas to caseins, bovine collagen, rabbit collagen and egg yolk.

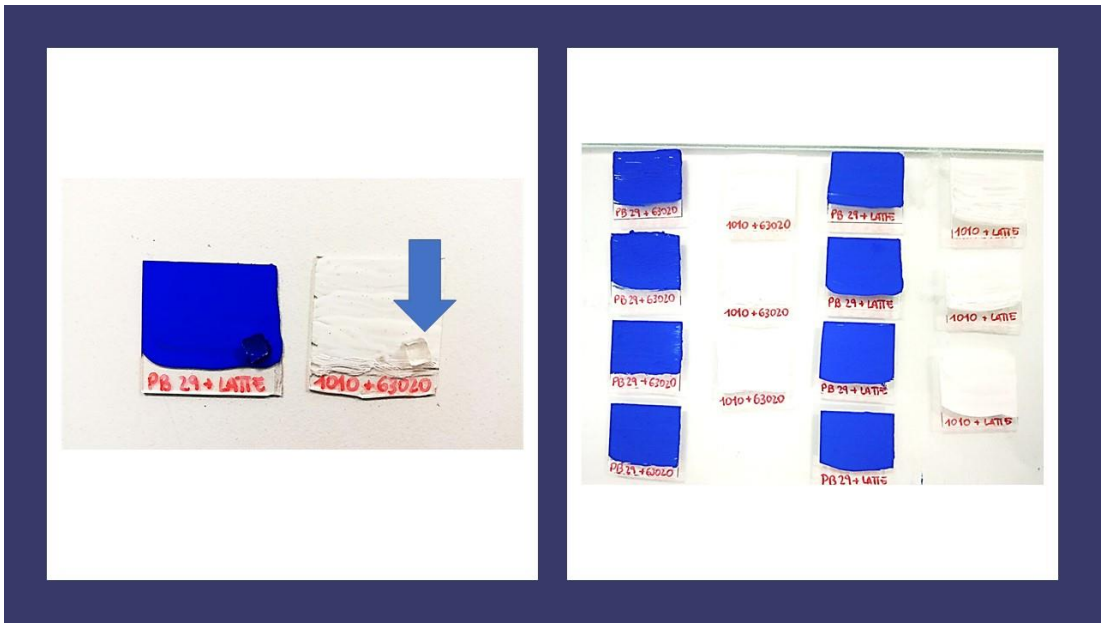

Figure 1. Pictures of some paint replicas examined by the proposed protocol.

To ensure a reliable sequence assignment, the same tryptic digests were also analysed by RPLC-ESI-MS and some selected peptides were subjected to tandem MS experiments by collision induced dissociation (CID). These LC-MS/MS experiments lead to a confident identification of the proteinaceous binders also with a few numbers of matched peptides because isobaric peptides were chromatographically separated. Finally, the same protocol was successfully applied to a painting on wood mockup, a statue exposed in San Lorenzo church (Bisceglie, Bari, Apulia), and a liturgical scroll *Benedictio ignis et fontis (Benedizionale)* of the Museo Diocesano of Bari.

Discussion/Conclusions

The proposed minimally invasive *in situ* sampling and digestion protocol was proved very useful for proteinaceous binder analysis; the conventional digestion gave rise to a sequence coverage comparable with that one obtained through the *in-situ* protocol, but the whole processing was reduced from about 12 h to less than 1 h. Along with the unaffected trypsin activity into the hydrogel, the tiny contact area was enough to obtain reliable results also for low BSA concentrations. The paint replicas confirmed the reliability of the protocol since in each case the media were correctly detected. Finally, the proteinaceous binder was successfully identified in aged samples and works of art pieces as well [7]. The key advantages of the proposed protocol rely on the almost non-invasiveness and on the straightforward sampling process that does not require any specific technical expertise. It can be easily applied to ancient objects of cultural heritage, since it does not require micro sampling and the protein extraction can be performed directly *in situ*, leaving the surface unaltered.

References

1. S. Dallongeville, N. Garnier, C. Rolando, C. Tokarski, *Chem. Rev.* 116 (2016), pp 2–79.
2. C.D. Calvano, I.D. Van Der Werf, F. Palmisano, L. Sabbatini, *Anal. Bioanal. Chem.* 407 (2015), pp 1015–1022.
3. R. Vinciguerra, A. De Chiaro, P. Pucci, G. Marino, L. Birolo, *Microchem. J.* 126 (2016), pp 341–348.
4. M. Manfredi, E. Barberis, F. Gosetti, E. Conte, G. Gatti, C. Mattu, E. Robotti, G. Zilberstein, I. Koman, S. Zilberstein, E. Marengo, P.G. Righetti, *Anal. Chem.* 89 (2017), pp 3310–3317.
5. P. Cicatiello, G. Ntasi, M. Rossi, G. Marino, P. Giardina, L. Birolo, *Anal. Chem.* 90 (2018), pp 10128–10133.
6. D.J.C. Pappin, P. Hojrup, A.J. Bleasby, *Curr. Biol.* 3 (1993), pp 327–332.
7. J. Hardouin, *Mass Spectrom. Rev.* 26 (2007), pp 672–682.
8. C.D. Calvano, E. Rigante, R.A. Picca, T.R.I. Cataldi, L. Sabbatini, *Talanta.* 215 (2020), p 120882.

Concentrations and persistence of antibiotics in pig manure and amended soil

S. Sdogati[1], F. Paoletti[1], S. Moretti[1] C.Barola[1], D.Giusepponi1, G. Saluti[2], A. Agnelli[3], C.F. Magistrali[1] and R. Galarini[1]

[1]Istituto Zooprofilattico Sperimentale dell'Umbria e delle Marche "Togo Rosati", Via G. Salvemini 1, 06126 – Perugia, Italy; [2]Istituto Zooprofilattico Sperimentale dell'Abruzzo e del Molise "G. Caporale", Campo Boario, 64100 –Teramo, Italy; [3]Department of Agricultural, Environmental and Food Science, University of Perugia, Borgo XX Giugno 74, 06124 Perugia, Italy

Keywords: *Veterinary antibiotics; pig manure; amended soil; liquid-chromatography high-resolution mass-spectrometry (LC-HR-MS/MS)*

Introduction

Antimicrobial drugs are broadly used to treat disease in livestock breedings [1]. These substances are mainly excreted via animal urine and feaces, which are often used in agriculture as soil fertilisers. Due to the growing concerns in the antibiotic resistance (AR) topic, it is quite important to evaluate the impact of the release of these substances in the environment and, on the other hand, to attest the presence of AR bacterial genes in soil through qRT-PCR. The aim of this project is to reveal and quantitate drugs in animal sewage and to explore how manured soils can retain these substances in time. For this purpose a multiresidue method for 58 veterinary antibiotics belonging to ten families was developed in sewage and soil samples.

Materials and Methods

Fifty liters of pig sewage were recovered from a storage pond of a swine local farm and used to manure eight boxes containing superficial soil (0-10 cm). Amended soil samples were collected at different days during a nine-month period (September 2019-May 2020). Sewage samples were analyzed via subsequent extractions at acidic and alkaline pH followed by filtration on NH_2 SPE columns. Soil samples protocol consisted of three consecutive extraction steps followed by tandem SPE purification (Oasis HLB and Strata X-C). After evaporation, the dry residues were reconstitued and injected in a Thermo Ultimate 3000 Ultra High Performance Liquid Chromatography system coupled to Q-Orbitrap analyser (Thermo Scientific, San Jose, CA, USA). The instrumental analysis was carried out in Full MS-ddMS^2 mode [2]. The collected sewage and soil samples were tested in parallel for the presence and characterization of microbial population (data not shown).

Results

In pig sewage the residues of ten antimicrobials were detected (Table 1).

Table 3. Antibiotic levels in sewage and amended soil (day 1 and day 270)

	Pig sewage		Soil (day 1)	Soil (day 270)
Class	Antibiotic	Concentration[a] (µg/kg)	Concentration[a] (µg/kg, d.w.)	
Tetracyclines	Doxycycline	3605	1073	420
	Oxytetracycline[b]	46	42	18
	Chlortetracycline[b]	20	13	6
Lincosamides	Lincomycin	1196	300	3
Pleuromutilines	Tiamulin	369	425	93
Sulfonamides	Sulfanilamide	29	27	28
	Sulfadimethoxine	5	7	3
Quinolones	Enrofloxacin[c]	16	8	7
	Flumequine	8	4	2

[a]Mean of two determinations; [b]Sum of parent compound and its epimer; [c]Enrofloxacin + ciprofloxacin

Doxycycline, lincomycin and tiamulin were the most abundant drugs (from 369 to 3605 µg/kg) followed by oxytetracycline, chlortetracycline and enrofloxacin. Despite the large usage of sulfonamides in pig farming, sulfanilamide and sulfadimethoxine were found at concentration lower than 50 µg/kg. This observation agreed with the data of Berendsen et al. [3] who observed fast dissipation of this drug family in manure of different livestock animals (pigs, calves and broilers). Accordingly, these researchers demonstrated that tetracyclines, lincomycin and tiamulin dissipated more slowly. In soil, among the three most abundant compounds, lincomycin decreased rapidly, whereas doxycycline and tiamulin persisted with about 20-40 % of the native compound measured after the nine months period (Table 1 and Figure 1).

Discussion/Conclusions

The high levels and persistence of tetracyclines in amended soils is well documented due to their chelating properties forming time-stable complexes with soil metals [4]. On the other hand, less data are available for tiamulin and lincomycin. Interestingly, although sulfadimethoxine and sulfadiazine have been administered in the swine farm from which manure was collected, no treatments with sulfanilamide have been recorded by the farmer. Therefore, sulfanilamide presence is not explainable. Since a plethora of different antimicrobials is used in pig farming, the degradation/transformation pathways of antibiotics in manure and amended soils must be better known to correlate residues and AR phenomena.

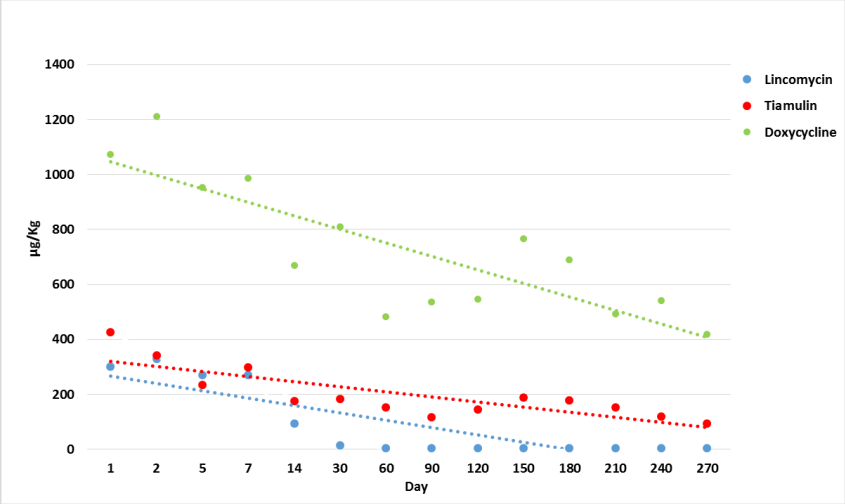

Fig. 14. Concentration trend of three antibiotics in amended soil

References

1. R.J. Erskine, S. Wagner, F.J. DeGraves, *Vet. Clin. North Am. Food Anim. Pract.* 19 (2003), pp 109-138
2. S. Moretti, G. Dusi, D. Giusepponi, S. Pellicciotti, R. Rossi, G. Saluti, G. Cruciani, R. Galarini *Journal of Chromatography A*, 1429 (2016), pp 175-188
3. B.J.A Berendsen, J. Lahr, C. Nibbeling, L.J.M. Jansen, I.E.A. Bongers, E.L Wipfler, M.G.M. van de Schans, *Chemosphere*, 204 (2018), pp 267-276
4. D. Grenier, M.-P. Huot, & D. Mayrand, *Antimicrobial Agents and Chemotherapy*, 44 (2000), pp 763–766.

Acknowledgements

This work was supported by the Italian Health Ministry (Project code: IZSUM RC0032018 "Antibiotic resistance in the surrounding environment of livestock: the black box").

Determination of chlorinated pollutants in environmental matrices using QuEChERS extraction and Gas-Chromatography Tandem Mass Spectrometry

F. Cardellicchio[1]

[1]University of Salerno, Department of Chemistry and Biology, 132 Giovanni Paolo II Street, 84084 Fisciano (SA), Italy

Keywords: *Chlorinated Pollutants, QuEChERS, Mass Spectrometry*

Introduction

In recent years the development of reliable and low-cost methods for determination of toxic persistent organic pollutants (POPs), such as polychlorinated dibenzo-p-dioxins and dibenzofurans (PCCD/F) has increased. PCDD/F are environmental contaminants regulated by the Stockholm Convention [1]. For these contaminants, international analytical methods requires long times, complex instrumentation (High Resolution Mass Spectrometry) and are not suitable for the analysis of a large number of samples in environmental monitoring [2]. Today, the trend is to develop and use "Green" analytical methods to reduce or eliminate the use of solvents, toxic reagents and preservatives, minimizing energy consumption and simplify management of analytical waste. QuEChERS extraction (Quick, Easy, Cheap, Effective, Rugged, and Safe) is a rapid and green multi-residue extraction [3] Briefly, QuEChERS uses a solid–liquid extraction in acetonitrile, followed by the partitioning of the acetonitrile from the solid and aqueous layers by salting out. An aliquot of the separated acetonitrile layer is then cleaned with dispersive adsorbents and analyzed. QuEChERS method is faster than traditional Soxhlet extraction with very limited use of organic solvents. Therefore, the aim of the present work has been to applied QuEChERS procedure for PCDD/F extraction in marine sediment samples. Gas chromatography coupled with triple quadrupole tandem mass spectrometry was used as a detection technique. This technique proved to be more effective than high-resolution GC-MS especially for screening a large number of samples. [4].

Materials and Methods

Superficial marine sediments (0-15 cm) to be analyzed were taken at various stations of first Inlet of the Mar Piccolo basin in Taranto (Ionian Sea, Southern Italy) an marin ecosystem subject to antrhopic impact. After collection, the samples were frozen, then lyophilized and homogenized. The samples (0.5 g) were spiked with known amounts of ^{13}C-PCDD/F and extracted by QuEChERS method using 20 ml acetonitrile (ACN) and sonicated for 60 minutes. Finally 15 mL of Milli-Q water, 6 g of Magnesium Sulphate and 1.5 g of Sodium Acetate were added. Following this step, the sample was centrifuged at 4000 rpm for 10 min. The organic phase (ACN) has been transferred to a Falcon tube, containing 15 mL of Milli-Q water. The analytes were then re-extracted with 3 aliquots of 10 mL of n-hexane each. The hexane extract was subjected to clean up on a column packed with activated carbon / silica gel. The interferences have been eliminated by eluting the column with a mixture of dichloromethane/hexane (1: 3). Finally, the dioxins and furans were eluted with 10 ml of toluene. The toluene extract was evaporated to dryness, diluted with 1 ml of nonane and analyzed by GC-MS triple quadrupole. GC-MS/MS analyses were performed with a gas-chromatograph (Agilent Technologies 7890B GC System) coupled to a triple quadrupole tandem mass spectrometer (QqQ) (Agilent Technologies 7000C GC/MS Triple Quad). The chromatograms were acquired in MRM (Multiple Reaction Monitoring) mode, monitoring two specific transitions for each precursor ion. For each target, two MRM transitions were used, one for quantitation and one for qualification. Quantitation was performed with the quantitative transition only, while the qualitative transition was used to verify the ion ratio between the two transitions. This approach minimized the risk of integrating interferences or the wrong peaks. Data analysis was performed with Agilent MassHunter Quantitative Analysis Software.

Results

The performance of the QuEChERS method was evaluate by calculating the recoveries, the reproducibility and limits of quantification for the various congeners. Under the optimized conditions, the recoveries (> 70%) of all targets are comparable with those recommended by US EPA method 1613 B [2], except for octa-chlorinated congener of dioxins. However, these congeners have low TEFs (Toxicity Equivalence Factors) and their effect on the final results is negligible. The linearity, determined by analyzing standard solutions (in triplicate) at five concentrations ranging from 0.05 and 200 ng/mL, was satisfactory, with correlation coefficients (R^2) > 0.9990. The repeatability, expressed as the relative standard deviation (RSD) of the spiked sample concentrations, was significantly better, with values of 20% or less. The limits of detection and quantification (LODs and LOQs) calculated for the various congeners by linear regression analysis, slope of the calibration lines and intercept standard deviation, showed values of a few dozen of pg/ml suitable to determine concentration levels normally found in contaminated environmental matrices.

Discussion/Conclusions

The QuEChERS method was applied to the determination of polychlorinated dibenzo-p-dioxins and dibenzofurans in contaminated sediment samples (named G and H). The analysis of distribution of the congeners are characterized by a clear predominance of octa-chlorinated dioxin (OCDD), whose percentage with respect to the total fluctuates between 60-80% (Fig.1). The evaluation of the distribution of the various congeners (Fingerprint) allows to hypothesize that the origin of the contamination in the examined samples derives mainly from the combustion processes mainly present in the industrial area of Taranto. In conclusion, the obtained results demonstrate not only the reduction of analysis times but, in general, the reliability and sensitivity of the method. In particular, the use of gas chromatography coupled with triple quadrupole tandem mass spectrometry can replace high resolution mass spectrometry, guaranteeing not only screening procedures, but also reliability in quantitative determination.

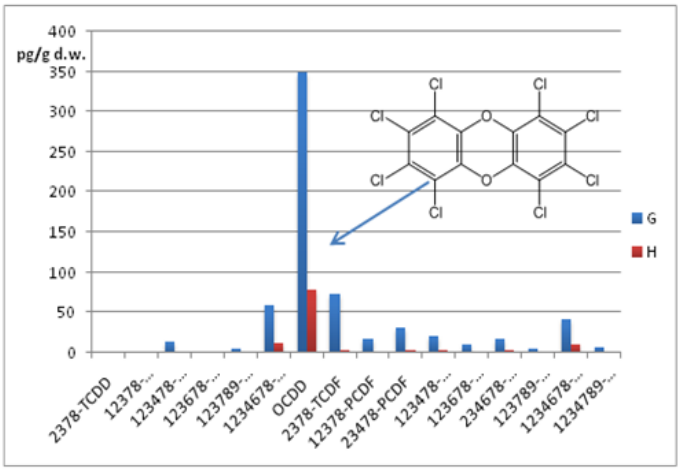

Fig. 1: *Profiles of PCDD/F congeners in the most contaminated sediments (G and H)*

References

1. Stockholm Convention on Persistent Organic Pollutants (POPs), (2001), 2256 U.N.T.S. 119, 40 I.L.M. vol. 532.
2. EPA Method 1613 revision B, October 1994, p.86.
3. M. Anastassiades, E. Scherbaum, B. Taşdelen, D. Štajnbaher, H. Ohkawa, H. Miyagama; P.W. Lee (Eds.), *Pesticide chemistry*, Wiley-VCH, Weinheim, (2007), pp. 439-458.
4. A. García-Bermejo, M. Ábalos, J. Sauló, E. Abad, M.J. González, B. Gómara; *Analytica Chimica Acta*, 889 (2015) pp. 156-65.

Forensic

Determination of capsaicin type compounds in forensic samples by UHPLC-HRMS: the case of Corinaldo

***F. Vincenti*[1,2], *C. Montesano*[1], *F. Pagano*[3], *A. Gregori*[4], *W. K. Cipriani*[5], *L. Micheli*[5], *R. Curini*[1] *and M. Sergi*[3]**

[1]Sapienza University of Rome, Department of Chemistry, 00185 Rome, Italy, [2]Sapienza University of Rome, Department of Public Health and Infectious Disease, 00185 Rome, Italy, [3] University of Teramo, Faculty of Bioscience and Technology for Food, Agriculture and Environment, 64100 Teramo, Italy, [4] Carabinieri, Department of Scientific Investigation (RIS), 00191 Rome, Italy, [5] University of Rome "Tor Vergata", Department of chemical Science and Technologies, 00133 Rome, Italy

Keywords: *Oleoresin Capsicum; capsaicin; HPLC-HRMS/MS*

Introduction

Red chilli (Capsicum annum) is a plant belonging to the Solanaceae family. Given its stinging properties, and in particular of some of its compounds such as Oleoresin Capsicum (OC) [1], the use of OC-based sprays has been reported in Europe since the 1950s, as a defence tool to resolve the problem of biting dogs and a few years later it was also adopted by the German and American police forces, as non-lethal self-defense tools [2]. Nowadays, they are well known also among civilians. The stinging pepper spray represents a very useful tool in case of aggression, but when it is used incorrectly it can turn into an instrument of panic and death, as demonstrated by what has happened in recent years, where sometimes it is used to cause a diversion to carry out thefts.

The aim of the work was the development and validation of an analysis method for the determination of capsaicinoids contained in the most common OC-sprays.

Materials and Methods

A method for the extraction of several capsaicinoids from the pre-packaged supports usually used by law enforcement for surface sampling has been developed.

A µSPE clean-up was carried out by means of OMIX C18 tips; it allowed to reduce the matrix effect caused by the dirty on the sampled surfaces. Qualitative and quantitative analysis of capsaicinoids was carried out by means of UHPLC-HRMS/MS.

The validated method was applied to the investigations concerning a case that occurred recently in an Italian disco. Here, was hypothesized the use of a spray with the aim of creating panic among the crowd.

Results

118 exhibits were sampled through the use of swabs from the disco surfaces, including floors and balustrades. The samples were treated with µSPE clean-up and analysed in a Full scan followed by a data dependent acquisition mode in order to identify and quantify the presence of capsaicinoids. Thanks to the large number of samples, it was possible to develop a concentration map of the analytes of interest within the disco in Corinaldo. In this way it was possible to verify the sector of the room from which the spray delivery started, as shown in figure 1.

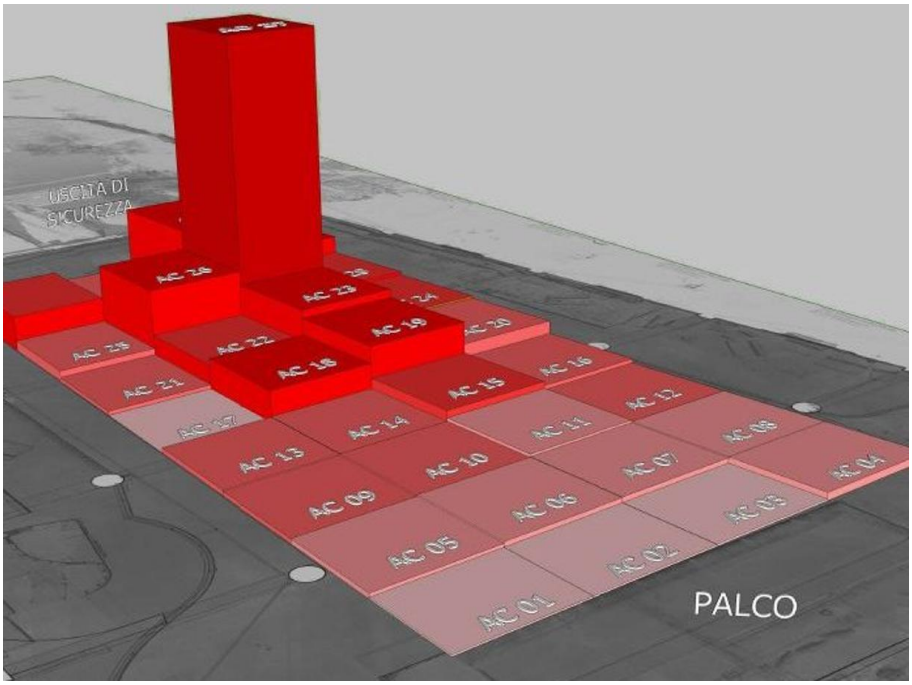

Fig. 15. Distribution of the concentration of Capsaicin in the different zones of the crime scene.

In order to identify the brand of spray used, 10 of the most common products sold in Europe were analysed. Thanks to the statistical analysis of the data, it was possible to identify the brand of the spray used.

Discussion/Conclusions

The development of the clean-up conducted by means of OMIX µSPE tips allowed an effective cleaning of the sample from interferers of different nature, which may include dust, sebum, sugary solutions and other compounds possibly present in places such as discos and pubs. Thanks to the miniaturization of the technique it is possible to use only 100 µL of sample, which is very useful when it is necessary to save an aliquot of the sample for any subsequent analyses. The analysis conducted in Full-dds mode allows the identification and quantification of the analytes of interest and the characterization of all the components of the spray cans. Only thanks to the principal components analysis it was possible to uniquely identify the brand of the spray used.

References

1. H. Krishnatreyya, H. Hazarika, A. Saha, P. Chattopadhyay; *European Journal of Pharmacology*, 819 (2018), pp 114-121.
2. T.C. Chan, G.M. Vilke, J. Clausen, R. Clark, P. Schmidt, T. Snowden, T. Neuman; *U.S. Department of Justice Office of Justice, Programs National Institute of Justice*, (2011), 1-8.

Genoa: huge cocaine-laden hidden in a cargo ship

***F. Nicoletta*[1], *A. Pescione*[1], *S. Beccarisi*[1], *P. Carrea*[1] *and C. Canali*[1]**

[1]Gabinetto Regionale di Polizia Scientifica per la Liguria

Keywords: *cocaine, quali-quantitative analysis*

Introduction

In February 2018, the cargo Dimitris coming from South America was invited to dock in the port of Genoa by the Port Captain's office following an alert by the Master who had detected a suspect cargo well concealed on board. The Police boarded the ship and found several sacks allegedly containing bricks of drug.

Materials and Methods

The Forensic Police carried out the inspection of the ship and accomplished laboratory activities of research of latent fingerprints on the bags containing drug as well as the quali-quantitative analysis of the substance.

Results

The narcotic analysed consisted of 248 bricks of 1 kg each one, with three different logos and purity level of basic cocaine between 91 and 89%. The treatment with cyanoacrylates of the sacks containing drug showed 31 fragments, 24 of which were attributed to one of the crew members.

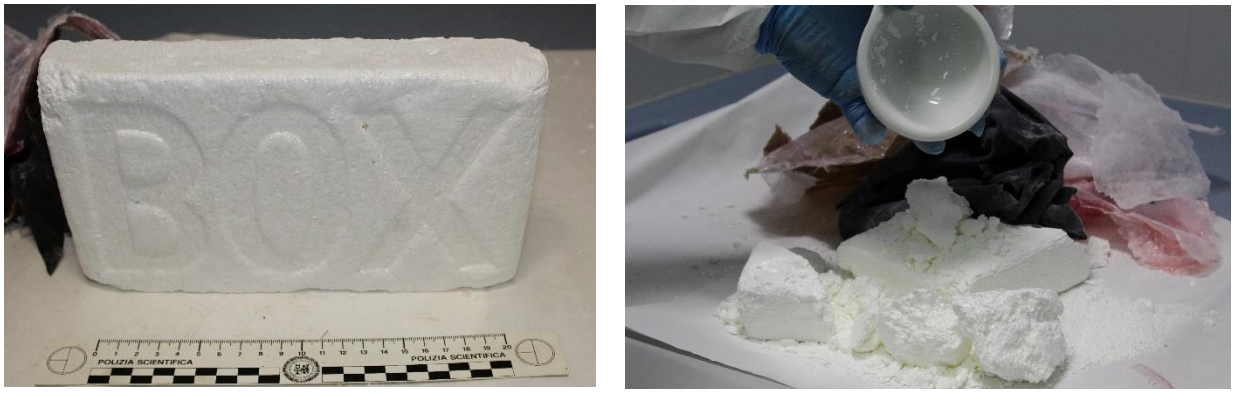

Fig. 1. photos of one sample.

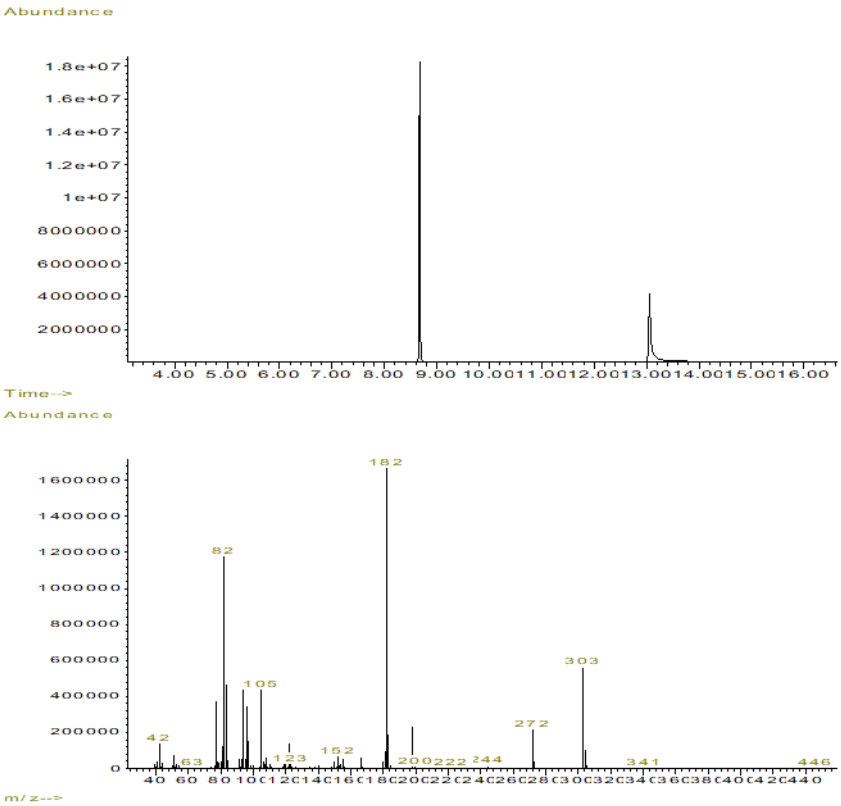

Fig. 2. GC-MS results of cocaine samples.

Table 4. quantitative analysis.

REPERTO	**Net weight (g)**	**A. P. (average)**	**Basic Cocaine (g)**
1	239.396,400	91%	194.509,575
2	7.028,840	89%	5.585,418
3	1.001,960	89%	796,200

Discussion/Conclusions

During the investigation crew remained at the disposal of the Judicial Authority in Genoa. The analysis in GC-MS was decisive to allow immediately detection of the Cocaine.

Kitchen laboratory 2.0 in Turin

***R. Rumonato*[1], *R. D'Angelo*[1], *M. Strano*[1]**

[1]Gabinetto Interregionale di Polizia Scientifica per il Piemonte e la Valle d'Aosta

Keywords: *BHO extractor – e-cigarette – butane hash oil*

Introduction

This communication deals with the first case found and reported in Italy of a kitchen laboratory equipped with materials and reagents to produce e-liquids for consumption in e-cigarettes together with a viable BHO (butane hash oil) extractor. The equipment has already been used and the seizure was also about e-cigarettes ready to use, hashish and marijuana.

Materials and Methods

The analysis wre performed in GC-MS and in GC-FID for the quantification of the drug. A close examination of the seized items was performed to assess their viability.

Fig. 16. BHO extractor

Fig. 2. Ready to use e-liquid

Results

The analysis performed with GC-FID and GC-MS on the e-cig liquid showed the presence of glycerol, cannabinol, cannabidiol and Δ-9-THC up to 0,3% (p/v).
The method of THC extraction with the BHO extractor, the working mechanism of the e-cigarette and the related risks are herein discussed. The equipment was viable and ready to use.

Discussion/Conclusions

The equipment, the reagents, and the drug (620 grams of marijuana and hashish) seized in the site, were suitable for the production of the e-cig liquid. The extractor was already used and capable of being used for the production of the BHO though this product wasn't found in the site, neither butane cans. It is not clear if the laboratory was producing intentionally e-liquid with low concentration of Δ-9-THC or it was only the result of an attempt of extraction. Furthermore, the risk of using such kind of equipment was assessed.

Drug test false positive on 50 kg of "fake" hashish requires GC-MS to solve the case

M. Sc. Commissario Capo Tecnico L. Magliato[1]

[1]Gabinetto Regionale Polizia Scientifica per la Calabria – Polizia Scientifica

Keywords: *drug test, hashish, abietic acid*

Introduction

Field tests are used on daily basis as preliminary screening analysis on presumptive psychoactive materials from seizures. Here we report a 50 kg presumptive hashish seized by Italian Police which turned into a tricky laboratory case. In fact, the main component of this complicate mixture that emulates hashish, reacts with the drug test reagent for THC, giving nonetheless a positive result. So what to do? Instrumental analyses are mandatory to identify and quantify psychoactive materials but in this particular case something that is quite routinely has been the key to understand that something unusual was going on.

Fig. 17. A view of the "fake" hashish seizure.

Materials and Methods

- GC System 7890A – VL MSD 5975C Agilent
-Thermo Scientific Nicolet iS5 iD5 ATR
- Commercial violin rosin

Results

GC-MS routine analysis showed the absence of any illicit psychoactive substance, in fact chromatogram peaks are not related to Δ^9-THC. Nevertheless, a list of chemicals consistent to a rosin wax material like has been identified: Abietic acid and analogues, Longifolene, Octacosane, Octadecane, Heinecosane and a lot of non-solved peak with low match in libraries.

No traces of Δ^9-THC were found even performing the analysis in SIM mode.

High similarity of sample's mass spectra with that of commercially available violin rosin a.k.a. "Pinus Palustric extract" or similar less raffinate product was found.[1]

FTIR analysis showed also a high match index for similar waxes.

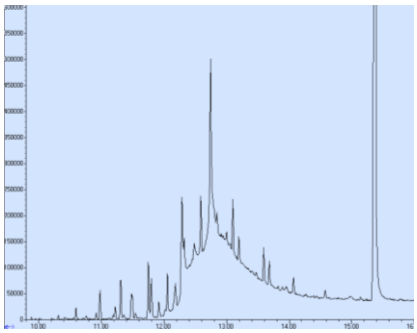

Fig. 2. GC-MS chromatogram of "fake" hashish.

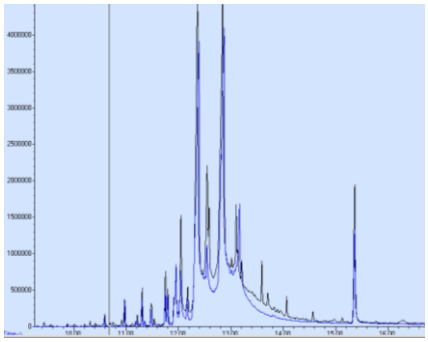

Fig. 3. GC-MS overlay chromatogram of "fake" hashish and "commercial violin rosin".

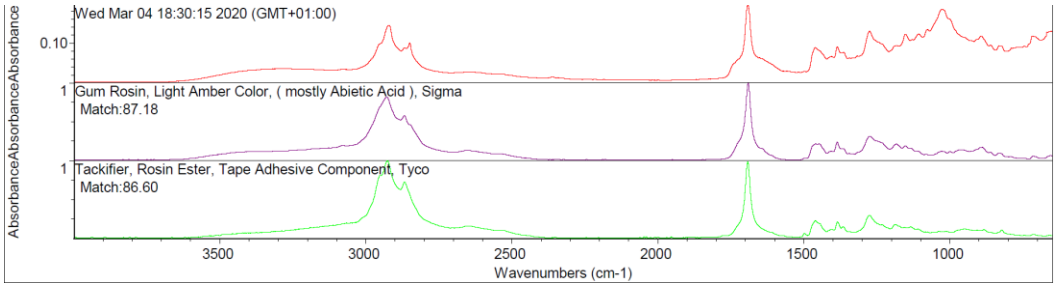

Fig. 4. FTIR ATR Spectrum of "fake" hashish vs library match

Discussion/Conclusions

A common hashish seizure endorsed by a positive field drug test showed through GC-MS analysis its real nature: a material very similar to hashish with no psychoactive substances.
GC-MS analysis revealed the presence of a mixture of Abietic acid and analogues.
What if someone tries to put on the market 50Kg of "fake" hashish? Is it possible to make it in an economic way? Which materials have similar properties to what we have seen?
Several products containing this kind of mixture are commercially available and among them violin rosin GC-MS chromatogram showed the best match.
Maybe we are going too far but what if we perform a field test on this material? Will it react as "real" hashish?
Indeed this product showed positive results to field drug test for THC.
These results led us to conclude that the material analysed could be used as a cutting agent for hashish thanks to its similar properties. In fact, we discovered that the high content of Abietic acid may be responsible of the color change in field drug test based on the Fast Blue B Salt Reagent leading to a false positive.

References

1. Lum ır O. Hanu sa, D. De La Vegab, M. Romanc and Tom cekc; *Israel Journal of Plant Sciences*, 62 (2015), pp 277-282

Pharma

Development of a HPLC-MS/MS method for the pharmacokinetic studies of Pirfenidone in pig plasma

***M. Pallecchi*[1], *M. Menicatti*[1], *G. Bartolucci*[1]**

[1]NEUROFARBA Università degli Studi di Firenze

Keywords: *HPLC-MS/MS, Pirfenidone, Drug Plasma Stability*

Introduction

Pirfenidone is a drug active against idiopathic pulmonary fibrosis, but recently its use was evaluated also in the myocardial infarction to reduce the heart damage[1-2]. The aim of this study was the development and validation of a HPLC-MS/MS method for the quantitative determination of Pirfenidone in pig plasma for preliminary pharmacokinetic studies in order to confirm the activity against heart attack.

Materials and Methods

For this study, a HPLC Varian Prostar coupled with a triple quadrupole Varian 1200L was employed. The development of the HPLC-MS/MS method started with an Energy Resolved Mass Spectrometry (ERMS) experiment on the Pirfenidone for study its fragmentation in order to select the best MRM transitions. Phenacetin, was chosen as internal standard due to its structural and molecular weight similarities. The chromatographic parameters employed to analyse the samples, were finely tuned to minimize the run time, maintaining the sensitivity and the reliability requested for the study. The best performances were obtained by using a Phenomenex Luna PFP 30x2 mm, 3 μm of particle size, column with a gradient elution of 10 mM formic acid and 5 mM ammonium formate solution (Solvent A), 5 mM formic acid and 10 mM ammonium formate in methanol solution (Solvent B). The elution gradient was started at 90 % solvent A, then decreased to 5 % in 4.0 min, kept for 4.0 min, returned to initial conditions in 0.1 min and maintained for 3.9 min for reconditioning, to a total run time of 12 min. Finally, the mobile phase flow, sample injection and column temperature were kept at 0.25 mL/min, 5 μL and 20°C respectively.

The pharmacokinetic studies involved three different Pirfenidone administrations to Pigs (ev, im and os). Then plasma samples in different times (0, 30, 60, 90, 120, 180 and 240 minutes) have been collected.

Moreover, in order to establish the chemical stability of Pirfenidone in studied samples, a series of experiments in PBS buffer and pig plasma were carried out.

Each sample was prepared by simply protein precipitation and dilution of supernatant, in order to increase productivity.

The evaluation of matrix effect was carried out by following the guidelines of Matuszewski et al[3] using Pig plasma.

Accuracy and Precision experiments were performed to validate the proposed HPLC-MS/MS method.

Results

Concerning the pharmacokinetics studies, the different administrations shown different kinetic profiles and the related PK parameters were calculated.

	AUC (ng h/mL)	AUC (mg h/L)	Bioavailability	T max (h)	Vd (L)	CL (L/h)	$t_{1/2}$ (h)
M1	19364	19.4	100.0%	0.5	42	20.7	1.4
M2	10125	10.1	52.3%	0.5	58	20.7	1.9
M3	14943	14.9	77.2%	0.5	41	20.7	1.4

Fig. 18 PK parameters obtained..

The drug plasma stability experiments demonstrated that the Pirfenidone was stable in all matrices and incubation times.
The method didn't show matrix effect while recovery, precision and accuracy values were 97.2%, 1,9-4% and 83-94% respectively.

Conclusions

The proposed HPLC-MS/MS method has proven to be suitable for the determination of Pirfenidone in the pharmacokinetic studies described above. Moreover, the obtained preliminary data will be useful to support the Pirfenidone study to reduce the heart damages in the myocardial infarction.

References

1. K.W. Lee, T.H. Everett, D. Rahmutula, et al. *Circulation*. 114 (2006), pp 1703-1712.
2. D. T. Nguyen, C. Ding, E. Wilson, G. M. Marcus, J. E. Olgin. *Heart Rhythm*. 7 (2010), pp 1438-1445.
3. B. K. Matuszewski, M. L. Constanzer, and C. M. Chavez-Eng; *Analytical Chemistry* 75 (2003), pp 3019-3030.

A chemoproteomic approach for the characterization of new covalent drugs

***S. Castelli*[1], *P. Orsini*[2], *F. Casuscelli*[2], *P. Magnaghi*[2], *A. Altomare*[1], *G. Aldini*[1], *B. Valsasina*[2] *and Sonia Troiani*[2]**

[1]Department of Pharmaceutical Sciences, University of Milan, Italy, [2]Oncology, Nerviano Medical Sciences Srl, Nerviano (MI)

Keywords: *chemoproteomic, click chemistry, target engagement*

Introduction

The recent success of covalent kinase inhibitors such as Ibrutinib, Neratinib and Afatinib in oncology targeted therapy led to the development of new covalent drugs.
Small molecule drugs, named Target Covalent Inhibitors (TCI), were designed in order to covalently bind and inhibit target proteins that are involved in tumorigenesis [1].
They have many desirable features, including increased biochemical efficiency of target inhibition, being not subjected to classical equilibrium kinetics and prolonged mechanism of action as the target activity can only be recovered by new protein synthesis [2].
Covalent binding is usually obtained by introducing an electrophilic warhead in the molecule able to bind specific nucleophilic sites of proteins.
However, such electrophilic groups could also bind additional proteins thus leading to unanticipated toxicities in drug development programs.
The characterization of the protein-drug interaction is therefore extremely important in the process of drug development, in order to measure the target engagement of the drug in a physiological environment and clarify the proteome-wide selectivity of covalent inhibitors.
Here we present the development of a chemoproteomic approach that takes advantage of a click chemistry reaction, a 1,3-dipolar cycloaddition of azide and alkyne groups to generate a 1,2,3-triazole ring [3], both for studying the target engagement and for identifying the off-target proteins of covalent inhibitors.

Materials and Methods

An alkyne group was incorporated into a covalent inhibitor with minimal disruption of the cell permeability and binding interactions compare to the parent molecule. This new molecule is named probe. Then, click chemistry was applied to bind an azide-functionalized reporter tag to the labeled proteins after cell or tissue lysis and homogenization.
For the target engagement studies a fluorescent reporter tag had enabled the visualization of the derivatized proteins after SDS-PAGE separation. Then, in order to identify the potential off-targets of the probe, a desthio-biotin reporter tag was used to affinity purify the tagged proteins, with a streptavidin resin, and identify them by a standard MS-based proteomic workflow.

Results

Concerning the verification of target engagement, click chemistry was performed and optimized on recombinant protein derivatized with the probe in order to select the best reaction conditions: the reaction performed better in 0.1% NP40. Then, the target engagement was performed in cells: cells in which the protein is expressed, were treated with the probe for 24 hours. After proteins extraction, click chemistry was applied and fluorescence detection was obtained after SDS-PAGE. The yellow band in Figure 1, confirmed that click chemistry reaction is efficient and the probe labels the protein target in cells.
The identification of probe off-targets was performed labelling to the probe an azide coupled with a desthiobiotin molecule. Proteins were enriched on streptavidin resin and separated on SDS-PAGE. The identification of the bands in elution lane was obtained with the digestion of gel bands and MALDI-MS analysis. As it is shown in table 1, different proteins were identified by mass spectrometry analysis and they may represent possible off-targets and false positive hits.

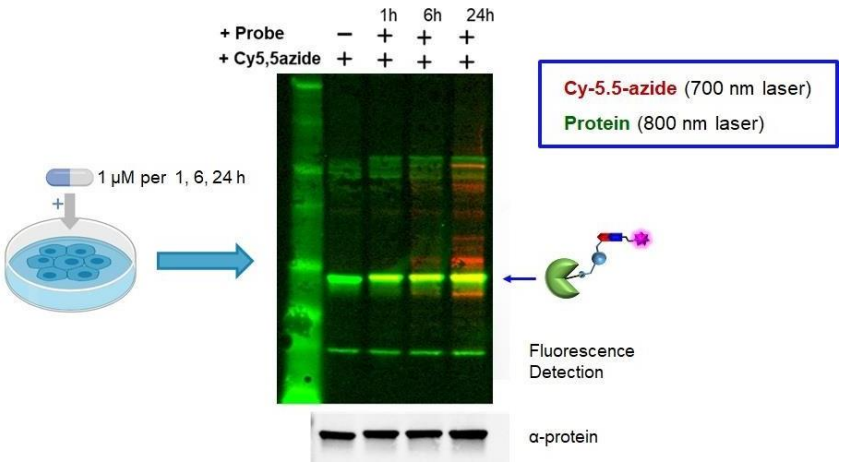

Figure 1_Fluorescence detection of probe target engagement in cells

Table 1_Proteins identified with MASCOT analysis

Band	Protein ID	Score	Molecular Weight
2	Miosin-9	75	226 KDa
3	eEF2	86	95 KDa
4	αHSP-90	128	90 KDa
5	Pyruvate Kinase	86	58 KDa
8	β-actin	172	43 KDa
9	GAPDH and Annexin A2	199	37 KDa – 38 KDa
10	Pyruvate Kinase	169	58 KDa
11	Tubulin α and β	192	55 KDa
12	α-enolase and tubulin α and β	288	47 KDa – 50 KDa

Discussion/Conclusions

In conclusion, click chemistry reaction has been optimized in order to verify the target engagement of covalent inhibitors. The probe shows a good selectivity profile and the probe-target binding results to be effective and predominant in the cellular context. Thus, click chemistry reaction is a useful approach to characterize the chemoproteomic profile of covalent inhibitors in drug discovery.

References

1. B. K. Mishra and P. M. Parikh *Medical journal, Armed Forces India,* 62 (2006), 169-173
2. D. S. Johnson, E. Weerapana and B. F. Cravatt; *Future Medicinal Chemistry,* 2 (2010)**,** 949-964
3. H. C. Kolb, M. Finn and K. B. Sharpless; *Angewandte Chemie International Edition*, 40 (2001), 2004-2021

Detection of a Catalytically Active Self-Assembled Resorcinarene Capsule by Mass Spectrometry

P. La Manna[1], G. Ferrino, M. De Rosa[1], C. Talotta[1], A. Rescifina[2], G. Floresta[2], A. Soriente[1], C. Gaeta[1] and P. Neri[1]

[1] Laboratorio di Chimica Supramolecolare, Dipartimento di Chimica e Biologia "A. Zambelli", Università degli Studi di Salerno [2] Dipartimento di Scienze del Farmaco, Università di Catania.

Keywords: *Resorcinarenes, Self-Assembly, FT-ICR, Supramolecular Catalysis*

Introduction

In the last decades, many efforts have been devoted to the study of reactions catalyzed in nanoconfined spaces for the synthesis of drug candidates.[1] In particular, pyrrole and *C*-alkylated pyrroles are among the most important fundamental constituents of biologically and physiologically active molecules, such as chlorophyll, porphyrin, hemoglobin, Vitamin B12 and bile pigments.[2] In addition *C*-alkylated pyrroles play important roles in medicinal chemistry, where they act as anticancer agents.[2]

The hexameric capsule ($\mathbf{1}_6(H_2O)_8$ in Figure 1), originally reported by Atwood,[3] is obtained by self-assembly of six resorcinarene **1** units and eight water molecules (Figure 1), and has been largely exploited as nanoreactor thanks to its capacity to host the substrates selectively and to accelerate the organic reactions with excellent chemo-, regio-, and stereoselectivity.[1,4]

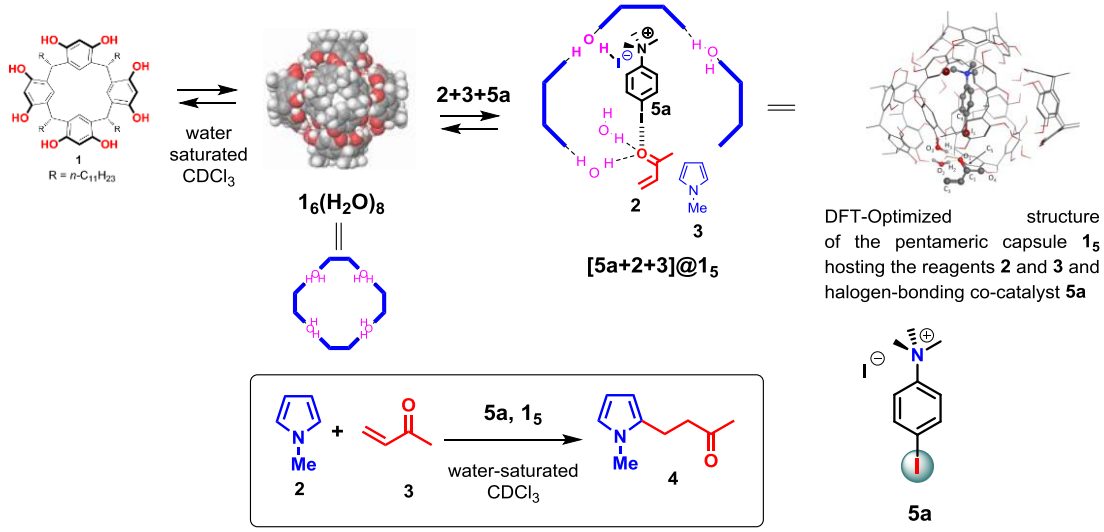

*Fig. 1. Top: Self-assembly[2] of six C-undecylresorcin[4]arene **1** and eight water molecules to form the hexameric capsule $(\mathbf{1})_6\bullet(H_2O)_8$.[2] Formation of the catalytically active pentameric capsule in presence of **2**, **3** and **5a**.[6] (Bottom) Halogen bonding[4] catalyzed Michael reaction between N-methylpyrrole **2** and methylvinylketone **3** in the presence of the pentameric capsule and the halogen-bond donor catalyst **5a**.[6]*

Halogen-bonding (XB)[4] is a secondary interaction between a covalently bound halogen atom in a R–X compound (the "XB donor", where X = I, Br, Cl, F, and R = C or any other atom including even I, for example) and a Lewis base (the "XB acceptor"). Recently, increasing attention has been devoted to exploiting the XB interaction in organocatalysis.[5]

On the basis of these considerations, we investigated[6] the Michael reaction between substrates **2** and **3** to give the *C*-alkylated pyrrole **4** in the presence of the catalyst **5a** inside the resorcinarene capsule (Figure 1).[6]

Materials and Methods

High-Resolution Mass Spectra were acquired using a Bruker Solaris XR Fourier transform ion cyclotron resonance mass spectrometer equipped with a 7 T refrigerated actively-shielded superconducting magnet. The samples were ionized in positive ion mode using the ESI ion source. An external calibration using a NaTfa solution in positive ion mode was performed.

Results

The Michael reaction between *N*-methylpyrrole **2** and methyl vinyl ketone **3** is catalysed in the nanoconfined space inside the pentameric capsule $\mathbf{1}_5$ (Figure 1) by activation of the carbonyl of **3** by halogen bonding interaction with the co-catalyst **5a** (see Figure 1).[6] Quantum-mechanical investigations highlighted that the Michael reaction proceeds through the activation of the carbonyl by synergistically enhanced halogen/hydrogen bonding interactions, and takes place in an open pentameric capsule (Figure 1).[6] Experimental evidences of the presence of a pentameric resorcinarene capsule **C** under the catalytic reaction conditions were obtained by HR FT-ICR ESI MS (Figure 2). [6]

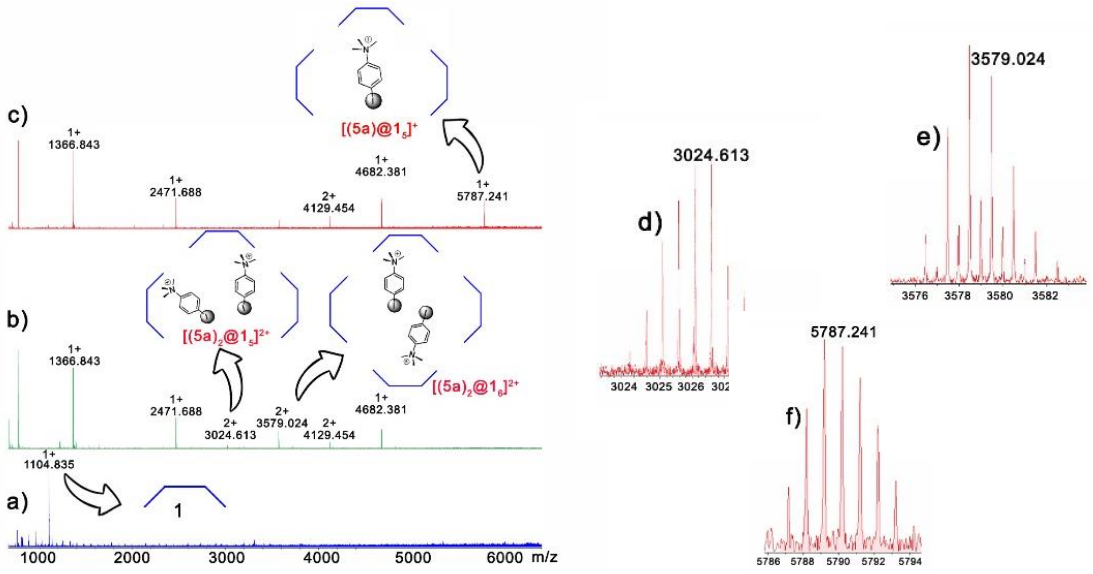

*Fig. 2. ESI-FT ICR mass spectra of: a) 250 μM solution of **1** in water-saturated $CHCl_3$, b) after addition of a stoichiometric amounts of **5a**, c) mixture in (b) in the presence of **2** and **3** (same reaction conditions), Experimental patterns of d) **[(5a)$_2$@1$_5$]$^{2+}$**, e) **[(5a)$_2$@1$_6$]$^{2+}$**, and f) **[5a@1$_5$]$^{2+}$**.*[6]

Discussion/Conclusions

When resorcinarene **1** was ionized with an ESI source in the absence of catalyst **5a**, then only the molecular peak of **1** at 1104.835 *m/z* was detected (Figure 2a).[6] Differently, when an equimolar mixture of resorcinarene **1** and catalyst **5a** was ionized with an ESI source according to the conditions reported previously by Schalley and coworkers,[7] then the mass spectrum reported in Figure 2b was obtained. The results in Figure 2b suggested that the organic cation of **5a** templates the formation of pentameric (**5a**)$_2$@**1**$_{5a}$ and hexameric (**5a**)$_2$@**1**$_6$ aggregate, which were detected at 3024.613 *m/z* and 3579.024 *m/z*, respectively, and in which two units of **5a** were present inside the capsules.[6] Significantly, when the reactants **2** and **3** were added to the mixture in Figure 2b then the mass spectrum in Figure 2c was obtained, in which a peak at 5787.24 *m/z* was revealed attributable to the pentameric aggregate containing a single unit of catalyst **5a**, (**5a**@**1**$_a$). Under these conditions, no hexameric capsule was detected. In conclusion, MS studies confirm the presence of the pentameric capsule postulated by DFT calculations.

References

1. C. Gaeta, C. Talotta, M. De Rosa, P. La Manna, A. Soriente, P. Neri, *Chem. Eur. J.* 25 (2019), pp 4899-4913.
2. A. Joule, K. Mills, G.F. SmithHeterocyclic Chemistry (4th ed.), Blackwell Science, Oxford (2000)
3. L. R. MacGillivray, J. L. Atwood, *Nature* 389 (1997), pp 469-472.
4. Q. Zhang, L. Catti, K. Tiefenbacher, *Acc. Chem. Res. 51 (*2018),pp 2107−2114.
5. G. Cavallo, P. Metrangolo, R. Milani, T. Pilati, A. Priimagi, G. Resnati, G. Terraneo, *Chem. Soc. Rev.*, 116 (2016), pp 2478-2601.
6. D. Bulfield, S. M. Huber *Chem. Eur. J.* 2016, *22*, 14434–14450.
7. P. La Manna, M. De Rosa, C. Talotta, A. Rescifina, G. Floresta, A. Soriente, C. Gaeta, P. Neri, *Angew. Chem., Int. Ed.* 59 (2020), pp 811-818.
8. N. K. Beyeh, M. Kogej, A. Ahman, K. Rissanen, C. A. Schalley, *Angew. Chem. Int. Ed*. 45 (2006), pp 5214–5218.


9 788894 952025